Characterizing the Variability of Kinematic Outcome Measures and Compensatory Movements using Inertial Measurement Units

by

Benjamin F. Cornish

A thesis

presented to the University of Waterloo

in fulfilment of the

thesis requirement for the degree of

Master of Science

in

Kinesiology

Waterloo, Ontario, Canada, 2019

Author's Declaration

I hereby declare that I am the sole author of this thesis. This is a true copy of the thesis, including any required final revisions, as accepted by my examiners.

I understand that my thesis may be made electronically available to the public.

Abstract

Cost-effective wearable sensors to measure movement have gained traction as research and clinical tools. The potential to quantify movement with a portable and inexpensive way could provide benefits to patient populations (e.g. amputees) to supplement or replace current clinical evaluations. For example, characterization of frontal plane kinematic outcome measures is a relevant movement pattern to a complex amputee population. The ability to capture such movements could have important therapeutic opportunities. The current research worked towards characterizing frontal plane compensatory movement patterns with kinematic outcome measures described by inertial measurement units (IMU) data in healthy adults. This was an initial step towards developing a future toolkit that could characterize normal and aberrant movement patterns in clinical populations.

The thesis is comprised of two related studies. The first study set out to evaluate the numerical accuracy of IMU estimated spatial measures when compared to a gold standard system. Six subjects completed six different movement tasks while instrumented with optical motion capture and IMUs. Each movement task probed the accuracy of specific deviations (e.g. vertical deviation). The hypothesis was that outcome measures would be strongly associated ($r>0.8$) and mean error would not be significantly different from zero and the coefficient of repeatability would be within priori set limits of agreement (± 18 mm). Kinematic outcome measures had small mean error bias compared to gold standard measures and range of subject specific mean errors showed minimal differences. Task specific differences were evident when movement patterns exhibit large transverse rotations. These results showed the devices have a level of accuracy that may be suitable to characterize changes in movement patterns clinically.

The second study aimed to utilize the same techniques from study 1 to describe compensatory kinematic outcome measures during a clinical obstacle avoidance task to differentiate between compensatory and normal movement patterns. Twelve subjects wore IMUs bilaterally on the ankles and on the belt above the right hip. An off the shelf orthotic knee brace was used to restrict lower limb knee

joint kinematics (reduce range of motion). Participants completed 15 walking trials for three different brace conditions (No Brace, Unlocked Brace, Locked Brace) and two obstacle task conditions (Level Ground Walking and Obstacle Avoidance) to elicit a comparison of normal and compensatory movements. During the walking task, IMUs were able to characterize compensatory movements typical of the amputee population. Lateral deviation of the swinging foot was significantly larger during obstacle crossing with a locked brace compared to no brace. Maximum elevation of the limb was significantly larger while crossing obstacles compared to level ground walking and was precise enough to discern elevation differences of No Brace elevation from both Unlocked and Locked Brace conditions. Hip hiking was also significantly larger in the locked brace obstacle crossing from no brace obstacle crossing. Swing time was longer when the limb was braced and during obstacle crossing when compared to level ground walking. Healthy subjects had no significant changes to double support time compared those exhibited by amputees during walking.

Overall, differences between IMU and gold standard measures are present. Mean error differences are present for certain tasks and criteria for agreeability between devices is not satisfied. Descriptive analysis of low subject mean error ranges across the majority of tasks indicate a potential utility in these measures to distinguish between movement patterns. During the clinical task, when knee mobility was manipulated compensatory movements were significantly different across conditions. This study provides evidence for the utility of IMU devices to support clinical gait analysis with quantifiable measures.

Acknowledgements

First, I would like to thank my supervisor Dr. Bill McIlroy, his ability to challenge and encourage me throughout the entirety of this thesis project has been instrumental in the development my scientific thinking and motivation. I would also like to acknowledge Dr. Stephen Prentice, his support during both my graduate and undergraduate work has allowed me to explore research with a unique perspective. I am forever grateful for the opportunity to study with the guidance from both of these professors.

Second, I would like to thank my examination committee, Dr. Andrew Laing and Dr. Steve Fischer. Their support never wavered throughout the duration of this project and their unique perspectives on this project helped strengthen the end results. During my time at the University of Waterloo, I have also had the privilege to have interactions with Drs. Nancy Theberge, Jim Frank, and Ron McCarville, all who have mentored and supported me in one way or another. To all my friends within the Kinesiology department, you have been instrumental in my success and I am happy to have developed such strong friendships within the department. In particular, I would like to recognize Benoit, Jordan, Jeff, Maureen, and Gary for the support in the early years.

Last, I would like to thank my family. Cheryl and James, for their continued support throughout these past years, I know you are as thrilled as I am for this part of my journey to be finished and I am happy to share that success with you. To Valerie Bigelow, for constantly supporting me in every decision I make and always approaching difficult situations with optimism. Your personality is inspiring and I am lucky to have you by my side.

Table of Contents

List of Figures viii
List of Tables x
Introduction 1
Chapter 1 : Literature Review 3
1.1 Prevalence of Amputee Population and Scope of the Rising Issue 3
1.2 Factors Contributing to Gait Deviations in the Amputee Population 4
1.3 Clinical Gait Analysis 7
1.3.1 The Gait Cycle 10
1.4 Inertial Measurement Units 12
1.4.1 Accelerometer 13
1.4.2 Gyroscope 14
1.5 Accuracy of Data Acquisition Using Inertial Measurement Units 14
1.5.1 Error Types in MEMS Accelerometers and Rate Gyroscopes 15
1.5.2 Environmental influence on data quality 16
1.5.3 Estimating Spatial Measurements from Acceleration Data 17
1.6 Application to Human Movement Analysis 21
1.7 Thesis Objectives and Rationale 22
Chapter 2 : Investigating the Agreeability between Inertial Measurement Units and 3D Motion Capture during Isolated Movement Tasks 24
2.1 Spatially Derived Estimates (IMU) compared to Gold Standard Measures 24
2.1.1 Other applications of IMU and their Clinical Significance 25
2.2 Rationale, Objective, and Hypothesis 27
2.3 Methods 28
2.3.1 Participants 28
2.3.2 Instrumentation 28
2.3.3 Collection Protocol 30
2.3.4 Data Analysis 34
2.3.5 Outcome Measures 37
2.3.6 Statistical Analysis 37
2.4 Results 38
2.4.1 Concurrent Validity of IMU Spatial Estimates and Optical Motion Capture 39
2.5 Discussion 53
Chapter 3 : Characterizing the Variability of Compensatory Movement Strategies in Healthy Subjects Using Inertial Measurement Units 62
3.1 Introduction 62

3.1.1 Defining the Gait Cycle with Instrumentation 63
3.1.2 Spatiotemporal Measures Change for Obstacle Avoidance 64
3.1.3 Exploring obstacle negotiation strategies in healthy subjects with movement manipulations 66
3.1.4 Support measures to probe stability – healthy and compromised 68
3.1.5 Detecting changes kinematic outcome measures with IMUs 70
3.1.6 Rationale, Objective, and Hypothesis 73
3.2 Methods 74
3.2.1 Participants 74
3.2.2 Collection Protocol 75
3.2.3 Instrumentation 77
3.2.4 Data Processing 79
3.2.5 Outcome Measures 82
3.2.6 Statistical Analysis 82
3.3 Results 83
3.3.1 Gait Event Detection Algorithm 83
3.3.2 Effect of Unlocked and Locked Brace Conditions on Normal Unrestricted Movement Patterns 84
3.3.3 Main Effect of Brace and Obstacle Condition 85
3.4 Discussion 94
Chapter 4 : Conclusion 102
References 104

List of Figures

Figure 1. Shimmer3 Inertial Measurement Unit (Shimmer Sensing Inc., Dublin, Ireland) with factory calibrated local coordinate system denoted. 13
Figure 2. Rigid body and IMU placement on lower limb (4 cm above lateral malleolus). The rigid body is instrumented with four smart IRED markers and setup to allow IMU attachment over rigid body construction. 29
Figure 3. Block diagram outlining collection sequence for Study #1 with all 6 tasks. 30
Figure 4. Sequence of movements for Task 1. Subject complete sagittal plane hip range of motion, starting at and returning to rest. 31
Figure 5. Sequence of movement for Task 2. Subject start at rest, hip abduction laterally deviates the leg, and they return to resting position. 31
Figure 6. Sequence of movements for Task 3. Subjects start at rest, lift their knee towards their chest (hip and knee flexion) and return to rest. 32
Figure 7. Sequence of movements for Task 4. Subjects start at rest, flex their knee and return to resting position. 32
Figure 8. Sequence of movements for task 5. Subjects start in a staggered foot position (left in front of right), complete a single isolated step and volitionally induce hip circumduction. 33
Figure 9. Sequence of movements for task 6. Subjects start in a staggered foot position (left in front of right), complete a single step and volitionally induce hip circumduction and hip rotation. 33
Figure 10. Bland-Altman plot of differences between IMU spatial estimate and motion capture measurement for anterior deviation during sagittal plane hip range of motion task. 40
Figure 11. Bland-Altman plot of differences between IMU spatial estimate and motion capture measurement for posterior deviation during sagittal plane hip range of motion task. 42
Figure 12. Bland-Altman plot of differences between IMU spatial estimate and motion capture measurement for lateral deviation during isolated hip abduction task. 44
Figure 13. Bland-Altman plot of differences between IMU spatial estimate and motion capture measurement for vertical deviation during hip and knee flexion task. 46
Figure 14. Bland-Altman plot of differences between IMU spatial estimate and motion capture measurement for vertical deviation during knee flexion task. 48
Figure 15. Bland-Altman plot of differences between IMU spatial estimate and motion capture measurement for lateral deviation during swing phase of stepping with hip circumduction task. 50
Figure 16. Bland-Altman plot of differences between IMU spatial estimate and motion capture measurement for lateral deviation during swing phase of stepping with hip circumduction and rotation task. 52
Figure 17. Trajectory of both lead and trail limb during obstacle crossing conditions (solid, fragile, no obstacle). Different toe and hip trajectories are evident from tracings of lead versus trail as they cross the obstacle. Image from (Patla et al., 1996) 65
Figure 18. Comparison of toe trajectory during obstacle clearance with increased limb flexion and hip hiking movement strategies (Patla & Rietdyk, 1993). 66
Figure 19. Block diagram outlining collection block details and sequence for Study #2. 75
Figure 20. (a) CTI® OTS Knee Brace (Ossur (UK) Ltd, Stockport, UK) used on the present study. (b) Flexion Stops (Ossur (UK) Ltd, Stockport, UK) used as the locking mechanism for the knee brace to reduce knee flexion. 76
Figure 21. Gait task walkway. Obstacle was placed halfway between the start and end sections and was removed on level ground walking tasks. Beam breakers were start up at start, end and middle of walkway to synchronize step counts within a certain distance and obstacle crossing timing. 77
Figure 22. IMU placement on lower limb (4 cm above lateral malleolus). Footswitches were secured with Hypafix® tape to the bottom of the heel and forefoot for gait event confirmation. 78

Figure 23. Lateral deviation of the right limb during clinical gait tasks comparing the lateral deviation that is present during obstacle avoidance and level ground walking with three different brace conditions (no brace, unlocked, locked brace). Negative values represent movement to the right (laterally) for the right limb. Significant differences (*) and not significant differences (*n.s.*) are denoted on figure. 86
Figure 24. Lateral deviation of the left limb during clinical gait tasks comparing the lateral deviation that is present during obstacle avoidance and level ground walking with three different brace conditions (no brace, unlocked, locked brace). Negative values represent movement to the right (medially) for the left limb. Significant differences (*) and not significant differences (*n.s.*) are denoted on figure. 87
Figure 25. Hip hiking measures of the right hip during clinical gait task comparing hip vertical deviation during obstacle avoidance and level ground walking with three different brace conditions (no brace, unlocked, locked brace). Significant differences (*) and not significant differences (*n.s.*) are denoted on figure. 90
Figure 26. Right limb swing time during clinical gait task comparing swing time during obstacle avoidance and level ground walking with three different brace conditions (no brace, unlocked, locked brace). Significant differences (*) and not significant differences (*n.s.*) are denoted on figure. 92
Figure 27. Left limb swing time during clinical gait task comparing swing time during obstacle avoidance and level ground walking with three different brace conditions (no brace, unlocked, locked brace). Significant differences (*) and not significant differences (*n.s.*) are denoted on figure. 93

List of Tables

Table 1. List of common amputee gait deviations, outline in the *Atlas of limb prosthetics: surgical, prosthetic, and rehabilitation principles* (Bowker et al., 1992) 5
Table 2. Clinical tasks and objectives for Amputee Mobility Predictor (Gailey et al., 2002) 9
Table 3. Example of task description from Amputee Mobility Predictor (Gailey et al., 2002) 10
Table 4. Mean error (SD) reported by Trojaniello et al., (2015) for step length estimates in four different populations using OFDRI techniques to de-drift, calculate, compare spatial measurements from IMUs, and pressure sensor mat. 25
Table 5. Summary and definition of each outcome variable. 34
Table 6. Subject specific IMU calculated and optical motion capture measured spatial anterior deviation during a sagittal plane hip range of motion movement. 39
Table 7. Subject specific IMU calculated and optical motion capture measured spatial posterior deviation during a sagittal plane hip range of motion movement. 41
Table 8. Subject specific IMU calculated and optical motion capture measured spatial lateral deviation during an isolated hip abduction task. 43
Table 9. Subject specific IMU calculated and optical motion capture measured spatial vertical deviation during an isolated hip and knee flexion task. 45
Table 10. Subject specific IMU calculated and optical motion capture measured spatial vertical deviation during an isolated knee flexion task. 47
Table 11. Subject specific IMU calculated and optical motion capture measured spatial lateral deviation during swing phase of an isolated step with volitional hip circumduction. 49
Table 12. Subject specific IMU calculated and optical motion capture measured spatial lateral deviation during swing phase of an isolated step with volitional hip circumduction and rotation. 51
Table 13. Mean-error, confidence interval (95%) and coefficient of repeatability for all outcome variables during each task. 52
Table 14. Clinical significance determined by correlation coefficients and error analysis for all subjects and tasks. Cells highlighted in green show a significant agreement utilizing the outlined technique, while red shows a significant difference. 61
Table 15. Participant anthropometric and descriptive information for Study #2. 75
Table 16. Brace sizing guideline. 76
Table 17. Outcome measure description to characterize compensatory movements typically seen in the amputee population. 82
Table 18. Results from correlations of gait event detection using IMU algorithm compared to the timing from foot-switches on the bottom of feet. 83
Table 19. Summary of results of PRE and POST brace condition outcome measures. 84
Table 20. Mean, SD and ANOVA results summarizing spatial measures during clinical gait task 91

Introduction

In clinical settings, compensatory behaviours are quantified using visual observations and basic task evaluation (e.g. Can the patient complete the task?). Clinician abilities to detect aberrant movements are valuable however, limited when quantitative analysis is required (Ong, Hillman, & Robb, 2008). Clinical assessment tools are quick to administer but subject to a ceiling effect that can decrease the sensitivity of assessments. In contrast, incorporating wearable sensors to provide information about the complexities of compensation (sagittal and frontal plane) could be used to provide a more meaningful gait evaluation to guide clinical decision making in a manner that is efficient and simple to administer. Understanding the application of inertial measurement units (IMUs) to detect compensatory movements in alternate anatomical planes has the potential to support the application and implementation of these tools to a clinical setting.

The long-term objective of this work is to progress towards the development of a clinically relevant tool-kit that quantifies a patient's movement patterns using wearable inertial sensors. As the initial steps, the current thesis explores the ability of wearable inertial sensors to measure specific lower limb movement characteristics/compensations in healthy adults that are often associated with clinical gait characteristics. The first study provided a comparison of estimated spatial measurements derived from the linear acceleration values of the inertial measurement units against gold standard kinematic measurements. Subjects completed a series of isolated movement tasks focusing on movements in the frontal plane and those movements that may reveal themselves during compensatory movements. Comparing two measurement tools, IMU derived spatial estimates and motion capture spatial measurements, outlines the precision and repeatability of derived spatial measurements when compared to research-grade measurement tools. The second study utilized inertial measurement units to determine if derived spatial measurements from IMUs are sensitive to distinguish between normal and compensatory kinematic outcome measures. Individuals completed an obstacle avoidance task while normal walking patterns were manipulated with the use of a mechanical device (i.e. commercially available functional

knee brace) that limits the amount of attainable knee flexion. The study aimed to distinguish adopted crossing strategies employed by young healthy adults during this difficult task compared to baseline avoidance strategies.

Chapter 1: Literature Review

Throughout the day, humans depend on an adaptable walking pattern to move around in their surroundings. The robust nature of our movement allows us to navigate complex environments and avoid potential hazards; as we encounter hazards, we are able to maintain stability and continue with forward progression. When components of our control system are altered (e.g. pathology, mechanical perturbations, or injuries) the flexibility of our system is revealed. The loss of a functional joint via amputation is an example of a disruption to the intact locomotor system (Hill et al., 1997). Amputation is the surgical removal of a part of or an entire limb segment or extremity (Bowker, Michael, & American Academy of Orthopaedic Surgeons, 1992). The removal of a limb segment is associated with mechanical (e.g. functional joint) and sensory dysfunction (e.g. afferent information) related to normal movement patterns (Pitkin, 2010). Assessing movement patterns in the amputee population is important for assistive device prescription and rehabilitation intervention. Quantitative assessment can be difficult because each amputation is unique in its own way (e.g. level of amputation, individual abilities prior to amputation, length of residual limb, etc.). Among other difficulties, the dispersion of these individuals across geographical regions decreases the likelihood to capture of access to fully equipped clinics or laboratories for robust analysis of movement patterns. The accessibility to portable analysis tools is important for improving patient assessment. Wearable sensor systems have gained widespread usage in human movement analysis; however have been limited to sagittal plane movement description.

1.1 Prevalence of Amputee Population and Scope of the Rising Issue

In Canada, 5342 patients underwent lower limb amputation between 2006 and 2009; this dataset was limited to acquired loss of limb, therefore did not include pediatric or trauma related amputations (Kayssi, de Mestral, Forbes, & Roche-Nagle, 2016). Among these amputees; 29% were above-knee amputations, 65% below-knee, and 6% were ankle-foot or toe amputations and the main cause for these amputations were diabetic complications (81% of reported amputations) (Kayssi et al., 2016). In larger

populations, such as the United States, an estimated 185 000 persons undergo amputation of an extremity each year (upper or lower). A main cause for amputation are complications arising from diabetes mellitus or vascular disease. Due to the prevalence and rise of diabetes, the number of amputations associated with vascular complications continues to rise (Dillingham, Pezzin, & MacKenzie, 2002; Ziegler-Graham, MacKenzie, Ephraim, Travison, & Brookmeyer, 2008). Improvement of prescribed devices and surgical practice has improved care for those living with amputations; however, these improvements have not eliminated secondary complications associated within the amputee population.

In the United States, amputation associated complications are prevalent in the long-term prosthetic users (Ephraim, Wegener, MacKenzie, Dillingham, & Pezzin, 2005). These complications include phantom, residual, or intact limb pain, and lower back pain. For traumatic amputees, lower back pain was recorded as being equally comparable to phantom limb pain, and was more prevalent in above-knee amputees than in below-knee amputees (Kulkarni, Gaine, Buckley, Rankine, & Adams, 2005). Anatomical issues, such as unbalanced hypertrophy of the psoas muscle, can be a contributing factors in back pain. Likewise, biomechanical issues such as, decreased shock absorption (leading to increase impulse forces), slower walking speeds (Kulkarni et al., 2005) or greater transverse plane rotational excursions of the lumbar spine (Morgenroth et al., 2010) may contribute to pain or be maladaptive movements as a result of pain. These are also secondary issues to the amputation procedure and are in part, caused by our adaptation to the prosthetic device or due to our rehabilitation procedure. Accurate and robust movement analysis (i.e. motion capture, force plates, etc.) of individuals would be necessary in order to determine root cause of secondary pain. The utility of accurate and portable wearable gait analysis system prove to be valuable and satisfy many of these issues.

1.2 Factors Contributing to Gait Deviations in the Amputee Population

Current clinical examination of amputees involves a battery of functional tasks to assess the ability of the amputee with their new device. From the *Atlas of Limb Prosthetics: Surgical, Prosthetic, and Rehabilitation Principles* a full description of these tests are available (Bowker et al., 1992) (Table

1). The definition of a gait deviation is as any movement pattern that is different from that seen in a healthy intact population. Common deviations in amputee populations can be caused by: misalignment or dimensions of the prosthetic, restricted range of motion at a specific joint, muscular weakness or contractures, habits and fear of falling (Bowker et al., 1992).

Table 1. List of common amputee gait deviations, outline in the *Atlas of limb prosthetics: surgical, prosthetic, and rehabilitation principles* (Bowker et al., 1992)

Movement Deviations	Descriptions	Causes
Lateral Trunk Bend	• Leaning towards the prosthetic limb during stance phase	• Amputee may bend laterally due to weakness or pain indicators from their amputation or when an individual walks with an abducted gait
Wider Step Width	• Increased size of base of support with abduction at the hips	• Contracted hip abductors or insecurity in the individual's ability to maintain stability
Hip Circumduction During Swing	• Amputated limb follows a laterally curved trajectory during swing phase	• Insufficient knee flexion, knee lock (decreasing knee flexion), foot set in plantar flexion
Vaulting with Intact Limb	• Increase in height of the entire body by employing plantar flexion with the stance limb	• Insufficient knee flexion, knee lock (decreasing knee flexion), foot set in plantar flexion
Swing Phase Whips	• Medial and lateral movement of the toe immediately after toe-off	• Mainly due to alignment and functional features of the prosthetic
Foot Rotation at Heel Strike	• Lateral movement of the foot at heel strike	• Heel cushion issues with prosthetic foot
Foot Slap	• After heel strike the foot plantar flexes uncontrollably	• Plantar-flexion bumper doesn't provide enough friction

Uneven Heel Rise	• Uneven heel rise refers to the height the heel reaches after toe-off occurs while the knee flexes during early swing phase	• Insufficient heel rise:
		  ○ Prosthetic device knee lock
		• Excessive heel rise:
		  ○ Tension within the prosthetic device

Terminal Impact	• At heel strike the prosthetic limb enter full extension	• Fear of buckling, therefore conservative walking pattern adopted
Uneven Step Length	• Asymmetry exists between the limb step lengths	• Pain or insecurity with prosthetic • Restriction to hip range of motion
Exaggerated Lordosis	• Posterior lean of the trunk during stance phase	• Contractures to hip flexors • Weakness to hip extensors or abdominal muscles

Transtibial amputees may experience gait deviations due functional abilities of the individual after surgery. Bi-articular muscles, spanning two joints, are uniquely impacted by amputation. Two examples of these muscles are the rectus femoris in the quadriceps group and gastrocnemius in the posterior compartment of the shank. The rectus femoris muscle provides extension at the knee and supports hip flexion. The gastrocnemius plantar flexes the ankle and assists the hamstrings and popliteus during knee flexion (Moore, Dalley, & Agur, 2006). Damages to these muscles during amputation can effect strength at the knee and may cause change to their action or increase stiffness at the proximal joint (e.g. increase stiffness at the hip joint). In early stance, the transtibial amputees can experience excessive knee flexion due to inappropriate alignment of the socket and the prosthetic foot or inability produce sufficient knee stiffness. On the contrary, absent or decreased knee flexion during early stance may occur in response to weakness of the quadriceps muscle (Bowker et al., 1992). Commonly, the quadriceps muscle of the residual limb experiences muscle atrophy after below-knee amputation. Quadriceps atrophy decreases the ability of the knee extensors to balance external knee flexor moments during early stance and weight acceptance phases of the gait cycle (Powers, Rao, & Perry, 1998; Schmalz, Blumentritt, & Reimers, 2001). Adopting a stiff knee gait pattern is an adaptation that decreases the need for a powerful eccentric contraction by the quadriceps muscles during early stance (Powers et al., 1998).

Adaptations to pain and discomfort are also prevalent in amputees. To avoid pain, the amputee may adopt short steps with the affected limb or increase sway in the trunk during walking. At mid-stance, the timing of knee flexion can occur earlier or later than required and lower the height of the amputee during stance (Bowker et al., 1992). During swing phase, foot whips can occur in response to reduce knee flexion, movement control and prosthetic alignment for transtibial amputees. Foot whips occur when the prosthetic foot moves medially or laterally during swing and are associated with tripping in amputees during walking (Seymour, 2002). Movement pattern changes can occur in order to avoid discomfort at the intact joints or at the socket-limb interface.

1.3 Clinical Gait Analysis

Analysis of gait in clinical settings is focused on both primary and secondary gait deviations. Primary gait deviations are those that are directly associated with the impairment or change in control where secondary gait deviations can be considered adaptive or compensatory to primary deviations. When patient populations are severely impaired they often rely on such compensatory movements to travel among their environment (Winter, 1991). Lower limb amputees require the use of compensatory movements and assistive devices to improve their day-to-day lives (Pitkin, 2010). In special populations, such as amputees, movement patterns are associated with large bands of variability because the level of mechanical and neurological control is unique to each amputation. Local and confined laboratory space may limit the ability capture the variability necessary for comprehensive understanding of population-wide gait deviations. This pitfall to laboratory confined movement analysis decreases the potential for evidence based practice interventions and device manipulations in the final stages of rehabilitation (Geil, 2009). Limited access to quantitative tools has impacted amputee research as the majority of current studies with sufficient power mainly report self-reported qualitative results (Condie, Scott, & Treweek, 2006). The application of portable wearable devices for quantitative clinical gait assessment could improve the comprehension of movement pattern characterization for patient populations.

Essential to successful management and treatment is the identification of primary or secondary gait deviations. Quantifying meaningful measures of movement characteristics are also beneficial to patients with respect to evaluating rehabilitation and/or device fitting (Cole, Durham, & Ewins, 2008). The combination of therapist knowledge of concepts and current challenges and cost-effective tools can increase the impact of rehabilitation. In most cases, clinicians have a difficult time implementing some of the more advanced tools due to training and cost (Geil, 2009). There is a continuing need to develop new methods to quantify movement that will be more successfully translated to clinical practice.

Of the available tools used clinically, movement-screening tools are quick and inexpensive methods to evaluate mobility and movement characteristics of patient populations. These tools are subject

to rater-error and commonly report inaccuracies when assessing severe gait deviations or when accurate quantified measures are required (e.g. joint angle) (Del Pilar et al., 2016; Maathuis, van der Schans, van Iperen, Rietman, & Geertzen, 2005). With advancing technology in human movement science, accurate assessment of progression will help improve the quality of devices and rehabilitation interventions. In an optimal scenario, clinical use of 3D gait analysis to drive interventions would be common practice. Cost-effective tools provide a potential utility to meet these special requirements.

The Edinburgh Visual Gait Analysis (EVGS) and the Amputee Mobility Predictor (AMP) are two assessment tools used to evaluate patient populations who could have severe gait deviations. For experienced clinicians (10+ years), gait deviations are detectable with observational assessment and screening tools (Del Pilar et al., 2016). Read, Hazlewood, Hillman, Prescott, & Robb, (2002), developed the EVGS to evaluate joint and segment angles at gait events of children with cerebral palsy. Discrepancies across and within raters arises when quantitative (e.g. joint angle, lateral deviation) evaluation is required for the progress of rehabilitation or assistive devices (Del Pilar et al., 2016; Maathuis et al., 2005). Reasons for discrepancies across raters was due to joint angle estimation technique. A main difference in quality of results depends on the experience of the raters. Reliability is larger in those that had extensive gait analysis experience and when reviewing children with higher function (Del Pilar et al., 2016; Ong et al., 2008). The variable nature and difficulty of visually estimating quantitative measurements indicates the potential for unreliable examinations with visual gait analysis and movement screening. The Amputee Mobility Predictor evaluates amputee performance of 20 different tasks with and without their assistive devices to assess mobility (i.e. balance, turning, obstacle avoidance, and stairs) (Table 2) (Gailey et al., 2002). Clinicians are required to evaluate the walking pattern by analyzing certain characteristics, such as: foot height during swing, variable cadence, step length, and step width (Gailey et al., 2002). Quantitative assessment of these specific tasks can help provide fall prevention or identify patterns that are associated with increase fall risk (Barak, Wagenaar, & Holt, 2006). Clinicians evaluate the amputee's ability to complete the task with a 0-2 rating, where zero score

represents inability to complete and a two score represents completion without assistance and no visible interruptions (Table 3) (Gailey et al., 2002). Gailey et al., (2002) proved to have high inter-rater reliability ($r = 0.99$), the examiners were all taught concurrently in a single session, with one instructor. Therefore, the transfer of knowledge was not different between examiners. Additionally, the tested AMP tasks were not extensive assessments and need little description or quantitative output from the examiner. Inter-rater reliability is lower when tests are more extensive and include reporting of quantitative measures.

Table 2. Clinical tasks and objectives for Amputee Mobility Predictor (Gailey et al., 2002)

Item	Task
1	Sitting balance
2	Sitting reach
3	Chair to chair transfer
4	Arises from a chair
5	Attempts to arise from a chair
6	Immediate standing balance
7	Standing balance
8	Single-limb standing balance
9	Standing reach
10	Nudge test (balance reaction)
11	Eyes closed standing balance
12	Picking up objects off the floor
13	Sitting down
14	Initiation of gait
15	Step length and height
16	Step continuity
17	Turning
18	Variable cadence
19	Stepping over obstacle (4 inches or ~10 cm)
20	Stairs
21	Assistive device selection

Table 3. Example of task description from Amputee Mobility Predictor (Gailey et al., 2002)

Score	Description of Variable Cadence
	The examiner instructs the patient to walk a distance of 12ft fast as safely possible 4 times for a total of 48ft (14.63m). Speeds may vary from slow to fast and fast to slow, varying cadence. his task may also be completed with an assistive device although care must be taken that the patient is not extended beyond his/her capabilities.
0	The patient is unable to vary cadence in a controlled manner.
1	The patient asymmetrically increase his/her cadence in a controlled manner so that step length markedly differs between legs, and/or balance must be re-established with each step.
2	The patient symmetrically increases his/her cadence in a controlled manner so that step lengths are equal and balance is maintained.

Although these assessments require minimal time to administer (5-25 minutes) (Maathuis et al., 2005) and provide information in a simplistic manner, the inability to produce reliable assessments increases the concern of singularly relying on these elements for proper rehabilitation and assessment of interventions. The tests can also provide inaccurate or variable data about the patient's movement pattern, as seen with the reliability across examiners (Del Pilar et al., 2016; Maathuis et al., 2005; Ong et al., 2008). Associated with movement screening tools are patient reported outcome measures. Pain and subject perception influence these reported measures (Stevens-lapsley, Schenkman, & Dayton, 2011). Using tools to quantify movement patterns provide more objectivity compared to self-reporting scores that can be influence by perception.

1.3.1 The Gait Cycle

The gait cycle is defined as the period between two heel strikes of the ipsilateral limb (Winter, 1991). There are two distinct periods within the gait cycle, stance and swing (58-61% and 42-39% respectively) which indicate whether the foot is in contact with the ground or not and bounded by heel strike (HS) and toe-off (TO) gait events. Heel strike (HS) is the moment at which the foot touches the ground regardless of the anatomical landmark. In pathological gait, these events are also known as initial contact and final contact because events may not align with anatomical definitions. Final contact is the instance at which the limb finishes stance phase and enters swing phase. The use of experimental

equipment to determine heel strike is important for stride definition and step characteristics. Explicit definitions for these gait events help define the event for clinical practice. Measuring human movement with force plates, heel strike and toe-off are defined when the force signal passes the threshold of 20 N (Johnson, Buckley, Scally, & Elliott, 2007; Kiss, 2010; Zeni, Richards, & Higginson, 2008). When force plates are not used, kinematic data can define these gait events. When individuals are walking, the foot oscillates around the pelvis. The heel marker is maximally anterior to the pelvis cluster at heel strike. The toe marker is maximally posterior to the pelvis cluster at toe-off (Zeni et al., 2008). During over-ground walking, using the optoelectronic technique provided 98% of gait events within two data frames (0.0334 s) of the ground reaction force technique used in the same trial, providing an accurate determination of gait events with optoelectronic techniques (Zeni et al., 2008).

Spatial measures define gait characteristics using measurement of distance (e.g. meters, millimeters). Temporal measures of gait describe the movement pattern using measurement of time (e.g. seconds). A step is the distance between the same gait events on contralateral limbs. For example, the left step period is between the RHS of the right foot to the LHS of the left foot. Between these two events step length and step time are calculated. Stride time and distance defined by two consecutive gait events (e.g. RHS to RHS) of the ipsilateral limb. Stance time, double support time, single leg support and swing time are all temporal measures that add quantitative value to the amount of time individuals spend in certain support phases (Winter, 1991). Changes to spatiotemporal measurements can reveal control in support, forward progression, and the implications of impairment on walking patterns in patient population during level ground walking (e.g. asymmetrical gait, cadence/stride length relationship) (Hak, Van Dieën, et al., 2013). Obstacle avoidance threatens an individual's stability with increased risk of tripping by altering the clearance required during swing phase. Modifications to level ground walking kinematics are needed to overcome barriers in our walking path, and have been well documented for healthy (Austin, Garrett, & Bohannon, 1999; Huang, Lu, Chen, Wang, & Chou, 2008; Sparrow, Shinkfield, Chow, & Begg, 1996), elderly (H.-C. Chen, Ashton-Miller, Alexander, & Schultz, 1991; Hahn & Chou, 2004; Hill et al., 1999;

Lu, Chen, & Chen, 2006), and impaired walking conditions (Evangelopoulou, Twiste, & Buckley, 2016; a. H. Vrieling et al., 2007; A. H. Vrieling et al., 2009). Changes to spatiotemporal and kinematic outcome measures can probe control strategies for obstacle avoidance.

1.4 Inertial Measurement Units

The portable and lightweight nature of wearable sensors diversifies their application to a variety of scenarios. Extracting valuable information uses difficult computational techniques that limits the expansion of these measurement devices to widespread clinical use without proprietary software and expensive user subscriptions. These compact and lightweight tools provide extensive data relative to a fixed axes system built within the IMU. Some of these manufactured devices can stream data via Bluetooth devices or log with on-board storage. This allows data collection in any natural environment suitable for the participant and for long periods without constraining them to a laboratory setting.

Inertial Measurement Units (IMUs) are typically comprised of tri-axial accelerometers and gyroscopes. The inclusion of these three tools describes movement with 6 degrees of freedom. Current IMU systems typically act as strap down systems that each have their own local coordinate system (LCS) (Figure 1). The IMU components (i.e. accelerometers, gyroscopes) are commonly micro-machined electromechanical systems (MEMS). One example of an inertial measurement unit is the Shimmer3 IMU (Shimmer Sensing, Dublin, Ireland) (Figure 1).

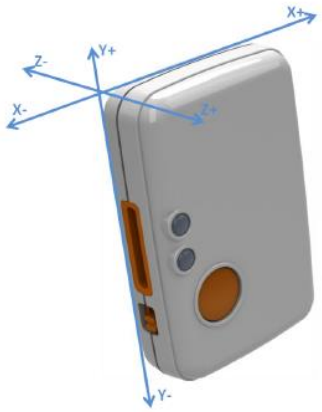

Figure 1. Shimmer3 Inertial Measurement Unit (Shimmer Sensing Inc., Dublin, Ireland) with factory calibrated local coordinate system denoted.

1.4.1 Accelerometer

Accelerometers measure linear acceleration along the three axes of the local coordinate system. Combination of gyroscope measurements and trigonometry techniques can help define acceleration in the global coordinate system and define vectors that exist along two different axes.

Mechanical accelerometers have a physical load suspended by a series and sequence of springs. When movement occurs, the displacement experienced by the load is proportional to the force acting on the load. Acceleration is calculated with the second law of motion:

$$F = m\vec{a} \qquad (1)$$

Solid-state accelerometers work using surface acoustic waves (SAW). The accelerometer consists of a long beam supported at one end and a mass at the other. When the beam bends there is a change in wave frequency produced by the beam and this change is proportional to acceleration.

MEMS accelerometers have piezo resistive, capacitive sensing, and piezoelectric components for movement sensing. MEMS have many advantages compared to traditional accelerometers making them the preferred method for today's devices:

- Lightweight and small
- Durable

- Long lasting battery life
- Inexpensive
- Portable devices
- Low maintenance (i.e. calibrating, repairs, etc.)

1.4.2 Gyroscope

A gyroscope is a tool used to measure the rate of angular velocity of an object in space. The number of axes available for the gyroscopes indicates how many orientation angles are measurable with the device. Current MEMS tools typically have tri-axial gyroscopes that can measure rotations about all three local axes. The positive advantages of these gyroscopes are similar to those mentioned regarding accelerometers.

Classic mechanical gyroscopes were tools that contained three rings that twisted about gimbals that defined the ring's axes of rotation. These mechanical gyroscopes had an object centered within the three rings. Angles between these adjacent rings output the amount of rotation that occurred when an object moved. The most accurate gyroscope mechanism uses optical devices, which use light interference to measure angular velocity. Current MEMS gyroscopes use the Coriolis Effect to measure angular rate movement. Vibrating elements within the device measure the Coriolis effect which records a force that is explained in a "frame of reference rotating at an angular velocity (ω), a mass (m) with a velocity (v) experience a force" (Woodman, 2007). The vibrating devices can range from a wheel to a tuning fork, or a mass that will vibrate along an axis, or MEMS technology.

1.5 Accuracy of Data Acquisition Using Inertial Measurement Units

Systematic errors due to calibration sequences, calculations or issues with model application during processing can affect entire data collection sessions. Random errors occur from uncontrollable events such as, electronic noise or marker flickering (Chiari, Della Croce, Leardini, & Cappozzo, 2005). Environmental factors and processing requirements are among the main sources of error when estimating position from IMU data.

1.5.1 Error Types in MEMS Accelerometers and Rate Gyroscopes

Error that affects MEMS devices comes from different sources categorized into two themes: random error and systematic error. Random error is unavoidable and unpredictable error sources that can affect the outcome of data but is typically small and captured with processing techniques or statistical models. Systematic errors are methodological, operator, or instrumental error sources (Evans, Goldie, & Hill, 1997; Litman, 2015). Methodological errors are present when proper protocol is not used during collection or processing of raw data. Operator errors occur when recorded signals are contaminated or erroneous due to equipment misuse. Instrumental error occurs when error is present due to errors in the instrumentation. These can be due to misaligned axes of sensors, invalid calibration, or errors to the calibration constants/formulas. Many hardware companies provide systematic process for calibrating and configuring devices to an acceptable range, however understanding the properties of the hardware is important for quality data collection. The environment where the MEMS device is used can also affect instrumental error. Ferrous metals and magnetic fields within vicinity of the IMU affect the accuracy and precision of the devices (Picerno, Cereatti, & Cappozzo, 2011). Picerno et al., (2011) compared the accuracy of inter and intra MEMS precision and found that calibration validity determines the accuracy of current MEMS performance. In addition to previous error, electromechanical systems are subject to both electrical and thermal-based noise contamination. Allowing sensors to adapt to their environment reduces temperature effects (de Pasquale & Somà, 2010). These errors can appear in different forms, such as:

- Constant bias
- Thermo-mechanical white noise
- Flicker noise/bias stability
- Temperature effects
- Calibration errors

Constant bias is an offset in the output signal (from the accelerometer or rate gyroscope) causing an error in integrated orientation data that grows quadratically over time (Woodman, 2007).

Thermo-mechanical white noise is the contamination of a signal output through the thermo-mechanical interference. Integration of the interfering white noise can cause random walk and increased variability of the position estimation (Woodman, 2007).

Flicker noise or *bias stability*, which is an effect of the *constant bias*, mentioned earlier. Flickering can cause the *constant bias* to change over time. This complicates the removal of bias which can affect integration techniques (Woodman, 2007).

Temperature effects are changes to the temperature of the recording device. These changes can also affect the *constant bias* mentioned earlier and complication the integration techniques (Woodman, 2007).

Calibration errors are bias errors calculated during calibration process. These are errors in scale factors, axes alignment and the calibration of the output value in correspondent to the raw voltage (Woodman, 2007).

Bias error present in the signal can appear as a drift of the signal. When drift is present, using integration techniques to obtain position/orientation data will cause error in the velocity and position estimations (Woodman, 2007) and correction factors need to be utilized.

1.5.2 Environmental influence on data quality

Structural elements of buildings (i.e. ferrous metals, elevators, etc.) influence IMU data and orientation estimation. An evaluation of the microelectronic measuring IMUs in both static and dynamics environments allows for an understanding of these potential affects. Karen Litman (2008) tested the effect of environmental and structural influence on Shimmer2r Inertial Measurement Units (Shimmer Sensing, Dublin, Ireland) data collection quality. Different conditions (i.e. rural and clinical settings, influence of large amount of ferrous metal and an acrylic box) compared the quality of raw IMU data (e.g. acceleration and gyroscope) and orientation information. For acrylic box measurements, a spirit level helped align the acrylic cube axis with gravity. A transformation of IMU signals to match the cube's axis aligned vertical acceleration with gravity vector and were considered accurate if percent error was within

predetermined 1% magnitude (Gill and O'Connor, 1997). Changes in environment (rural vs clinical) did not affect the static accelerometer and magnetometer data, but changes to location within a building did affect both magnetometer and accelerometer data. Magnetometer measurements were unaffected by location of the cube; however, changes to the location (inside or outside of acrylic cube) of the IMU influenced the accuracy of measured acceleration. IMU location inside the cube were not statistically significant when compared to the calibrated 1.0000 g, while outside the cube was statistically different. When located outside the cube difficulty balancing on the edges of the IMU casing could have caused variability of axis alignment compared to using the secured equipment within the box. The variability that may exist in the casing structure outside the box compared to the secured nature of the IMU in the box could have been the source of this error and statistical difference. In dynamic scenario, the angular velocity of the long axis (Y-axis) of the IMU was statistically different from the turntable values and could be due to the instability of the orientation used to measure the Y-axis angular velocity (Litman, 2015). Ferrous metals, often used in building materials, can affect data acquisition by a magnetometer in a clinical setting (de Vries, Veeger, Baten, & van der Helm, 2009). This is important when considering the implications of erroneous magnetometer data and sensor fusion algorithms. Shimmer Sensing Inc. (Dublin, Ireland) have incorporated both nine and six degrees-of-freedom on-board algorithms to determine the accuracy of recorded data (Madgwick, Harrison, & Vaidyanathan, 2011). Using six-degrees of freedom boycotts the influence of magnetometer data and relies on the accuracy of acquired acceleration and rate gyroscope data to predict the next iteration of the dataset. Careful setup needs to be attended to when securing IMU devices to align with anatomical reference frames and the development of inertial reference frames needs special consideration due to the errors that can occur with local frame data acquisition.

1.5.3 Estimating Spatial Measurements from Acceleration Data

The effects of low frequency noise during double integration acceleration data has been well documented (Pezzack, Norman, & Winter, 1977; Ryo Takeda et al., 2014; Thong, Woolfson, Crowe,

Hayes-Gill, & Jones, 2004; Thong, Woolfson, Crowe, Hayes-Gill, & Challis, 2002; D.A. Winter, 2009). IMU users have adopted several techniques to reduce the effect of low frequency noise when integrating rate gyroscope measure to calculate orientation of the IMU and accelerometer to obtain position data. These major steps when deriving position data from acceleration are as follows: (1) representing data in a known coordinate system, (2) divide into shorter and known segments of data, and (3) remove integration drift by updating segmented data to known values.

1.5.3.1 Creating Motor Task Coordinate Systems

Calibration processes create a local coordinate system (LCS) aligned to the casing of IMUs. The LCS may not align within axes of interest when the IMU moves and rotates during movement (i.e. anterior-posterior axis may be measuring vertical acceleration components). Magnetic north (magnetometers), the gravity vector (accelerometer) and their cross product can create a global coordinate system (GCS) (McGinnis & Perkins, 2012). Building material interference can cause large errors with respect to quality of magnetometer data collection; therefore representing these data based on orientation change from GCS may not be practicable. Securing IMUs with anatomical relevance allows a representation of the limb movement through space, often referred to as the anatomical frame (Cappozzo, Della Croce, Leardini, & Chiari, 2005). Representing data in these frames allows accurate intra- and inter-subject reliability and evaluating segment movements with respect to anatomical planes of movement. A task specific frame of reference (motor task coordinate system (MTCS)) is often recommended and used during human locomotion analysis (Cappozzo et al., 2005; Wu et al., 2002). An orthogonal coordinate system typically has the direction of progression as the anterior posterior axis (x-axis), vertical (y-axis), and medio-lateral axis (z-axis) during gait analysis (Cappozzo et al., 2005; Trojaniello, Cereatti, & Croce, 2014). A stride-by-stride analysis allows for flexible updating of the MTCS to align with gait progression. Using ankle-worn IMUs varying the swing time windows altered the estimated mean differences in direction of progression average of 15 degrees during healthy and mild-traumatic brain injury populations (Trojaniello et al., 2014). The estimation of foot displacement had more variation and larger discrepancies

across these different heading directions when compared to motion capture (Trojaniello et al., 2014). Using discrete periods of swing time and successive gait cycles may not be applicable to patients with altered swing phase characteristics or large gait deviations. An anatomical relevant frame of reference relying on principle component of sagittal plane angular velocity (Cain et al., 2016) also has the potential to be influenced by aberrant swing phase movement patterns. An alternative method could be to develop an inertial frame reference system that uses gravity and projects the x- and y-axis onto a horizontal plane (Cain et al., 2016; McGinnis & Perkins, 2012). The representation of accelerometer signals in a known orientation will allow calculable clinical gait parameters to evaluate movement patterns and behaviours in both healthy and pathological gait regardless of movement pattern.

1.5.3.2 Segmenting Data for Short Integration Intervals

Low frequency noise can introduce inaccuracies when integrating accelerometer signals (Pezzack et al., 1977; Thong et al., 2004). When quantifying segment angles using unilateral gyroscopes, Tong & Granat (1999) used two different drift correction methods. One technique was to reset the original inclination angle when drift occurs and another was to apply a high-pass filter with a 0.3 Hz cut-off. Correlations for joint angle and inclination angle were strong when compared across shank gyroscope locations ($r = 0.94$) and when compared to motion analysis system ($r > 0.90$). The application of high-pass filters and resetting to known values has proved to be valuable when integrating accelerometer signals. The goal of high pass filtering is to create a drift/noise free signal for integration over time to estimate position (Thong et al., 2004). The length of integration time and the noise-contaminated signals are the main influencers of inaccuracies associated with position estimation (Thong et al., 2004, 2002). Integration drift is assumed to act as a linear function during short integration intervals (Zok, Mazzà, & Della Croce, 2004). Difficulties exist when selecting the window of integration to capture human movement of interest. Efforts to increase the accuracy of position estimation focused on improving post-processing of accelerometer signals and techniques to outline accurate and shorter integration time-periods.

Segmenting the time series data into known time intervals, stride-by-stride analysis, is one common technique to reduce the integration interval. This segmentation technique divides larger time series data into smaller segments between two known points within the gait cycle. Although the foot continuously moves during gait, instances of assumed zero-velocity are advantageous because it allows for an assumed known removal of integration drift over the short time period (Kose, Cereatti, & Della Croce, 2012; Peruzzi, Della Croce, & Cereatti, 2011; Sabatini, Martelloni, Scapellato, & Cavallo, 2005; Trojaniello et al., 2014). Different definitions have described zero foot velocity: the entirety stance phase (Sabatini et al., 2005), discrete sections (Rebula, Ojeda, Adamczyk, & Kuo, 2013), and specific instances (Trojaniello et al., 2014) of the stance phase. Although the zero-velocity assumption is commonly used there are inaccuracies embedded into algorithms when this assumption is used. Derived velocity data from different optical motion capture locations revealed errors in stride length estimations when zero-velocity was assumed (Peruzzi et al., 2011). Depending participant's gait speed and the location of the movement tracking device there are differences in stride length estimation (from -0.07 to -3.3 percent differences) and timing of minimum velocity (31% - 57% stance phase duration) (Peruzzi et al., 2011). Errors associated with derivation may influence error in outcome measure comparison (Peruzzi et al., 2011). Understanding the influence of these differences between measures for clinical utility is unclear. Incorporating these limitations to the evaluation of IMU spatial accuracy is important for a wholesome understanding of the limitations to these integrated estimations.

1.5.3.3 Removing Noise and Drift Contamination

Removing signal noise has underwent phases of filtering techniques. High-pass filters are commonly used to remove low frequency noise with a range of frequency cut-offs from 0.025 – 0.1 Hz (Boonstra et al., 2006; Kose et al., 2012; Trojaniello et al., 2014). The Optimally Filtered Direct and Reverse Integration (OFDRI), an expansion to the Optimal Filtered Integration (OFI) technique, filters data with a series of high-pass frequency cut-off values to determine an optimal cut-off frequency. The cut-off frequency that produces minimum error in the final known data point, after high-pass filtering and

single integration, is deemed the optimal cut-off frequency (Cereatti, Trojaniello, & Croce, 2015; Kose et al., 2012; Trojaniello et al., 2014; Zok et al., 2004). A weighted average between a forward and reverse integrated acceleration is used to calculate a drift-free velocity estimation (Kose et al., 2012; Trojaniello et al., 2014). Without correcting for time to peak amplitude or the weighted function, this technique can attenuate peaks of interest, which ultimately affect the estimation of positon. Implication of signal attenuation could alter maxima when time series data is not symmetrical. Assuming linear drift is unaffected by temporal alignment and corrects velocity measures creating a drift-free estimation. Rebula, Ojeda, Adamczyk, & Kuo, (2013) assumed linear drift over short time periods to remove drift from the velocity estimate over time. This simpler method assumes the difference between the beginning and final integration accumulates to the amount of drift during the integration process. Results indicated comparable estimations of stride length (within 1% error) and estimated directional change in stride variability (RMS within 4% for step width and length variability) when walking with their eyes closed (Rebula et al., 2013). A variety of drift removal and estimation techniques corrects estimations of velocity and position from acceleration. Error prone estimations may be inevitable but understanding the implications and assumptions surrounding each technique will mitigate compounding error when extracting conclusions.

1.6 Application to Human Movement Analysis

Inertial measurement units (IMUs) are gaining momentum as a motion-measuring device because their lightweight and cost-effective nature. Onboard sensor fusion exists with these devices providing valuable and accurate information about the sensor's local reference frame (Faragher, 2012; Madgwick, Harrison, & Vaidyanathan, 2011; Mazza, Donati, Mccamley, Picerno, & Cappozzo, 2012).

Inertial measurement units (IMUs) can accurately detect and measure gait events and stride definitions when compared to instrumented gait mats (Trojaniello et al., 2014). IMU data has successfully defined gait event definitions in amputee population (Selles, Formanoy, Bussmann, Janssens, & Stam, 2005). The pattern of foot to ground contact is unique in special populations (e.g. amputee gait).

Amputations at the ankle or higher can remove or limit ankle articulations. In these scenarios, initial contact spatially coincides with final contact and phases such as flat foot, heel rocker and heel-off are missing. Due to these changes, gait event algorithm development should be applicable to the population of interest rather than applying general heuristics across all populations. Combination of the gyroscope and accelerometers used for healthy individuals has proved to be robust enough for healthy populations as well as some neurodegenerative populations when detecting initial and final contact events (Trojaniello et al., 2014).

In the amputee population, spatiotemporal and kinematic gait deviations are not restricted to the sagittal plane. Significant gait deviations can occur in the frontal plane (e.g. lateral foot deviation) during the swing phase of the gait cycle. When foot clearance is challenged (i.e. stepping up onto a raised surface or over an obstacle), these deviations become a major contributor to clearance values (Hill et al., 1997). Obstacle avoidance occurs many times in a single day and serves as a valuable task when evaluating movement patterns. When crossing obstacles complex multiplane compensations maintain stability and increase limb movement, specifically when normal movements are unattainable, and therefore is sensitive to reveal aberrant movement patterns when mobility deficiencies are present.

1.7 Thesis Objectives and Rationale

The first objective of this thesis is ***to determine the agreement between spatial measures using cost-effective wearable sensors and a motion capture system when calculating kinematic outcome measures.*** These kinematic outcome measures quantify compensatory movements (in both frontal and sagittal planes) during simple isolated movement tasks. A key focus is to determine the ability in revealing specific frontal plane movements relevant to gait compensations tested in healthy adults but simulate those movements particular to the use of prosthetics (e.g. lateral foot deviations).

The second objective, of this thesis will be focused on the use of wearable sensors ***to investigate compensatory movement patterns in the during normal and restricted limb movement conditions during an obstacle avoidance task***. Principally the objective is to determine if the devices can detect

kinematic characteristics of provoked compensatory movements. Subsequently, an objective will be to outline variability of temporal and spatial outcome measures to provide an initial indication of the potential to reveal variability of compensatory strategies. In the current study, healthy adults will walk under different task conditions with and without a unilateral limb constraint to evoke compensatory behavior in response to simulations of the movement challenges imposed by amputation and prosthetic use. The simulation of a movement restriction seen in the amputee population (e.g. decreased knee range of motion) applied to the healthy population will serve as a first attempt to differentiate between normative and compensatory movement patterns necessary for future evaluation in an amputee population. This information can help support defining gait deviations and development of a tool-kit available for future clinical use.

Chapter 2: Investigating the Agreeability between Inertial Measurement Units and 3D Motion Capture during Isolated Movement Tasks

2.1 Spatially Derived Estimates (IMU) compared to Gold Standard Measures

Current position estimations from IMU data are comparable to gold standard measurements, however results are confounded with assumptions underlying accuracy claims. Inertial measurement units (IMU) analyze human movement in a spatial manner. During self-selected level-ground walking, vertical center of mass movement derived from inertial measurement data in a global reference frame compared to gold standard measurements. Mean vertical displacement error between IMU and motion-capture (MC) data was -0.047 ± .060 m across all subjects, with a range of -0.128 – 0.06 m across subjects (Esser, Dawes, Collett, & Howells, 2009). Accuracy of COM vertical displacement is improve when velocity and positional data is de-drifted. De-drifting requires the last temporally known integrated value which is typically assumed zero and applies zero-velocity updating technique (ZUPT) to de-drift between these time points. Utilizing the ZUPT can affect stride lengths estimations by -0.3% error for foot worn IMUs and rises to -3.3% error for shank worn IMUs (Peruzzi et al., 2011). Evaluation of the ZUPT was completed on derived motion capture data and in a global frame of reference (Peruzzi et al., 2011). Stride length estimations are strong when the ZUPT and optimal filtering techniques are applied. Stride length errors from a single hip worn IMU compared to MC are 0.009 ± 0.017 m for the right leg (ipsilateral to the IMU) and -0.008 ± 0.016 m for the left leg (contralateral side). These derived stride lengths undergo correction methods to reduce the influence of pelvic rotation on hip worn IMUs (Kose et al., 2012). IMU sensors placed bilaterally on the feet (Rebula et al., 2013) or lower shank segments (Trojaniello et al., 2014) can remove the post-processing and assumptions required from a single hip mounted. Mean stride length parameters agreed within 1% error when comparing estimations from foot mounted IMU to a portable MC device (Rebula et al., 2013). Mean error of stride length errors range from 1-3% stride length for five different populations when comparing shank mounted IMUs and instrumented walkways (e.g.

healthy, elderly, hemiparetic, parkinsonian, and choreic) (Trojaniello et al., 2014). Reporting mean error can decrease the perceived error between two devices, however range of data from provided Bland-Altman plots (Table 4) has low variability error estimates (less than ±5 cm) (Trojaniello et al., 2014). Vertical displacement of the COM during walking was well defined using IMU data (Esser et al., 2009). Using similar data vertical displacement of the foot can be recorded using ankle or foot mounted IMUs. In elderly and Parkinson disease patients, differences between MC and IMU vertical estimates were not significantly different during over ground walking or obstacle crossing tasks (Trojaniello, Cereatti, & Della Croce, 2015). The variability of errors comparing MC and IMU is greater than stride length data reported early using identical methods (vertical mean error: elderly (1 ± 10 mm), PD (2 ± 20 mm)) indicating changes to movement patterns or larger amounts of variability. General distinction of movement patterns was the focus and precision of the devices were not discussed. Research revolves around the application and utility of these devices during walking and balance tasks. Little research focuses on the precision between the gold standard MC and the spatial estimations from IMU data with focus on the movements in the frontal plane and excursion through multiple planes of motion.

Table 4. Mean error (SD) reported by Trojaniello et al., (2015) for step length estimates in four different populations using OFDRI techniques to de-drift, calculate, compare spatial measurements from IMUs, and pressure sensor mat.

Population	Mean Error (m)	+2 SD (m)	- 2 SD (m)
Elderly	-0.001	0.043	-0.046
Hemiparetic	0.008	0.062	-0.046
Parkinson	-0.002	0.043	-0.047
Choeric	0.01	0.077	-0.58

2.1.1 Other applications of IMU and their Clinical Significance

Instrumented gait analysis using wearable sensors may support clinical decision-making because of ceiling effects and inaccuracies associated with movement screening tools. Many wearable toolkits for clinical evaluation are on the market (Roetenberg, Luinge, & Slycke, 2009) and proprietary to laboratory use (Cutti et al., 2010; Yang, Zheng, Wang, McClean, & Newell, 2012). Evaluation outside the developer centers test the reliability across environmental settings and end-user errors. Leardini et al., (2014) compared Riablo™ (CoRehab, Trento, Italy) to optical motion capture to evaluate the reliability knee and

thorax angles during clinical tasks. Mean error between devices falls within clinical acceptable range (±5º) for knee flexion and extension but extends to the limits of clinical acceptance range for lunges and squatting. Although mean error falls within the acceptable boundaries maximum error sizes consistently fall outside the acceptable range. Similar results were reported for thorax angles during functional tasks (lunges, squatting). Bolink et al., (2016) studied frontal and sagittal pelvis angles during four different clinical tasks (gait, sit-to-stand, and stepping onto a block) using IMU and optical motion capture. Frontal and sagittal plane pelvis angles have strong agreement for correlation measures (ICC > .90, r > .85). For the majority of individuals and clinical tasks reported mean errors are within the suggested clinical agreement (error less than ± 5º). IMU outcome measures have reported spatiotemporal and trunk and pelvis range of motion differences between healthy and OA populations during these clinical outcome measures (Bolink, Van Laarhoven, Lipperts, Heyligers, & Grimm, 2012). Using the combination of accelerometer and gyroscope signals two dimensional sagittal plane thorax, pelvis and upper leg angles correlate highly to the optical motion capture system (r > .9) and indicated low RMS values for segment angle error (RMS error < 3.9º) (Boonstra et al., 2006). Evaluating lower limb joint angles with IMUs in both the sagittal and frontal planes also report high correlation values (Takeda, Tadano, Natorigawa, Todoh, & Yoshinari, 2009a). Measurement tools have high agreement for hip and knee flexion-extension joint angles (r > .85) but variability between subjects influences the agreement for hip abduction and adduction (r = .89, r = .62, r = .64). Error in hip abduction-adduction measures were attributed to error in the internal-external rotation at the hip. Reported measurement error magnitudes are borderline clinically acceptable when evaluating measurement error (Hip F-E (6.57º), Hip Ab-Ad (3.30º), Knee F-E (4.65º)), however standard deviations and variability of individual trials are not expressed which limits our ability to make claims about clinical significance using an error analysis (Takeda, Tadano, Natorigawa, Todoh, & Yoshinari, 2009b). The application of more IMUs to a segment increases the available information for segment angles. A 3D reconstruction of foot angles using four IMUs attached to the foot produced significant detail about foot orientation (Rouhani, Favre, Crevoisier, & Aminian, 2012). Although mean errors for all subjects and gait cycles was clinically acceptable, according to correlation strength, there

were no variability and subject specific data reported. Nonetheless, IMUs were on average reporting correlations values (r = .93), which are considered clinically significant. In a clinical setting joint angle descriptions were able to distinguish between ankle osteoarthritis groups and healthy groups for joint range of motion in all movements of interest (Rouhani et al., 2012). This section reflects upon some of the current validation and reliability studies using IMUs to detect specific kinematics during clinical tasks. Strong correlation values are reported (r > .85) but most studies do not report measurement error as a reliability or validation tool. Determination of tool accuracy incorporating error measurement encompasses random and systematic error and allows for an interpretable understanding of accuracy for clinicians (Vaz, Falkmer, Passmore, Parsons, & Andreou, 2013). Understanding the error associated with wearable tool implementation help build the base knowledge for these devices and their potential application to clinical settings. Initiating the investigation of wearable sensor's ability to discriminate movement patterns is a second pillar for these devices to gain momentum and to excel our knowledge about advantages and disadvantages in these toolkits (Bonato, 2005). Past research and application of tools suggest operational acceptance in a clinical setting.

2.2 Rationale, Objective, and Hypothesis

To advance use of IMUs to assess human movement in clinical settings there needs to be continued work to determine the agreement between gold-standard measures of motion and spatially derived IMU movement tracking. While proprietary wearable systems (e.g. APDM, XSENS) have undergone the rigor of reliability and validity studies within their respective tasks. The objective of this first study is to understand the agreement between spatially derived movements, measured with commercially available and cost-effective IMUs, in contrast to a gold standard measurement (optical motion capture). Contrasting the peak deviation during a series of isolated movements will explore the differences between these two devices. To analyze this objective:

(1) It is hypothesized that spatially derived (IMU) and spatially measured (optical motion system) movements will be highly correlated (r>0.8) for all peak amplitudes calculated.

(2) It is hypothesized that mean error between devices will have high agreement. Specifically high agreement will be determined if no significant error bias exists, a 95% confidence interval encompasses the line of equality (zero error), and amount of error variability will be low, the coefficient of repeatability (CR) of all errors measured will fall within the a priori set limits of agreement (±18 mm).

Accepting these hypotheses, would suggest that agreement between the two devices is acceptable and spatially derived movements would be statistically accurate compared to optical motion capture.

2.3 Methods

2.3.1 Participants

Six young healthy adults, absent of neurological or mechanical dysfunction, were recruited for this study. University of Waterloo Office of Research and Ethics reviewed the study protocol. All subjects provided informed consent prior to participation. Participant anthropometric data (SD) was collected and summarized, mean age 27.33 (1.2) years, height 1.70 (0.04) m, weight 75.92 (12.42) kg.

2.3.2 Instrumentation

2.3.2.1 Motion Capture

Participants were instrumented with motion capture and inertial measurement units. Six Certus Optotrak motion capture sensors (NDI, Waterloo, Ontario) recorded movement of rigid body attached to the lower leg, 4 cm above the lateral malleolus (Figure 2), during six isolated movement tasks. Custom lower limb rigid bodies accommodated a single Shimmer3 IMU fastened directly onto the rigid body. Hypafix (BSN Medical Canada, Laval, Quebec), double sided tape, and a hook and loop band were used to fasten the rigid body and IMU to the participant's lower shank. Motion capture collection frequency was 100 Hz and global axis system was created so the z-axis was mediolateral, y-axis vertical, and x-axis anterior-posterior.

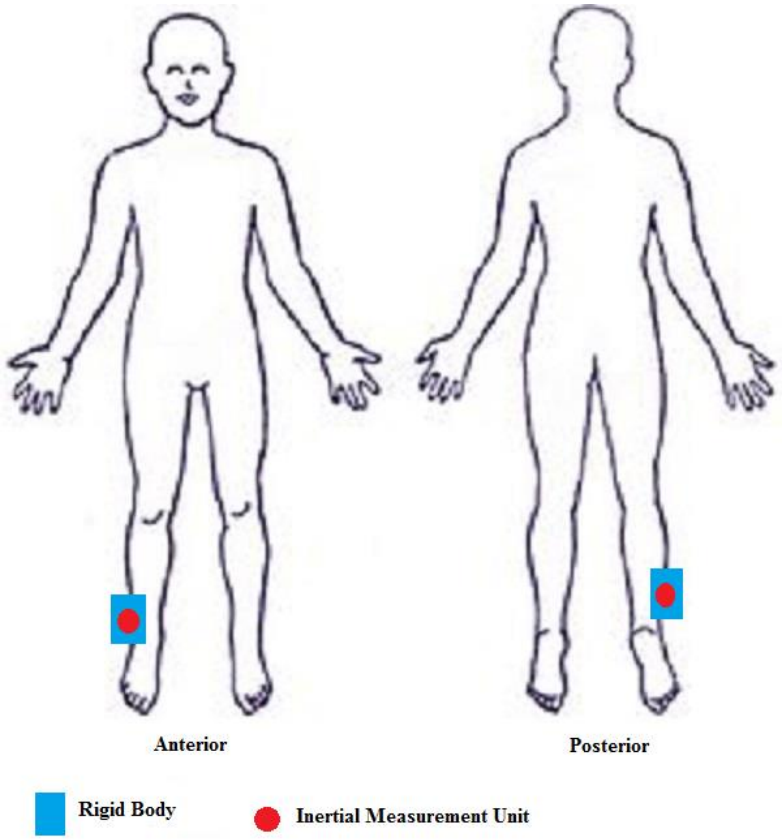

Figure 2. Rigid body and IMU placement on lower limb (4 cm above lateral malleolus). The rigid body is instrumented with four smart IRED markers and setup to allow IMU attachment over rigid body construction.

2.3.2.2 Inertial Measurement Unit

Shimmer3 inertial measurement unit (Shimmer Sensing Inc., Dublin, Ireland) recorded movement during six isolated tasks. The Shimmer IMU was fixed to the center of the rigid body. All calibration sequences followed Shimmer Sensing instructions and utilizes an API LabVIEW (NI, Texas, U.S.A.) program 9-Degrees of Freedom (Shimmer Sensing Inc., Dublin, Ireland) and the local coordinate system orientation is outlined in Figure 1. All configuration settings were completed using proprietary software ConsensysPRO (Shimmer Sensing Inc., Dublin, Ireland). Shimmer3 IMU were configured with both low-noise (±2g) and wide-range (±4g) accelerometers, gyroscope (±1000 degrees per second), magnetometer (1.3 kPa), and timestamped with UNIX clock time. Shimmer3 IMU units streamed via Bluetooth for visual purposes and data for processing was logged onto a 32 GB SD card for data analysis purposes to

avoid missing data points lost during streaming. IMU collection frequency was set to a priori available frequency, determined by Shimmer Sensing Inc., at 102.4 Hz.

2.3.2.3 Data Synchronization

A sync pulse output from NDI First Principles Motion Capture Software (NDI, Waterloo, Ontario, Canada) synchronized motion capture and Shimmer3 IMU units. A 9-pin output cable sends a step pulse from the First Principles software to the resistance amplifier sensor of a Shimmer3 Bridge Amplifier+ Unit (Shimmer Sensing, Dublin, Ireland), via a 3.5 mm AUX cable, that was sitting on a table. Sync pulse had a magnitude of 5V and indicated the start and end of each collected trial. UNIX timestamps from both IMUs aligned Shimmer3 IMU data and using the sync pulse data was windowed into collection trials aligning with motion capture.

2.3.3 Collection Protocol

During data collection, participants completed twenty-five repetitions of six different movement patterns (Figure 3). The right limb completed all movement patterns and participants were provided with ample rest time. Isolated movement patterns were selected to probe the accuracy of spatial measures along a single axis (e.g. maximum A/P deviation, etc.) and represent a deviated movement that amputees may exhibit. Seven different outcome measures calculated from all isolated movement patterns (Table 5).

Task #1 - Sagittal plane hip ROM - 5 repetitions	**Task #2** - Frontal plane hip ROM - 5 repetitions	**Task #3** - Hip and knee flexion -5 repetitions	**Task #4** - Isolated knee flexion - 5 repetitions	**Task #5** - Isolated stepping with volitional hip circumduction - 5 repetitions	**Task #6** - Isolated stepping with volitional hip circumduction and rotation - 5 repetitions
Repeat randomized order 5x (25 repetitions/task)					

Figure 3. Block diagram outlining collection sequence for Study #1 with all 6 tasks.

At the beginning of each task, subjects maintained 2 seconds of quiet standing required for IMU initial orientation. Collected trials included five repetitions of each movement, starting and ending with a stationary anatomical position. Participants freely selected speed of movement for each task and

repetition. Prior to collections, specific instructions were explained for each task and movement practice was completed. During collection, subject-to-subject and trial-to-trial variability was captured by allowing subjects to naturally vary their movement patterns.

Task 1 & 2: Hip Range of Motion

Sagittal plane hip range of motion (hip flexion-extension) evaluated anterior and posterior deviation from rest (Figure 4). Frontal plane hip range of motion (abduction-adduction) tested the lateral deviation from rest (Figure 5). Hip ROM tests will record the maximum amplitude within the plane of movement (i.e. maximum anterior deviation of the foot when hip flexion occurs) starting from the zero-velocity instance.

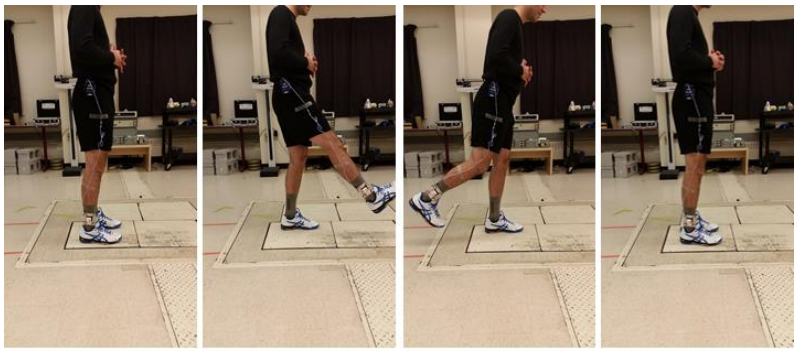

Figure 4. Sequence of movements for Task 1. Subject complete sagittal plane hip range of motion, starting at and returning to rest.

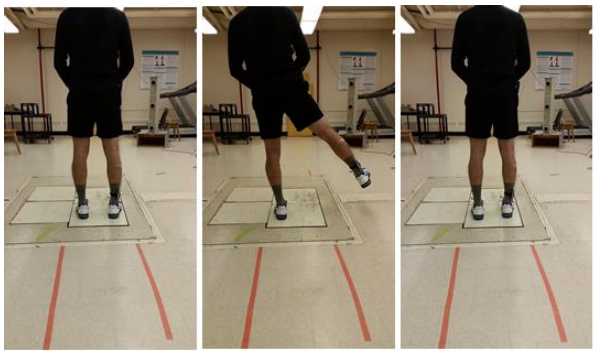

Figure 5. Sequence of movement for Task 2. Subject start at rest, hip abduction laterally deviates the leg, and they return to resting position.

Task 3: Vertical Translation/Hip and Knee Flexion Task

To assess vertical deviation from rest, subjects lifted their limb in a standing position (knee flexion and hip flexion) (Figure 6). This movement assessed height displacement (maximum elevation) during higher than normal trajectories in the vertical direction and replicated the movement of the lead limb clearing obstacles.

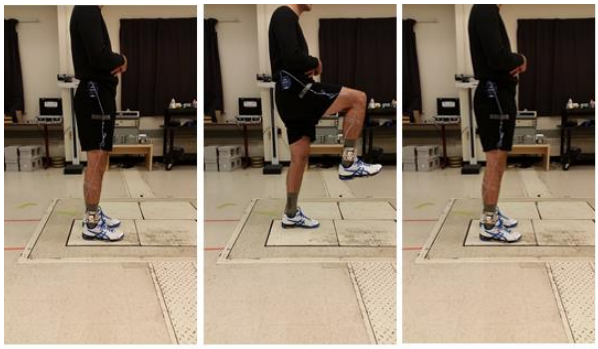

Figure 6. Sequence of movements for Task 3. Subjects start at rest, lift their knee towards their chest (hip and knee flexion) and return to rest.

Task 4: Heel Rise/Isolated Knee Flexion

To assess differences seen in heel rising measurements, subjects flexed their knee during standing (Figure 7). This assessed the ability of the IMU to measure height of the foot during knee flexion (maximum elevation) to replicate the height of the trailing limb during obstacle clearance.

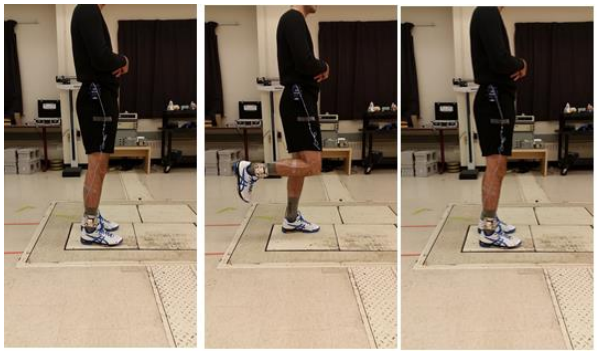

Figure 7. Sequence of movements for Task 4. Subjects start at rest, flex their knee and return to resting position.

Task 5: Stepping with Lateral Deviation of Foot (hip circumduction)

Volitional lateral deviations of the foot during swing phase during a single step with the right leg replicates hip circumduction (peak lateral deviation). The participants will begin by standing with their right foot slightly behind their left leg. When instructed, subjects will step with their right leg and include volitional hip circumduction (Figure 8).

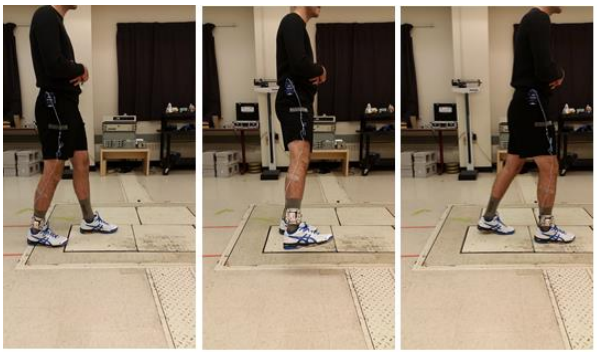

Figure 8. Sequence of movements for task 5. Subjects start in a staggered foot position (left in front of right), complete a single isolated step and volitionally induce hip circumduction.

Task 6: Stepping with Foot Whips (hip circumduction and rotation)

Clinically, foot whips characteristics are internal or external rotation of the foot during swing phase. Foot whips are defined as medial or lateral whip of the foot at toe-off (Bowker et al., 1992). Subjects mimic a foot whip (external transverse rotation of the IMU) during their stepping pattern with volitional hip circumduction and rotation and peak lateral deviation is calculated. Stepping instructions will be similar to those in the *Stepping with Lateral Deviation of Foot* task. Researchers visually confirmed the presence of foot whips; trials without adequate attempts were not be included (Figure 9).

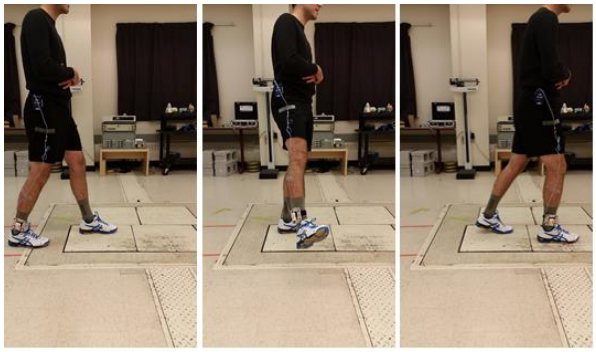

Figure 9. Sequence of movements for task 6. Subjects start in a staggered foot position (left in front of right), complete a single step and volitionally induce hip circumduction and hip rotation.

Table 5. Summary and definition of each outcome variable.

Task	Description of Outcome Measure
Sagittal Plane Hip ROM	Maximum anterior/posterior displacement
Frontal Plane Hip ROM	Maximum abduction displacement
Hip and Knee Flexion	Maximum elevation of ankle joint from vertical translation
Isolated Knee Flexion	Maximum elevation of ankle joint from knee flexion
Step with Lateral Foot Deviation	Peak lateral foot movement during stepping
Step with Foot Whips	Peak lateral foot movement during stepping with foot whips

2.3.4 Data Analysis

2.3.4.1 Motion Capture

Motion capture data was processed using custom Matlab script (Mathworks Inc., MA, USA). Missing data points were interpolated with a third order cubic spline (Heijnen, Muir, & Rietdyk, 2012). Missing data interpolation was limited to 10 data points or 200 ms of data (Howarth & Callaghan, 2010). A dual pass 2nd order Butterworth low-pass filter removed high frequency noise. Low-pass frequency cut-off was determined using previous literature and was set at 10 Hz (Heijnen et al., 2012; Winter, 2009). Outcome measures are the maximum deviation from rest and in the global coordinate system.

2.3.4.2 Inertial Measurement Units

Collection trials completed by all individuals were accepted or rejected during analysis procedure. An on-board SD card logged all movement trials. The first step to data analysis was to window all IMU recorded data into the appropriate collection trials. Using a threshold crossing method, when sync pulse data crossed a 2.5 V threshold (half the magnitude of the sync pulse) with a positive slope, indicated collection start, and with a negative slope, indicated collection end. These time markers allowed temporal alignment for all IMUs and data was windowed to correspond to the manually recorded collection details, each windowed time period included five repetitions of a single movement pattern.

Accelerometer signals are rotated into an inertial frame that is relative to gravity following techniques used by McGinnis & Perkins (2012) and Cain et al., (2016). Initial orientation was determined during the first 0.5 seconds of each collection trial. Normalized magnitude of acceleration during the first 0.5 seconds to determine the vertical vector of our initial orientation, aligned with gravity during quiet standing. In this phase, the accelerometer acts as an inclinometer to determine the orientation and relation to a global frame of reference (Cain et al., 2016).

$$\hat{Y}_{VERT} = \frac{\vec{a}_{standing}}{\sqrt{\vec{a}_{standing} \cdot \vec{a}_{standing}}} \quad (2)$$

World aligned Y-axis is a cross product of the gravity vector and a projection of a temporary anterior-posterior axis (Cain et al., 2016). The anterior-posterior axis is redefined to confirm orthogonality.

$$\hat{Z}_{M/L} = \frac{\hat{Y}_{VERT} \times \begin{bmatrix}1\\0\\0\end{bmatrix}}{norm\,(\hat{Y}_{VERT} \times \begin{bmatrix}1\\0\\0\end{bmatrix})} \quad (3)$$

$$\hat{X}_{A/P} = \hat{Z}_{M/L} \times \hat{Y}_{VERT} \quad (4)$$

All movement completed by participant is recorded by a local IMU reference frame and rotated into a inertial frame (Cain et al., 2016; McGinnis & Perkins, 2012). Rotations begin at the initial orientation and continue for the duration of the trial. Direction cosine matrix (DCM) is a resultant of an adaptation to integrating the angular velocity recorded at LCS level developed by McGinnis & Perkins (2012) and applied by Cain et al., (2016). The adaptation allows for numerical approximation of the change in orientation after integrating the angular velocity. The resultant is a time varying DCM that describes the movement of the local coordinate system (Λ). Rotating the accelerometer signals by their DCM will represent data in a task reference frame, which aligns gravity vertically and projects two horizontal vectors for ML and AP (McGinnis & Perkins, 2012). After inertial frame was established, gravity was removed algebraically.

$$\vec{a}_{inertial\ frame} = \Lambda\vec{a}_{LCS} \quad (5)$$

$$\vec{a}_{VERT} = \vec{a}_{VERT} - 9.81 \quad (6)$$

Data was dual=pass filtered with a 2nd order Butterworth filter with a pass-band between 0.05 – 18 Hz (Trojaniello et al., 2014; Winter, 2009). Thresholds applied to inertial frame magnitude acceleration data and gyroscope data to windowed repetitions for integration. When magnitude of acceleration was larger than 0.065 m/s^2 (Kingma, 2005) and angular velocity was larger than 0.17 rads/s (Hall & McCloskey, 1983) for greater than 200 ms, intentional human movement occurred. These threshold crossings sectioned SD logged IMU data into repetitions and periods for integration. Sensitivity of movement detection is a disadvantage of generic threshold applications. When resultant accelerometer and gyroscope data was below threshold during known movement pattern (e.g. at peak deviation), the repetition was removed from analysis.

$$\vec{a}_{mag} = \sqrt{\vec{a}_{LCS\,X} + \vec{a}_{LCS\,Y} + \vec{a}_{LCS\,Z}} \quad (7)$$

$$\vec{a}\left(\vec{a}_{mag} < 0.065\ \&\&\ \vec{\omega}_{mag} < 0.17\right) = 0 \quad (8)$$

Drift contaminated velocity was estimated by integrating inertial frame acceleration values using trapezoidal integration between threshold crossings (Pezzack et al., 1977). During short periods of integration, drift is assumed to be linear, therefore linear drift removal was used to remove drift effects and correct velocity estimation (Rebula et al., 2013).

$$\vec{v}_{drift\ contaminted}(t) \approx \sum_{t=1}^{N} \Delta t \left(\frac{\vec{a}_{t+1} + \vec{a}_t}{2}\right) \quad (9)$$

$$\vec{v}_{drift} \approx \left(\frac{\vec{v}_{end} + \vec{v}_1}{2}\right)\Delta t \quad (10)$$

$$\vec{v}_{corrected} \approx \vec{v}_{drift\ contaminted} - \vec{v}_{drift} \quad (11)$$

Integrating the corrected ("drift-free") velocity estimated position. After each repetition, the foot returned to the ground. Max deviation occurred when the foot was moving, not during static ground recording.

Difference between maximum flight period and position at rest (beginning of repetition) is the deviation during each isolated movement pattern. During isolated stepping, step width was considered negligible and therefore swing deviation was measured from initial rest not ending rest period (Mariani et al., 2010).

2.3.5 Outcome Measures

One outcome measure during each isolated movement pattern and each movement along a single global axis is calculated. During Task 1: Sagittal Plane Hip ROM peak anterior and posterior deviation from rest were derived.

$$AP_{ant} = \max(\vec{p}_x(1,2,3 \dots n) - \vec{p}_x(1)) \quad (12)$$

$$AP_{pos} = \min(\vec{p}_x(1,2,3 \dots n) - \vec{p}_x(1)) \quad (13)$$

Peak lateral deviation is the main outcome of interest during Task 2, Task 5, and Task 6, which probed the accuracy of lateral deviation while the foot moves through different motions.

$$ML_{max} = \max(\vec{p}_z(1,2,3 \dots n) - \vec{p}_z(1)) \quad (14)$$

Peak vertical deviation of the foot from rest is the main outcome measure in Task 3 and Task 4. Each movement pattern evaluated vertical deviation with emphasis on different movement patterns (high versus low rotation). The trailing limb primarily relies on knee flexion (Task 4) to elevate over obstacles while the lead limb primarily relies on hip flexion (Task 3).

$$VERT_{max} = \max\left(\vec{p}_y(1,2,3 \dots n) - \vec{p}_y(1)\right) \quad (15)$$

2.3.6 Statistical Analysis

All statistical calculations and tests were performed using SPSS Statistics (IBM Corporation, Armonk, New York, United States). Concurrent validity of IMU spatial estimates and optical motion capture is evaluated using Pearson correlation (*r*) and linear regression analysis. Pearson coefficients were considered significant when $r > .80$ (Shrout & Fleiss, 1979; Vaz et al., 2013). Repeated measures allowed subject specific statistical evaluation to view the within and between subject variability and its impact on

the agreement between two measurement tools. For error analysis Bland-Altman plots were used to visualize error within and between subjects (Bland & Altman, 1986). Mean error bias was compared to the line of equality (LOE) to determine if significant bias existed. If the 95% confidence interval (CI) of the mean error encompassed the LOE, a significant bias did not exist; if LOE was outside the CI then a significant error bias exists. The coefficient of repeatability (CR), corrected for repeated measures, described variability of error between the devices and subjects and was related to the limits of agreement described by Bland & Altman (1986). To determine variability quality CR measures compare to a priori set agreement limits. In previously reported studies, stride length distances average ±18 mm error between GAITRite and IMU estimations mean, therefore the differences expected within this study should fall within the range bounds. If the CR range is within these bounds the agreement is considered narrow (low variability) and if it is larger than these bounds it is considered to have a wide agreement (high variability) .

$$s_C = \sqrt{{s_D}^2 + \frac{1}{4}{s_1}^2 + \frac{1}{4}{s_2}^2} \quad (16)$$

$$CR = 1.96 \cdot s_C \quad (17)$$

2.4 Results

Subjects completed total 150 repetitions of movements across the six tasks, totaling 175 peak amplitude measurements per subject. Tasks were repeated when obvious movement mistakes occurred, however this study allowed individual movement selection to be a factor in movement execution. Unacceptable movement trials occurred when acceleration and gyroscope data detected as zero-velocity during known movement post-hoc. From the total peak amplitudes 1027 (97.8%) of repetitions were acceptable and contributed to correlation, regression, and error analysis.

2.4.1 Concurrent Validity of IMU Spatial Estimates and Optical Motion Capture

2.4.1.1 Task #1: Peak Anterior and Posterior Deviation during Sagittal Plane Hip ROM Task

Sagittal plane hip range of motion outputs two peak amplitudes, the maximum anterior and maximum posterior deviation from rest (quiet standing). Average anterior deviation estimated (double integrated) with IMU data (n = 139, M = 0.659 m, SD = 0.05) is lower than peak amplitude measured with optical motion capture (n = 139, M = 0.685 m, SD = 0.06). For all subject linear regressions IMU spatial estimations significantly predict optical motion capture measured deviations, 001, b = .379, $t(15)$ = 3.102, $p < .05$, 002, b = .790, $t(22)$ = 7.127, $p < .05$, 003, b = .763, $t(23)$ = 7.681, $p < .05$, 004, b = .456, $t(21)$ = 5.860, $p < .05$, 005, b = .828, $t(23)$ = 14.139, $p < .05$, 006, b = .248, $t(23)$ = 7.338, $p < .05$. Inertial measurement spatial estimations also explained significant amount of variance in optical motion capture measurement data, 001, R^2 = .397, $F(1,15)$ = 9.623, $p < .05$, 002, R^2 = .698, $F(1,22)$ = 5.788, $p < .05$, 003, R^2 = .719, $F(1,23)$ = 58.996, $p < .05$, 004 R^2 = .612, $F(1,21)$ = 34.343, $p < .05$, 005, R^2 = .897, $F(1,23)$ = 199.902, $p < .05$, 006, R^2 = .175, $F(1,23)$ = 4.875, $p < .05$ (Table 6).

Table 6. Subject specific IMU calculated and optical motion capture measured spatial anterior deviation during a sagittal plane hip range of motion movement.

	N	IMU Spatial Estimate	Optical Motion Capture Measurement	Pearson Correlation
Peak Anterior Deviation		$(\bar{x} \pm SD)$	$(\bar{x} \pm SD)$	r
001	17	0.608 ± 0.04	0.720 ± 0.02	.625**
002	24	0.676 ± 0.03	0.681 ± 0.04	.835**
003	25	0.632 ± 0.05	0.651 ± 0.04	.848**
004	23	0.707 ± 0.07	0.697 ± 0.04	.788**
005	25	0.599 ± 0.07	0.571 ± 0.06	.947**
006	25	0.733 ± 0.03	0.788 ± 0.02	.418*
TOTAL/MEAN	139	0.659 ± 0.05	0.685 ± 0.06	

* represents significant Pearson correlation p < 0.05.
** represents significant Pearson correlation p < 0.01.

Difference between anterior peak measurements had a mean error 0.0256 m, a lower average spatial estimation with IMU devices compared to optical motion capture (Figure 10). No significant error bias exists because the line of equality falls within the 95% confidence interval (-0.015 - 0.066 m) of the overall mean error. The coefficient of repeatability is greater than the a priori acceptable error range (± 0.018 m) (Trojaniello et al., 2014) therefore the agreement between measurements has a wide range. Mean error differences have a small absolute range across subjects (range: 0.069 m). The smallest subject mean error is 0.0048 m and the largest subject mean error is 0.1117 m.

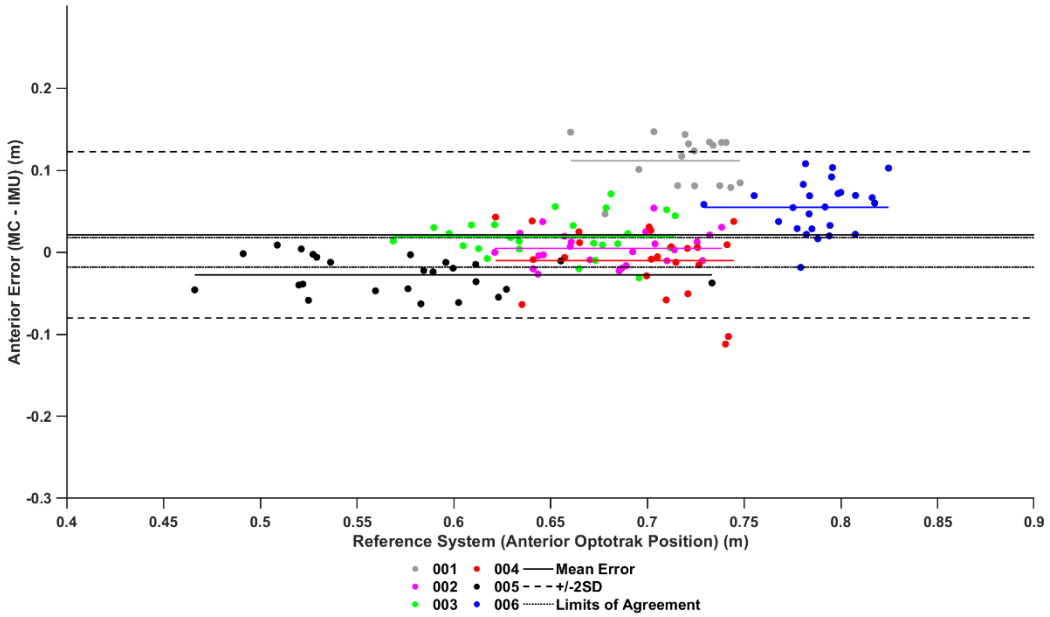

Figure 10. Bland-Altman plot of differences between IMU spatial estimate and motion capture measurement for anterior deviation during sagittal plane hip range of motion task.

Average posterior deviation estimated by IMU data (n = 139, M = -0.577 m, SD = 0.09) has a lower magnitude than peak amplitude measured by optical motion capture data (n = 139, M = -0.604 m, SD = 0.08). Linear IMU spatial estimations significantly predict measured spatial movements by optical motion capture, 001, b = .402, $t(23)$ = 3.250, p < .05, 002, b = .790, t (23) = 11.229, p < .05, 003, b = .957, t (23) = 18.682, p < .05, 004, b = .396, t (23) = 2.223, p < .05, 005, b = .807, t (23) = 8.759, p < .05, 006, b = .810, t (23) = 8.617, p < .05. Inertial measurement spatial estimation explained significant amount of variance in optical motion capture measurement data, 001, R^2 = .315, $F(1,23)$ = 10.566, p <

.05, 002, R^2 = .851, F (1,23) = 126.091, p < .05, 003, R^2 = .938, F (1,23) = 348.999, p < .05, 004, R^2 = .177, F (1,23) = 4.941, p < .05, 005, R^2 = .769, F (1,23) = 76.712, p < .05, 006, R^2 = .764, F (1,23) = 74.256, p < .05 (Table 7).

Table 7. Subject specific IMU calculated and optical motion capture measured spatial posterior deviation during a sagittal plane hip range of motion movement.

	N	IMU Spatial Estimate	Optical Motion Capture Measurement	Pearson Correlation
Peak Posterior Deviation		$(\bar{x} \pm SD)$	$(\bar{x} \pm SD)$	r
001	25	-0.495 ± 0.04	-0.542 ± 0.03	.561*
002	24	-0.675 ± 0.05	-0.679 ± 0.04	.923**
003	25	-0.597 ± 0.07	-0.597 ± 0.07	.969**
004	25	-0.688 ± 0.07	-0.718 ± 0.07	.421*
005	25	-0.440 ± 0.05	-0.474 ± 0.05	.877**
006	25	-0.566 ± 0.06	-0.614 ± 0.06	.874**
TOTAL/MEAN	149	-0.577 ± 0.09	-0.604 ± 0.08	

* represents significant Pearson correlation p < 0.05.
** represents significant Pearson correlation p < 0.01.

Difference between posterior peak measurements had a mean error -0.0271 m, since the deviation was negative direction lower average spatial estimation with IMU devices compared to optical motion capture was completed (Figure 11). Error bias is significant because the line of equality is outside the 95% confidence interval from the mean error (Table 13). Measurement repeatability is also poor because the coefficient of repeatability is greater than the a priori acceptable error range (± 0.018 m) (Trojaniello et al., 2014). Mean error differences have a small absolute range across subjects (range: 0.069 m). The smallest subject mean error is -0.0003 m and the largest subject mean error is -0.0472 m.

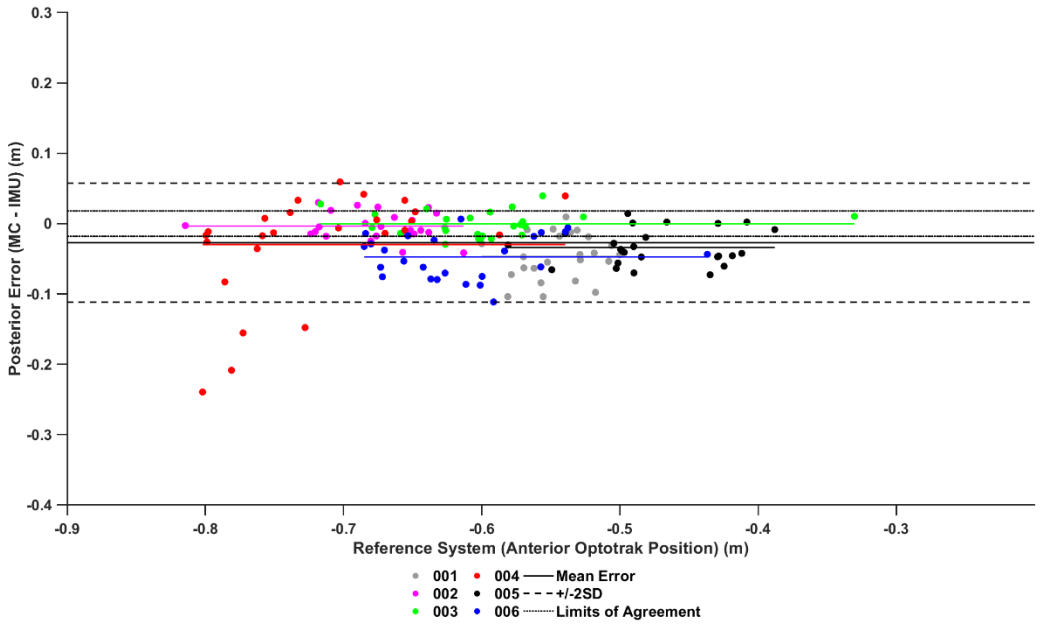

Figure 11. Bland-Altman plot of differences between IMU spatial estimate and motion capture measurement for posterior deviation during sagittal plane hip range of motion task.

2.4.1.2 Task#2: Lateral Deviation during Frontal Plane Hip ROM Task

Frontal plane hip ROM tasks output a single peak amplitude measures of lateral deviation from quiet standing. Average lateral deviation estimated with IMU data (n = 155, M = 0.537 m, SD = 0.05) is lower than peak amplitude measured with optical motion capture (n = 155, M = 0.553 m, SD = 0.05). Linear spatial estimations derived from IMU measurements significantly predicted the spatial measurements by optical motion capture, 001, b = .679, $t(23)$ = 6.342, $p < .05$, 002, b = 1.014, $t(23)$ = 9.599, $p < .05$, 003, b = 1.059, $t(23)$ = 17.127, $p < .05$, 004, b = .829, $t(23)$ = 15.927, $p < .05$, 005, b = .925 $t(23)$ = 13.381, $p < .05$, 006, b = .964, $t(28)$ = 19.914, $p < .05$. IMU estimations also explain significant amounts of the variation within optical motion capture measurements, 001, R^2 = .636, $F(1,23)$ = 40.215, $p < .05$, 002, R^2 = .80, $F(1,23)$ = 92.135, $p < .05$, 003, R^2 = .927, $F(1,23)$ = 293.320, $p < .05$, 004, R^2 = .92, $F(1,23)$ = 253.673, $p < .05$, 005, R^2 = .89, $F(1,23)$ = 179.064, $p < .05$, 006, R^2 = .93, $F(1,28)$ = 396.558, $p < .05$. (Table 8).

Table 8. Subject specific IMU calculated and optical motion capture measured spatial lateral deviation during an isolated hip abduction task.

	N	IMU Spatial Estimate	Optical Motion Capture Measurement	Pearson Correlation
Lateral Deviation		$(\bar{x} \pm SD)$	$(\bar{x} \pm SD)$	r
001	25	0.510 ± 0.03	0.554 ± 0.03	.798**
002	25	0.596 ± 0.02	0.610 ± 0.03	.895**
003	25	0.527 ± 0.05	0.560 ± 0.05	.963**
004	25	0.582 ± 0.05	0.559 ± 0.06	.958**
005	25	0.454 ± 0.03	0.454 ± 0.03	.941**
006	30	0.551 ± 0.04	0.578 ± 0.04	.966**
TOTAL/MEAN	155	0.537 ± 0.05	0.553 ± 0.05	

* represents significant Pearson correlation $p < 0.05$.
** represents significant Pearson correlation $p < 0.01$.

All repetitions (n = 155) were included in the analysis, mean error had a positive bias, 0.0233 m. Error bias is significant because the line of equality falls outside the confidence interval of the mean error (Figure 12). The repeatability of the spatial estimation is poor because the coefficient of repeatability is larger than the a priori acceptable error range (± 0.018 m) (Trojaniello et al., 2014). The subject mean errors have small absolute ranges (*range:* 0.0429 m). The lowest absolute subject mean error is 0.00017 m and the highest absolute subject mean error is 0.04305 m.

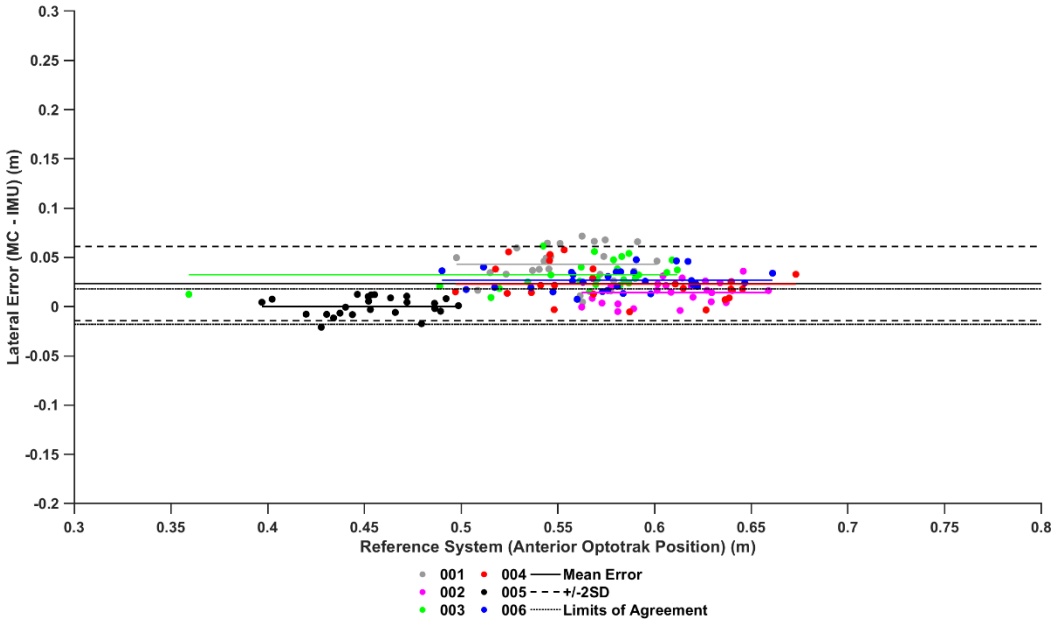

Figure 12. Bland-Altman plot of differences between IMU spatial estimate and motion capture measurement for lateral deviation during isolated hip abduction task.

2.4.1.3 Task #3: Vertical Displacement during Hip and Knee Flexion Task

Peak vertical displacement is measured during simultaneous hip and knee flexion. Estimated spatial deviation from IMU data (n = 144, M = 0.4635 m, SD = 0.02) is slightly lower than measured spatial deviation using optical motion capture from rest (n = 144, M = 0.4639 m, SD = 0.01). Linear spatial estimates from IMU data significantly predicted measured deviations using optical motion capture, 001, b = .757, $t(23)$ = 9.100, p < .05, 002, b = .730, $t(21)$ = 10.116, p < .05, 003, b = .909, $t(21)$ = 16.734, p < .05, 004, b = .898, $t(17)$ = 18.615, p < .05, 005, b = .836, $t(22)$ = 14.370, p < .05, 006, b = .817, $t(28)$ = 8.974, p < .05. IMU estimations also explain significant amounts of the variation of optical motion capture measurements, 001, R^2 = .636, $F(1,23)$ = 40.215, p < .05, 002, R^2 = .830, $F(1,21)$ = 102.338, p < .05, 003, R^2 =.930, $F(1,21)$ = 280.021, p < .05, 004, R^2 = .953, $F(1,17)$ = 346.508, p < .05, 005, R^2 = .904, $F(1,22)$ = 206.487, p < .05, 006, R^2 = .742, $F(1,28)$ = 80.538, p < .05 (Table 9).

Table 9. Subject specific IMU calculated and optical motion capture measured spatial vertical deviation during an isolated hip and knee flexion task.

	N	IMU Spatial Estimate	Optical Motion Capture Measurement	Pearson Correlation
Vertical Deviation		$(\bar{x} \pm SD)$	$(\bar{x} \pm SD)$	r
001	25	0.464 ± 0.02	0.464 ± 0.01	.885**
002	25	0.596 ± 0.02	0.610 ± 0.03	.911**
003	23	0.535 ± 0.02	0.528 ± 0.03	.964**
004	19	0.560 ± 0.04	0.560 ± 0.04	.976**
005	24	0.445 ± 0.04	0.459 ± 0.03	.951**
006	30	0.613 ± 0.02	0.623 ± 0.02	.861**
TOTAL/MEAN	146	0.536 ± 0.06	0.541 ± 0.06	

* represents significant Pearson correlation $p < 0.05$.
** represents significant Pearson correlation $p < 0.01$.

All repetitions (n = 144) were included in the analysis and mean error, 0.0038 m, has a positive bias. The error bias was not significant because the confidence interval encompasses the line of equality (Figure 13). The repeatability of the spatial estimation is not considered significant because the range of coefficient of repeatability is wider than the a priori acceptable error range (± 0.018 m) (Trojaniello et al., 2014), however, the coefficient of repeatability is lower than the a priori limits, 0.0172 m. The range of absolute subject mean errors is also low when considering the characteristics of the agreement (*range:* 0.014 m). The lowest magnitude subject mean error is -0.000043 m and the highest magnitude subject mean error is 0.01390 m.

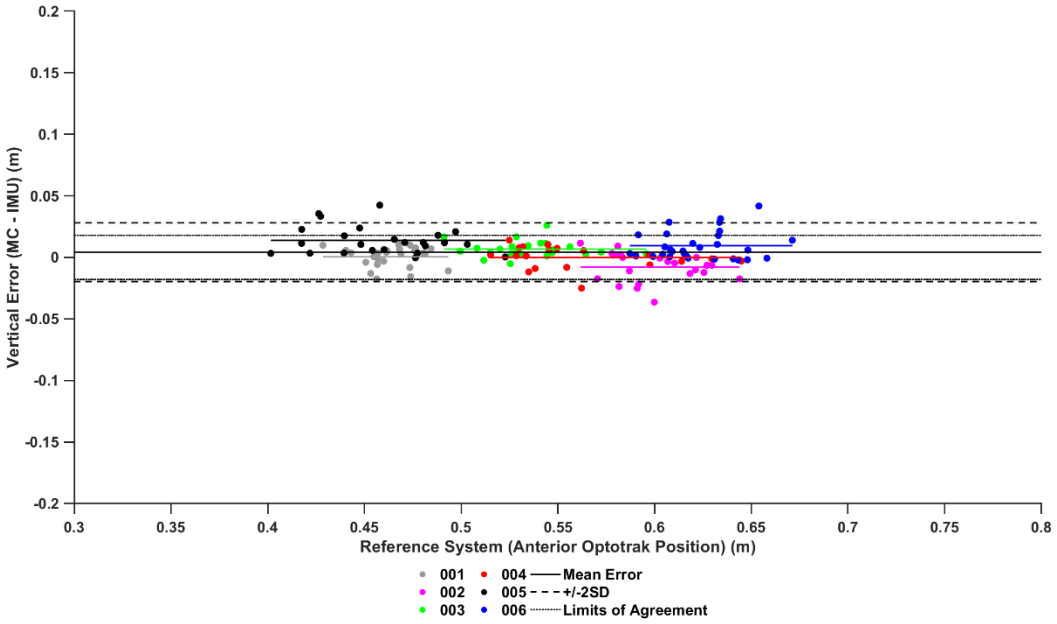

Figure 13. Bland-Altman plot of differences between IMU spatial estimate and motion capture measurement for vertical deviation during hip and knee flexion task.

2.4.1.4 Task #4: Vertical Displacement during Isolated Knee Flexion Task

Isolated knee flexion raises the foot in a non-linear fashion, this task revealed a single vertical deviation measurement from rest. Estimated spatial deviation from rest using IMU data (n = 147, M = 0.5085 m, SD = 0.034) is slightly lower than the measured deviation from optical motion capture (n = 147, M = 0.5095 m, SD = 0.034). IMU spatial estimations significantly predicted optical motion capture measurements, 001, b = .847, $t(23)$ = 17.841, p < .05, 002, b = .575, $t(23)$ = 6.823, p < .05, 003, b = .909, $t(23)$ = 6.088, p < .05, 004, b = .849, $t(20)$ = 14.954, p < .05, 005, b = 1.039, $t(23)$ = 35.129, p < .05, 006, b = .764, $t(23)$ = 8.937, p < .05. IMU spatial estimates significantly explain the variance of optical motion capture measures, 001, R^2 = .933, $F(1,23)$ = 318.314, p < .05, 002, R^2 = .669, $F(1,23)$ = 46.560, p < .05, 003, R^2 = .617, $F(1,23)$ = 37.060, p < .05, 004, R^2 = .918, $F(1,20)$ = 223.615, p < .05, 005, R^2 = .982, $F(1,23)$ = 1234.026, p < .05, 006, R^2 = .776, $F(1,23)$ = 79.862, p < .05 (Table 10).

Table 10. Subject specific IMU calculated and optical motion capture measured spatial vertical deviation during an isolated knee flexion task.

	N	IMU Spatial Estimate	Optical Motion Capture Measurement	Pearson Correlation
Vertical Deviation		$(\bar{x} \pm SD)$	$(\bar{x} \pm SD)$	r
001	25	0.490 ± 0.02	0.498 ± 0.02	.966**
002	25	0.499 ± 0.02	0.503 ± 0.01	.818**
003	25	0.523 ± 0.01	0.512 ± 0.02	.786**
004	22	0.490 ± 0.02	0.490 ± 0.02	.958**
005	24	0.476 ± 0.03	0.475 ± 0.03	.991**
006	25	0.579 ± 0.02	0.579 ± 0.02	.881**
TOTAL	146	0.5085 ± 0.034	0.5095 ± 0.034	

* represents significant Pearson correlation $p < 0.05$.
** represents significant Pearson correlation $p < 0.01$.

All repetitions (n = 147) were included in the analysis, mean error across subjects was not equal to zero and had a slight negative bias, -0.00098 m. Error bias is not significant because the 95% confidence interval encompasses the line of equality (Figure 14). Repeatability of spatial estimates is significant because the coefficient of repeatability of less than a priori acceptable error range (± 0.018 m) (Diana Trojaniello et al., 2014). Differences across subject mean errors have a range of 0.0113 m. The lowest magnitude subject mean error is -0.000381 m and the highest magnitude subject mean error is -0.01088 m.

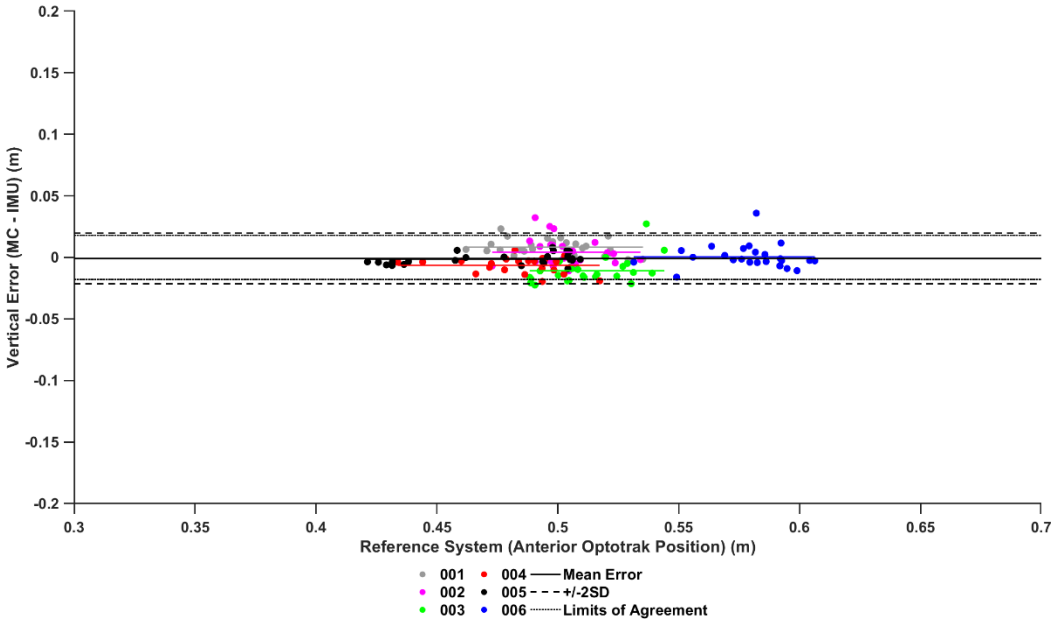

Figure 14. Bland-Altman plot of differences between IMU spatial estimate and motion capture measurement for vertical deviation during knee flexion task.

2.4.1.5 Task #5: Lateral Deviation during Isolated Stepping with Volitional Hip Circumduction

During isolated stepping with hip circumduction the foot deviates laterally during swing phase. Peak lateral deviation during swing is detected and used to characterise the movement pattern. Average lateral deviation of the foot calculated by IMU measures (n = 150, M = 0.304 m, SD = 0.08) is lower than average measured lateral deviation by optical motion capture (n = 150, M = 0.315 m, SD = 0.07). IMU spatial estimations significantly predicted optical motion capture measurements, 001, b = .696, $t(23)$ = 5.047, $p < .05$, 002, b = .731, $t(23)$ = 5.483, $p < .05$, 003, b = 1.133, $t(23)$ = 24.025, $p < .05$, 004, b = 1.134, $t(23)$ = 48.936, $p < .05$, 005, b = 1.111, $t(28)$ = 26.444, $p < .05$, 006, b = .931, $t(18)$ = 7.101, $p < .05$. IMU spatial estimates significantly show the variance of optical motion capture measures, 001, R^2 = .525, $F(1,23)$ = 25.470, $p < .05$, 002, R^2 = .548, $F(1,23)$ = 30.064, $p < .05$, 003, R^2 = .960, $F(1,23)$ = 577.203, $p < .05$, 004, R^2 = .990, $F(1,23)$ = 2394.756, $p < .05$, 005, R^2 = .960, $F(1,28)$ = 699.288, $p < .05$, 006, R^2 = .737, $F(1,18)$ = 50.430, $p < .05$ (Table 11).

Table 11. Subject specific IMU calculated and optical motion capture measured spatial lateral deviation during swing phase of an isolated step with volitional hip circumduction.

	N	IMU Spatial Estimate	Optical Motion Capture Measurement	Pearson Correlation
Lateral Deviation		$(\bar{x} \pm SD)$	$(\bar{x} \pm SD)$	r
001	25	0.378 ± 0.03	0.337 ± 0.03	.725**
002	25	0.252 ± 0.06	0.304 ± 0.06	.753**
003	25	0.203 ± 0.08	0.202 ± 0.09	.981**
004	25	0.370 ± 0.18	0.397 ± 0.20	.995**
005	30	0.232 ± 0.04	0.249 ± 0.05	.981**
006	20	0.390 ± 0.05	0.403 ± 0.06	.858**
TOTAL	150	0.304 ± 0.08	0.315 ± 0.07	

* represents significant Pearson correlation $p < 0.05$.
** represents significant Pearson correlation $p < 0.01$

Error analysis was completed on all repetitions (n = 150), mean error was not equal to zero and had a slight positive bias, 0.0113 m. Error bias is not significantly different from zero because the 95% confidence interval encompasses the line of equality (Figure 15). The agreement is considered to have wide variability because the coefficient of repeatability is larger than a priori acceptable error range (± 0.018 m). Differences in mean subject error contribute to variability of outcome measures, as the range of subject errors is 0.0515 m. The lowest absolute subject mean error is -0.000429 m and the highest absolute subject mean error is 0.0511 m.

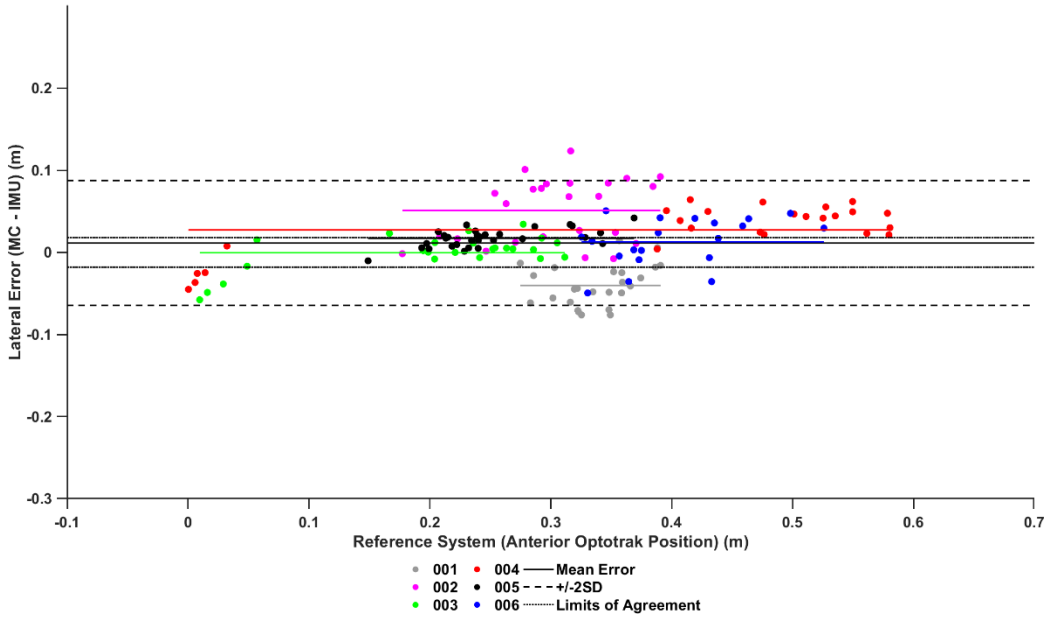

Figure 15. Bland-Altman plot of differences between IMU spatial estimate and motion capture measurement for lateral deviation during swing phase of stepping with hip circumduction task.

2.4.1.6 Task #6: Lateral Deviation during Isolated Stepping with Volitional Hip Circumduction and Rotation

Isolated stepping with hip circumduction and hip rotation causes a rotation and lateral translation of the IMU to peak lateral deviation during swing. During isolated stepping, the peak lateral deviation calculated from IMU data (n = 142, M = 0.266 m, SD = 0.06) is smaller than the peak deviation measured but optical motion capture data (n = 142, M = 0.314 m, SD = 0.08). Not all IMU prediction models predict optical motion capture significantly, 001, b = .760, $t(20) = 6.081$, $p < .05$, 002, b = .257, $t(19) = 1.571$, $p > .05$, 003, b = .986, $t(22) = 7.642$, $p < .05$, 004, b = 1.037, $t(23) = 16.013$, $p < .05$, 005, b = .985, $t(23) = 23.827$, $p < .05$, 006, b = 1.075, $t(23) = 12.525$, $p < .05$. Similar results are found when analyzing IMU models accounting for variance of optical motion capture measures, 001, R^2 = .649, $F(1,20) = 36.975$, $p < .05$, 002, R^2 = .115, $F(1,19) = 2.469$, $p > .05$, 003, R^2 = .726, $F(1,22) = 58.399$, $p < .05$, 004, R^2 = .918, $F(1,23) = 256.410$, $p < .05$, 005, R^2 = .961, $F(1,23) = 567.715$, $p < .05$, 006, R^2 = .867, $F(1,23) = 156.865$, $p < .05$ (Table 12).

Table 12. Subject specific IMU calculated and optical motion capture measured spatial lateral deviation during swing phase of an isolated step with volitional hip circumduction and rotation.

	N	IMU Spatial Estimate	Optical Motion Capture Measurement	Pearson Correlation
Lateral Deviation		$(\bar{x} \pm SD)$	$(\bar{x} \pm SD)$	r
001	22	0.181 ± 0.05	0.212 ± 0.04	.806**
002	21	0.267 ± 0.05	0.362 ± 0.04	.339
003	24	0.220 ± 0.03	0.245 ± 0.04	.852**
004	25	0.382 ± 0.08	0.449 ± 0.09	.958**
005	25	0.265 ± 0.07	0.287 ± 0.07	.980**
006	25	0.281 ± 0.05	0.331 ± 0.05	.934**
TOTAL	142	0.266 ± 0.06	0.314 ± 0.08	

* represents significant Pearson correlation $p < 0.05$.
** represents significant Pearson correlation $p < 0.01$.

All repetitions (n = 150) were included in the analysis of error, mean error across subjects was not equal to zero and is positively bias, 0.04857 m. Error bias is not significantly different from zero because the 95% confidence interval encompasses the line of equality (Figure 16). The repeatability of the spatial estimate is not significant because the coefficient of repeatability is larger than a priori acceptable error range (± 0.018 m). Range of differences across subject mean errors is larger than other isolated movement tasks (*range:* 0.07288 m). A specific subject, 002, had no significant Pearson correlation and had highest absolute subject mean error is 0.09485 m which contributes to larger mean error and variability. The lowest subject magnitude mean error is 0.02197 m.

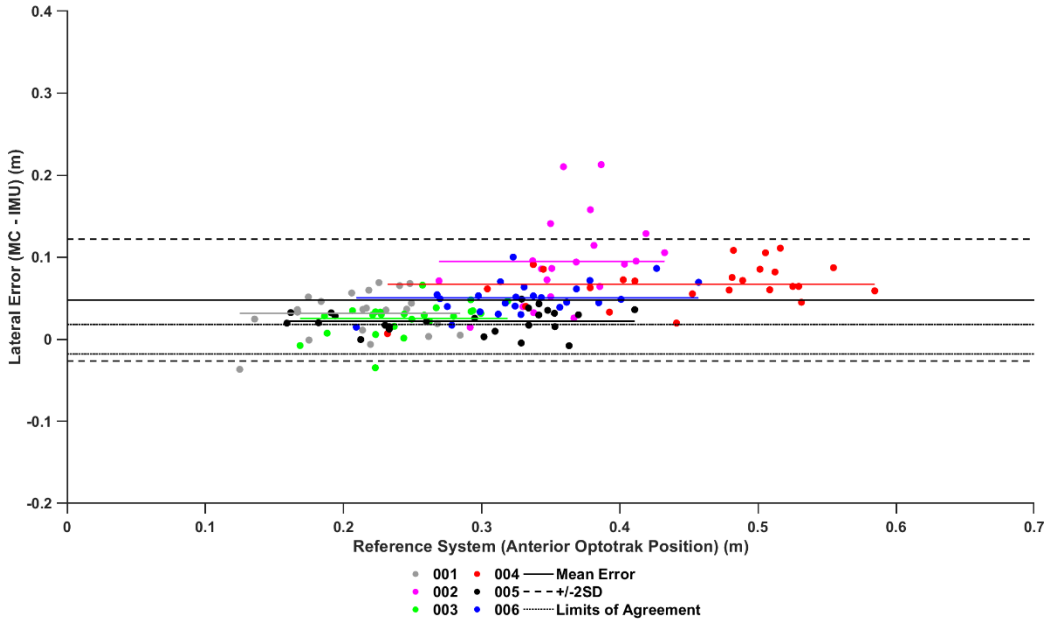

Figure 16. Bland-Altman plot of differences between IMU spatial estimate and motion capture measurement for lateral deviation during swing phase of stepping with hip circumduction and rotation task.

Table 13. Mean-error, confidence interval (95%) and coefficient of repeatability for all outcome variables during each task.

		Mean Error (m)	**Confidence Interval**		**Coefficient of Repeatability**	
		$(\bar{x} \pm SD)$	*-95% CI*	*+95% CI*	*Lower bound*	*Upper bound*
Task #1	Anterior	0.026 ± 0.05	-0.015	0.066	-0.03	0.0811
Task #1	Posterior	-0.026 ± 0.02	-0.043	-0.011	-0.058	0.004
Task #2	Lateral	0.023 ± 0.01	0.011	0.035	-0.002	0.0485
Task #3	Vertical	0.0038 ± 0.008	-0.002	0.010	-0.013	0.021
Task #4	Vertical	-0.00098 ± 0.007	-0.007	0.005	-0.018	0.0158
Task #5	Lateral	0.011 ± 0.03	-0.013	0.036	-0.027	0.0501
Task #6	Lateral	0.049 ± 0.028	0.026	0.071	0.0068	0.0904

2.5 Discussion

The purpose of this study was to continue to build towards understanding of the numerical accuracy of IMU spatial estimates as compared to motion capture measurement of kinematics for realizing the future potential application in clinical settings. The study set out to determine the accuracy between IMU calculated measurements and motion capture measured spatial data across specific movements. Each movement was designed to test the accuracy of spatial measures along a single axis of motion (e.g. vertical displacement during isolated knee flexion) and understand how estimated kinematic outcome measures could characterize movement patterns. Table 14 summarizes the main observations from study 1. This table highlights main learning points from the comparison between two measurement devices: (1) specific tasks have high accuracy (i.e. hip and knee flexion and isolated knee flexion) (2) statistical approach (correlation vs. error analysis) influences the agreement between the two devices, and (3) across subject differences are prominent compared to the devices or the analysis. The between subject differences may be associated with how tasks are performed rather than the processing techniques utilized.

As noted, the study revealed that IMUs can be very accurate when examining certain axes of movement in an inertial frame of reference. However this level of accuracy is not as strong for all planes or types of motion. For example, tasks that vertically translated the IMU (hip and knee flexion, *me* = 0.0038 m, and isolated knee flexion, *me* = -0.00098 m), compared to increase transverse rotation (stepping with hip circumduction and rotation, *me* = 0.049 m), had smaller mean differences. Although the majority of tasks did not have mean errors that were significantly different from zero, the coefficients of repeatability indicate low repeatability for all planes or types of motion. Tasks with less transverse rotation (hip and knee flexion, *CR range* = 0.034 m, and isolated knee flexion, *CR range* = 0.0338 m), report smaller coefficient of repeatability ranges compared to more transverse rotation (posterior deviation during sagittal plane hip ROM, *CR range* = 0.062 m, stepping with hip circumduction and rotation, *CR range* = 0.0836 m) (Table 13).

The first objective of this study was to investigate association of these tools by evaluating peak-amplitude outcome measures from two different methods of measurement. The majority (75%) of subject and task comparisons are statistically and clinically significant ($r > 0.8$). The second objective focused on the error between the two measurement devices to evaluate the agreement of these devices. The agreement between these two devices, on average, was not significantly different to the line of equality. However, the variability of measurement error was larger than the agreement boundaries during majority of movement patterns. Findings from these two tests indicate there is a level of statistically accuracy comparing the IMU to the gold standard however; it may not be clinically acceptable due to repeatability criteria. Across all movements tested the specific task goals and movement pattern execution appear to the main influence on accuracy rather than between subjects.

With respect to the association between IMU and optical measurement of kinematics the study relied, in part, on a criteria of $r>0.8$, which was exceeded in 75% of tasks (across each subject). Correlation values greater than .75 have been typically used to determine clinical significance when evaluating measurement association (Shrout & Fleiss, 1979; Vaz et al., 2013). These evaluations suggest good agreeance between the two measurement devices to estimate spatial measurements. However the measure of association alone is not sufficient to determine accuracy and evaluation of clinical measures and comparisons including error terms have been advised (Vaz et al., 2013). Examining the measurement error with the mean errors and the coefficient of repeatability (limits of agreement) is more applicable in this scenario (Bland & Altman, 1986; Vaz et al., 2013). The correlation coefficients, measurement error, and the coefficient of repeatability are tools used to evaluate the significance of association between two measurement devices. Correlation coefficients accept the agreement between devices with less scrutiny compared to the error analysis with Bland-Altman techniques. Measurement error and the coefficient of repeatability are used to evaluate the association between two measurement devices (Bland & Altman, 1986). Measurement error (mean, confidence intervals) can help outline whether a significant bias exists within the error data while the coefficient of repeatability compared to a priori established limits of

agreement can outline the characteristics of the agreement (wide versus narrow agreement) (Bland & Altman, 1986; Giavarina, 2015; Vaz et al., 2013). While 75% of conditions (tasks and subjects) met correlation criteria, only 50% of subject mean errors fell within previously set acceptable error band outlined. These a priori limits were referenced from a mean error value during a comparison of stride length measures between IMU estimates and GAITRite generated reports (Trojaniello et al., 2014). As a result, it was deemed important to emphasize the assessment of agreement based on not only on simple correlation but also measurement error and coefficient of repeatability.

The results of the current study revealed similar overall repeatability of outcomes as reported previous studies (Trojaniello et al., 2014). However, what is of interest are the differences across tasks and specific factors that may have influenced IMU accuracy. One factor that appeared to impact accuracy was the specific movement. The measurement of posterior deviation during the sagittal plane hip range of motion and lateral deviation during frontal plane hip ROM and stepping with hip circumduction and rotation are the only mean bias that is considered significantly different (i.e. line of equality is outside ±95% CI from mean) (Giavarina, 2015). Measurements during all tasks have some magnitude of systematic error because no mean bias are equal to zero. When testing the vertical deviation of the IMU devices, mean error bias was very small (less than 3.8 mm). Movement patterns evaluating lateral and anterior-posterior movements were larger in magnitude in all comparisons (from 11 to 49 mm). Vertical displacement tasks (Task 4: Hip and knee flexion & Task 5: Isolated knee flexion) have the smallest mean error when comparing accuracy between IMU and OPTO measures. Task 2 (Posterior deviation during sagittal plane hip ROM), 3 (Hip abduction), and 6 (Stepping with hip circumduction and rotation) performed similarly when comparing clinical significance and error measurement, they also have similar magnitude of ranges between maximum and minimum subject mean error. The largest significant discrepancies occur with task 6 (stepping with hip circumduction and rotation). This task has large amounts of measurement error within their estimates and the majority of subjects have strong agreement based on their R-values. Tasks that involved more transverse rotation in the local frame (yaw) of the IMU appear to have more error than those that do not. Furthermore, the repeatability of each task varies and

depends on similar issues discussed above. Tasks that may have larger transverse rotation exhibit larger ranges between the CR's upper and lower bounds. These differences in both mean error and CR indicate that movement patterns with more transverse rotation may by less precise and less repeatable.

In addition to task (movement differences), there were some influences associated with subject error. Independent of tasks, 50% of subject mean errors fall within previously set acceptable error band outlined compared to 75% of r-values. These a priori limits were referenced from a mean error value during a comparison of stride length measures between IMU estimates and GAITRite generated reports (Trojaniello et al., 2014). As a group, these acceptance rates produce similar conclusions and no one subject consistently contradicts agreeability of the two devices. During simple, uniplanar tasks, all subjects meet agreeability standards with respect to error analysis band and nearly all measures are highly correlated ($r > 0.80$). When tasks are multi-planar, marked differences become more evident. Differences arise due to subject specific movement patterns and devices begin to show statistical and biological differences with respect to error and correlation analysis.

A possible source for these inaccuracies is attributable to data acquisition and processing and specifically: (1) contamination integration drift when estimating change in local frame orientation (Pezzack et al., 1977) and (2) inaccurate orientation of the recorded data (Picerno et al., 2011). There are many techniques to correct for integration drift during position estimation (Kose et al., 2012; Mazza et al., 2012; Peruzzi et al., 2011; Rebula et al., 2013). Drift removal techniques are similar for all axes of movement; therefore, error due to inaccuracies in estimated drift removal should be consistent across all axes of movement. However, orientation errors will not be accounted for and will cause errors in derived spatial information. Accuracy of data captured is reliant and a product of manufacturing error. IMUs local coordinate systems align with anatomical reference to record and measure kinematic outcomes. Error in manufacturing sensor alignment may affect the assumptions imposed when creating specific reference frames after movement. Typical application of IMU data requires a stationary period prior to task completion or development of a reference from during data collection (e.g. direction of progression, angular velocity measures) (Cain et al., 2016; Trojaniello et al., 2014). All collections and inertial frame

creation followed the same mathematical techniques and all stationary periods were sufficient for reference frame creation. However, another potential reason for the error may be associated with the calibration algorithms that create local coordinate systems. Factory calibration techniques use a combination of gravity and perceived magnetometer vector (north). Errors with heading direction (reliant on magnetometer accuracy) during calibration are subject to interference from magnetic dip (Brodie, Walmsley, & Page, 2008b) and structural environment (de Vries et al., 2009). The kinematic outcome measures that have the largest bias and variability involve movement along the mediolateral or anteroposterior axis. These two local axes are developed using data that is capture and reliant on the absolute heading direction and potentially influenced during calibration sequencing. When evaluating the absolute orientation (global frame) of several IMUs error maximums ranged 5.2º - 21.6º when using factory calibration settings (Brodie et al., 2008b). Orientations were evaluated in 24 different orthogonal orientations on a custom-made rig. Evaluating the relative orientation of IMUs to a known orientation can also produce large errors in orientation estimates (max: 9.8º), with the largest errors occurring in transverse rotation (yaw), 2.68-5.2º, compared to 0.92-2.2º for other component angles. Recalibration of the IMU improved the accuracy of orientation estimations but in every iteration the heading error (transverse rotation) had the largest associated error (Brodie et al., 2008b). The effects of recalibration created maximum errors of 1.1-2.5º, however these results were recorded from static IMUs. During dynamic movement on a swinging pendulum, the application of a new fusion algorithm performed better than a proprietary Kalman filter output different orientation accuracy results (Brodie, Walmsley, & Page, 2008a). The fusion algorithm had a lower RMS error range, 0.8-1.3º, compared to the RMS error output by the proprietary Kalman filter, 8.5-11.7º, with the maximum error occurring around the Z-axis (longitudinal/yaw). Further, these errors are larger when the magnitude of acceleration is large. Errors in static orientation may cause errors to globally measured accelerations be exacerbated when these larger accelerations are recorded (Brodie et al., 2008a). Inter-IMU spot-checking found that the different sensed orientations exist for each individual IMU, because the sensed global coordinate systems during calibration sequences was different between IMUs (Picerno et al., 2011). During single IMU consistency

spot checking errors were statistically larger for transverse rotation (yaw) compared to both pitch and roll angles (Picerno et al., 2011). Ricci, Taffoni, & Formica, (2016) also recorded larger error about the yaw axis when checking orientation of the IMU. Larger error is attributed to error in the heading direction or rotation about the yaw axis because of the ability for IMUs to sense accurate changes in to the magnetic field during calibration sequences. Using on-board quaternion information, the orientation of an IMU compared to a measure angular deviation of turntable device were comparable (Taylor, Miller, & Kaufman, 2017). Angular movement derived from on-board orientation information reported minimal differences across small (0.2 ± 0.1°) and larger angular magnitudes (0.6 ± 0.1°), these magnitude of differences are also seen in previous studies that also utilized relative reference frames (Brodie et al., 2008b). These data are more accurate because of the relative reference frame and methodologically steps considered to improve accuracy (consistent recalibration techniques) (Taylor et al., 2017). Without recalibration sensors exposure to rapid movements and high accelerations can decrease the accuracy of the original predicted orientation from calibration (Brodie et al., 2008b, 2008a) which could ultimately affect the outcome data. The algorithm in the present study associated with the Shimmer3 units outputs the orientation information of the IMU as it moves compared to the initial calibrated orientation. Reported RMS error rates are also largest in the yaw direction (about vertical) at a magnitude of average of ~1.5^{o} but at least twice as large as any other axis estimation (Madgwick et al., 2011). This may be one potentially significant contributor to error in kinematic outcome measures since largest amounts of error variability occur when larger transverse rotations be recorded.

Other possible source of error, specifically linked to between subject differences, could be the movement characteristics each subject performed during the tasks. In tasks one (sagittal plane hip range of motion), two (hip abduction), and five (stepping with hip circumduction), little to no transverse rotation is required. If lower limb rotation was variable between subjects then significant error between devices may be present in some subjects but not others. The influence of speed has already been discussed and could influence data outcomes. Between subject movement pattern differences are factors inherent to clinical assessment and for IMU data to describe human movement with kinematic outcome measures it

needs to be robust enough to distinguish between these factors. Although these errors exist within the current set of data, in most cases the differences are small for the majority of these tasks. Research indicates errors up to 5^{o} difference can lead to misinterpretation for clinical intervention (Bolink et al., 2016), error rates for kinematic outcome measures are unknown. However, if the intended purpose is to detect difference between movement patterns, then more research needs to be conducted to determine if the IMUs are precise and repeatable enough to distinguish compensatory and normal movement patterns in the frontal plane.

Some noted limitations to this study are variability associated with movement execution, the approximate estimation of both angular movement (during rotation sequences) and drift removal, and the lack of clarity surrounding clinically detectable differences between two kinematic outcome measures. Instruction and practice were given to each participant prior to collection; however, during collection variability of individual movement patterns were unrestricted. There is benefit to include this variability because inherently during movement execution variability will always exist within and between subjects. When attempting to outline the agreeance between devices, restricting movement patterns to meet very specific standards could eliminate the variability associated within individual movement pattern execution. A second limitation is the estimation of linear drift during integration (from low frequency noise) and the approximation of angular movement during rotational sequencing. Approximation allows a certain level of assumption within the processing steps, and in turn allows certain levels of assumption to confound the results. Computational techniques to remove drift and estimate orientation changes receives a lot of discussion and attention. Currently, assumption need to be accepted and understood when interpreting results, however in the future it is recommended that these assumptions are outlined and interpretable in comparison with results for clinical awareness and understanding. The third noted limitation are unclear standards for clinically detectable change for kinematic outcome measures. Without clearly defined limits of agreement, it is difficult to determine if these devices are numerically accurate enough to distinguish between compensatory movements during a clinical task. Research should focus on detectable change with the ‘clinical eye’ in all ranges of movement deviations in order to understand the

accuracy and benefit of combining both experimental tools and clinical judgement to improve care and rehabilitation.

In summary, IMUs are used to characterize movement patterns in clinical and research settings. Little research has examined the ability to detect frontal plane movements, which is important when characterizing many multi-planar and compensatory movements. Overall, results reveal that IMU spatial measures are not significantly different from measured deviations both statistically and clinically however, task and subject factors task influence these differences. Next steps will need to disentangle the error characteristics including: (1) investigating how the size of error is associated with timing of peak deviation within segmented data and amount of recorded angular velocity at peak deviation and (2) determine if IMUs are precise enough to distinguish between normal and compensatory movements. The second study will focus on the ability to characterize compensatory movement patterns during a clinical obstacle avoidance task.

Table 14. Clinical significance determined by correlation coefficients and error analysis for all subjects and tasks. Cells highlighted in green show a significant agreement utilizing the outlined technique, while red shows a significant difference.

Movement	Sagittal Plane hip ROM	Sagittal Plane hip ROM	Hip Abduction	Knee/Hip Flexion	Knee Flexion	Isolated step with Hip Circumduction	Isolated step with Hip Circumduction and rotation
Measured Axis	Anterior	Posterior	Lateral	Vertical	Vertical	Lateral	Lateral
Clinical Significance WRT Pearson (*r* > *.80*)							
001	0.63	0.56	0.80	0.89	0.97	0.73	0.81
002	0.84	0.92	0.90	0.91	0.82	0.75	0.34
003	0.85	0.97	0.96	0.96	0.79	0.98	0.85
004	0.79	0.42	0.96	0.98	0.96	1.00	0.96
005	0.95	0.88	0.94	0.95	0.99	0.98	0.98
006	0.42	0.87	0.97	0.86	0.88	0.86	0.93
Percent Accepted	17%	67%	83%	100%	67%	67%	67%
Clinical Significance WRT Measurement Error (*-95% CI me* < *LOE* < *+95% CI me*)							
001	0.112	-0.047	0.044	0	0.008	-0.041	0.031
002	0.005	-0.004	0.014	0.014	0.004	0.052	0.095
003	0.019	0	0.033	-0.007	-0.011	-0.001	0.025
004	-0.01	-0.03	-0.023	0	0	0.027	0.067
005	-0.028	-0.034	0	0.014	-0.001	0.017	0.022
006	0.055	-0.048	0.027	0.01	0	0.013	0.05
Percent Accepted	33%	33%	33%	100%	100%	50%	0%

Chapter 3: Characterizing the Variability of Compensatory Movement Strategies in Healthy Subjects Using Inertial Measurement Units

3.1 Introduction

Compensatory movements are a change in movement patterns in response to dysfunction of an intact control system. Prosthetic fit (e.g. discomfort, misalignment), design, and amputation level (e.g. transtibial, transfemoral) are sources of compensations in the amputee population. The origin of these asymmetries dictates the ability clinicians have to restore normal movement patterns using rehabilitation techniques. Some researchers view these compensatory movements as adaptations by the control system to new mechanical abilities of the limb and are inherently the new movement pattern adopted (Hak, van Dieën, van der Wurff, & Houdijk, 2014; Winter & Sienko, 1988). The effect of these asymmetries and their relationship with secondary injuries (e.g. lower back pain) are unknown. This suggests that adaptive movement patterns may be optimized for gait progression while simultaneously being injurious to the amputee (Devan, Hendrick, Ribeiro, Hale, & Carman, 2014).

Walking is attainable with assistive prosthetic devices after the loss of a lower limb functional joint. Transtibial amputation, above the ankle and below the knee, is an example of loss of a single joint. Deviations from their original walking pattern can occur when fitted with a prosthetic device which is absent of the mechanical and sensory advantage of a functional joint (Bowker et al., 1992). One of these deviations comes in the form of asymmetrical gait, where amputees experience differences between their amputated and intact limbs. When an amputee has more control (e.g. transtibial amputees versus transfemoral) asymmetries may be minimal because of increased sensory and mechanical control. Detecting these asymmetries and compensations become increasingly difficult when patients have more control because the deviations become less prominent. Assistance of wearable devices could help increase detection and accuracy of these deviations and compensations from normal walking patterns. Moving outside the laboratory setting is much more difficult, however many researchers have begun the application of IMUs to elderly, hemiparetic, amputee, and osteoarthritic populations to characterize

movement patterns and help understand control strategies (Muro-de-la-Herran, García-Zapirain, & Méndez-Zorrilla, 2014; Shull, Jirattigalachote, Hunt, Cutkosky, & Delp, 2014; Trojaniello et al., 2014).

3.1.1 Defining the Gait Cycle with Instrumentation

Outside of the laboratory, gait events are detected using IMU data and algorithms with explicit searching steps. Gait events have been detected using a single IMU located on the lower back or hip (Bugané et al., 2012; Sejdić et al., 2016), bilaterally on the lower limbs (Aminian et al., 2004; Aminian, Najafi, Büla, Leyvraz, & Robert, 2002; Salarian, Burkhard, Vingerhoets, Jolles, & Aminian, 2013), shank (Greene, McGrath, Foran, Doheny, & Caulfield, 2011; Hanlon & Anderson, 2009; Trojaniello et al., 2014), shank and feet (McGrath, Greene, Walsh, & Caulfield, 2011; Rouhani et al., 2012), and feet (Dadashi et al., 2013; Rebula et al., 2013). The motivation to alter sensor configurations allows the ability to apply different detection methods that may be suitable for patient population or variables of interest. Impulse dampening is one challenge associated with different sensor configurations. The impulse detected by IMUs is smaller when the IMU is farther away from the location of heel strike (e.g. the hip compared to foot). To overcome these difficulties several algorithms (Kose et al., 2012; Trojaniello et al., 2014) , thresholds (Greene et al., 2011; Hanlon & Anderson, 2009; McGrath et al., 2011; Rebula et al., 2013) and wavelet analysis (Aminian et al., 2002; Millor, Lecumberri, Gómez, Martínez-Ramírez, & Izquierdo, 2014) techniques have been used for event detection. Trojaniello et al., (2014) developed a heuristic algorithm model to detect gait events using acceleration and gyroscopes attached bilaterally above the ankle joints for healthy, elderly, hemiparetic, parkinsonian, and choreic gait. The heuristic model outlined event search windows by removing known swing time intervals (threshold of peak angular velocity during swing phase). Within the respective search window, initial contact is the maximum AP acceleration and final contact is as the minimum ML angular velocity. These gait event detections showed small mean average error for initial contact timings and final contact timings when compared to footswitch data for all populations included (Trojaniello et al., 2014). Defining these gait events, as part of a person's movement pattern, help outline specific clinical measures that can be used to

evaluate the quality of gait or the effects of intervention (e.g. stride length, swing time, support times). These measurements are defined as spatiotemporal measurements as they relate to both spatial position of the steps as well as timing of events that outline the step taken.

3.1.2 Spatiotemporal Measures Change for Obstacle Avoidance

3.1.2.1 Effects obstacle properties on clearance strategy

Fundamental obstacle avoidance research reveals the effect visual information and obstacle properties has on obstacle avoidance strategies. Visually guided foot placement is necessary for successful obstacle avoidance, further, foot placement prior to obstacle avoidance is highly tuned for successful obstacle crossing (Patla & Greig, 2006). Obstacle size (Patla & Rietdyk, 1993) and perception of obstacle fragility (Patla, Rietdyk, Martin, & Prentice, 1996) influence clearance strategies. Healthy subjects tend to scale up their toe clearance and scale down their crossing speed and foot velocity values when stepping over the taller obstacle. Intuitively, when stepping over wider objects (increase depth) stride length increases but not when clearing taller objects (H.-C. Chen et al., 1991; Patla & Rietdyk, 1993). Crossing fragile obstacles, the lead limb increases toe clearance and hip hiking but there are no affects to the trailing limb clearance (Patla et al., 1996). Kinematic differences exist temporally and spatially between limbs for obstacle clearance. Trailing limb toe height driven by knee flexion during obstacle clearance whereas hip flexion and hip hiking drives lead limb toe height prior to obstacle clearance (Figure 17 & 18). These differences are evident when comparing changes to joint angles during level ground walking and examining maximum toe height characteristics of limb avoidance (Patla et al., 1996). Lead limb clearance has the benefit of real-time visual information whereas exteroceptive information (information of environmental characteristics) drives the trailing limb movement (Lajoie, Bloomfield, Nelson, Suh, & Marigold, 2012). Differences between limb clearance strategies appear to mitigate the risk of falling. Lead limb obstacle contact has greater risk to the stability of the system when compared to trail limb contact because COM movement during lead limb crossing is away from the base of support (BOS) while trail limb clearance moves towards the BOS. The control system reduces the risk

of lead limb contact by decreasing foot velocity over obstacle, increasing toe clearance and increasing hip hiking. These compensations are unneeded for trail limb clearance because the movement of COM is towards BOS and a more stable position.

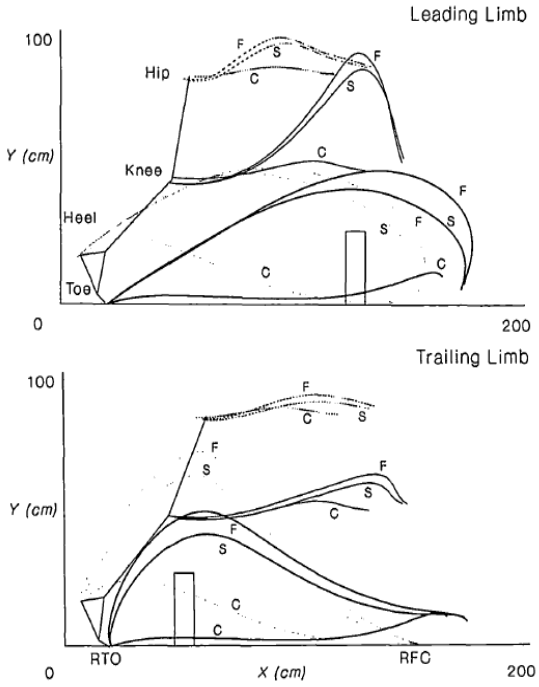

Figure 17. Trajectory of both lead and trail limb during obstacle crossing conditions (solid, fragile, no obstacle). Different toe and hip trajectories are evident from tracings of lead versus trail as they cross the obstacle. Image from (Patla et al., 1996)

3.1.2.2 Effects impairments have on obstacle avoidance strategies

Compensatory movement patterns overcome obstacles when neurological disorders or mechanical constraints compromise the intact system. The state of the system dictates the adopted movement strategies utilized to maintain primary locomotion goals (e.g. upright posture, adequate clearance, forward progression). The amputee population has both a mechanical restriction and reduced peripheral sensory information. The amputee population is at a greater risk of falling and the majority of falls occur during ambulation (De Asha & Buckley, 2014). During self-selected walking, amputee populations reduce walking speeds and adopt asymmetrical spatiotemporal patterns to maintain posture stability and reduce the likelihood and consequence of tripping. At faster velocities, minimum clearance is unaffected in prosthetic limbs when compared to intact limbs, suggesting fine-tuned ankle motion

controls margin of safety in response to gait speed (De Asha & Buckley, 2014). Healthy individuals increase safety margin of clearance under conditions with greater risk of tripping (e.g. faster velocity, taller or fragile obstacles). Lead limb minimum clearance is similar between an amputee's intact and affected limb however crossing speed decreases during amputee obstacle crossing (Hill et al., 1997; Vrieling et al., 2007). Slower walking speeds over obstacles could reflect an increase control of COM movement over the obstacle when control is constrained.

Amputees compensate for reduce knee and ankle control by increasing the work at the stance ankle joint and maintain the lowering strategy by modifying the swing limb hip joint work during clearing (Hill et al., 1999). These power profiles attribute to toe clearance by using multi-planar movements or other compensatory movements such as: vaulting (Bowker et al., 1992) or ipsilateral hip hiking (Patla et al., 1996). Amputees also utilize a hip circumduction strategy to aid in the increase toe clearance during walking (Vrieling et al., 2007). Hip circumduction increases lateral deviation of the foot during crossing and aids in foot elevation. Patients with knee osteoarthritis and total knee replacements utilize the frontal plane to accommodate knee dysfunction, avoid onset of pain, or increase stability while clearing the obstacle (Byrne & Prentice, 2003; H.-L. Chen, Lu, Wang, & Huang, 2008; Levinger et al., 2012).

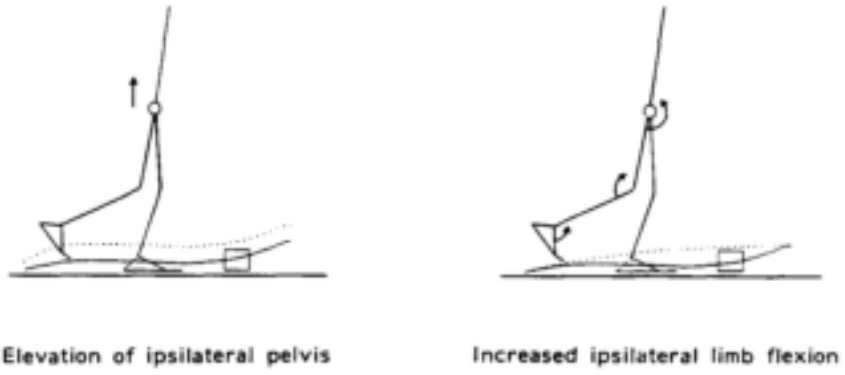

Figure 18. Comparison of toe trajectory during obstacle clearance with increased limb flexion and hip hiking movement strategies (Patla & Rietdyk, 1993).

3.1.3 Exploring obstacle negotiation strategies in healthy subjects with movement manipulations

Investigating patient populations increases the awareness of compensatory movements utilized by their associated restriction but is confounded by variable factors. Toe clearance is required for successful

obstacle avoidance and is a product of the lower limb joint angles and biased swing leg trajectories (Patla & Rietdyk, 1993; Winter, 1992). Restricting movement in a single lower limb joint examines the contribution of isolated kinematic properties absent of severe confounding variables. Change in movement pattern, as a response to single joint manipulations, in a healthy population help further our understanding of joint contribution and compensatory movement adoption. Using ankle-foot-orthotic devices (AFO), healthy subjects can replicate below-knee amputee impairments such as ankle immobilization. Toe height increases during obstacle avoidance with restricted ankle mobility (Evangelopoulou et al., 2016; Landy, 2010), however the clearance height decreases compared to unrestricted obstacle avoidance (Evangelopoulou et al., 2016). Assistive devices can also increase the lower limb mass of an amputee compared to healthy individuals. Immediate increases in ankle dorsiflexion are responsible for significant contribution to safe clearance when an external mass affects knee joint kinematics (Noble & Prentice, 2006). Ankle dorsiflexion appears to be critical for fine-tuned adjustments to toe clearance in both weight limb and joint restriction studies (Evangelopoulou et al., 2016). After adaptation to the new segmental properties of the limb (increased shank segment weight) knee flexion and ankle dorsiflexion change towards normal walking conditions in response to the change of work conducted at knee and hip joints (Noble & Prentice, 2006). Walking with mechanical (i.e. mobility restricting knee brace) and physiological (i.e. quadriceps external stimulation) interventions are two different ways to impose stiff-knee gait pattern and decrease attainable knee flexion during walking. In response to mechanical knee restriction hip hiking influence toe clearance whereas, a combined hip circumduction and hip hike strategy responds to physiologically controlled stiff-knee gait (Lewek, Osborn, & Wutzke, 2012). In both imposed restriction techniques, individuals decreased their stance time on their affect limb as strategy to increase stance on limb with more control. Overall, healthy subjects are able to adapt to new movement patterns in response to perturbations to normal walking patterns. Asymmetries can arise to control for stability and avoid potentially instable postures.

Distance of foot-off prior to obstacle clearance is another tightly controlled spatiotemporal measurement in obstacle avoidance (Patla & Greig, 2006). Foot placement around the obstacle also

changes in response to ankle restriction. Without full ankle mobility, foot placement increases before the obstacle to provide more time to increase the limb height for appropriate clearance. Trail limb placement before the obstacle increases and lead limb placement after the obstacle decreases, simultaneous change of these placements counteracts changes to the stride length (Evangelopoulou et al., 2016). Decrease in foot placement after the obstacle is also seen in amputee populations when crossing with their prosthetic limb (Hill et al., 1999). Decrease in foot placement after obstacle clearance allows for control of the center of mass clearing the obstacle and safe comfortable loading (e.g. decrease ground reaction force) of the affected limb. During early stance, the lower limbs act as a dampening tool to absorb the shock from the ground reaction force and weight acceptance (Winter, 1991). During amputee gait, the lower limb decreases ground reaction peak force and loading rate after obstacle clearance (Buckley, De Asha, Johnson, & Beggs, 2013). This is a similar compensatory movement seen in amputees and compensates for inability to utilize joint range of motion for support loading and ground reaction force (GRF) dampening. Conservative control and placement of the limb indicated by decreased peak force and loading rate in amputees (Buckley et al., 2013), decreased step length past obstacle in restricted ankle mobility (Evangelopoulou et al., 2016), and decreased foot velocity prior to foot contact after clearing tall obstacles (Patla & Rietdyk, 1993) could lead to investigation increased control of stability during obstacle clearance.

3.1.4 Support measures to probe stability – healthy and compromised

Base of support (BOS) size relates to the balance during walking, larger base of support is more stable. Base of support changes between *double* and *single leg support. Double leg support* is when two feet are in contact with the ground and is often the most stable portion of the gait cycle because the BOS is largest. Total double support time makes up 16-22% of the gait cycle (Winter, 1991). *Single leg support* is the period when one limb supports body weight while the contralateral limb is above the ground to prepare for the next step. The center of pressure is the summation of all the ground reaction forces acting on the body. During normal gait, the center of pressure corrals the center of mass to

maintain dynamic stability as the base of support changes state and size. Dynamic stability during walking to avoid falling is important for healthy and special populations. Compensations to increase stability or confidence in walking pattern can be common for amputees and include reduce walking speed, increase step width, and increase double support time (Kendell, Lemaire, Kofman, & Dudek, 2015). Analysis of center of mass movement with respect to the center of pressure during obstacle avoidance (Huang et al., 2008) and volitional and reactive stepping responses (Singer, McIlroy, & Prentice, 2014; Singer, Prentice, & McIlroy, 2013) probe the dynamic stability of the motor control system. Older adults tend to decrease the distance between their center of mass and center of pressure during obstacle crossing, level ground walking, and the restabilisation phase of volitional stepping (Huang et al., 2008; Lugade, Lin, & Chou, 2011; Singer et al., 2014). Older adults have lower COM control by exemplifying larger COM excursions when compared to the final resting center of mass position after volitional stepping (Singer et al., 2013). Analysis of the COM and COP in a laboratory setting allow for robust descriptions of dynamic stability, however are not applicable outside of the laboratory setting. Temporal measure of gait, double support time, can provide insight to the stability control of the motor system. The BOS is larger and encompasses the COM during double support, whereas the BOS is smaller and the COM may exist outside the BOS during single support. Unilateral transfemoral amputees, increase their double support time when transitioning into affected single leg stance when compared to transitioning onto their intact limb (Schaarschmidt, Lipfert, Meier-Gratz, Scholle, & Seyfarth, 2012; Schmid, Beltrami, Zambarbieri, & Verni, 2005). Single leg stance times are also shorter for the amputated limb compared to the intact limb (Hof, van Bockel, Schoppen, & Postema, 2007; Schaarschmidt et al., 2012). These two temporal control features reduce the risk of falling by increasing control of the COM movement towards a less stable limb and reduce the time of single leg support with a less stable limb (Hof et al., 2007; Schaarschmidt et al., 2012). Double support phases are asymmetric when evaluating a range of gait velocities produces. Change in asymmetrical pattern is driven by changes to the intact limb required to achieve gait velocity (decrease double support and single leg support times), rather than a change in affected limb pattern, indicating a preference/reliance of intact limb movement (Schaarschmidt et al.,

2012). Healthy individuals increase their double support time bilaterally when their normal swing phase is perturbed with decreased knee range of motion (Temel, Rudolph, & Agrawal, 2010); however, limited studies have examined the change in stability/support times in locomotor adaptation of healthy individuals.

Spatiotemporal parameters can probe the stability of locomotor control by evaluating step width (Owings & Grabiner, 2004). In the amputee population, increases in double support time when transferring to the affected limb and step width are techniques employed to increase stability during walking (Hak, Van Dieën, et al., 2013; Hak, Houdijk, Beek, & Van Dieë, 2013). Changes to double support time detected with an IMU have evaluated the stability of movement patterns with and without external mass (Cain et al., 2016). Walking with a weighted backpack significantly increases double support time of stride and stride time increases to provide more stability for the locomotor system (Cain et al., 2016). IMUs have yet to examine the difference between double support phases with constrained walking in healthy adults to probe changes in stability of the walking pattern as an indicator an potential tool for compromised gait patterns.

3.1.5 Detecting changes kinematic outcome measures with IMUs

The benefits of inertial measurement units in a clinical scenario provide valuable feedback for clinician decision making during gait assessments or haptic and sensory feedback during training (Shull et al., 2014). Audio biofeedback has provided increase postural control in patients with mobility and balance control problems (Chiari et al., 2005) and has the potential to outline compensatory or aberrant movements in patients with motor control problems. Sensors can track personnel walking direction and location without relying on GPS measurement (Ojeda & Borenstein, 2007). Clinical application of these devices is a smaller scale but requires more detail compared to larger scale tracking. One particular gait analysis method, stride-by-stride analysis, has proven to be suitable for spatiotemporal gait analysis using inertial measurement units (Trojaniello et al., 2014). Evaluation of the ability to detect changes to spatiotemporal characteristics of walking are important for clinical assessment. Stride length and width

estimates both increased when young healthy adults walked with their eyes closed compared to eyes open. Simultaneous collected motion capture data also distinguished between vision conditions and reported a low percent error between gold-standard MC and IMU estimation spatial data (Rebula et al., 2013). Tripping is main mechanism for falling in elderly and the amputee population and the ability to detect minimum ground clearance and the variability associated with minimum clearance can be explored with inertial measurement units (Mariani, Rochat, Büla, & Aminian, 2012). Spatiotemporal measures have evaluated elderly and neurological disorders with association to fall risk. Comparing stride length (SL), foot clearance (FC), and stride velocity (SV) to a motion capture system shows high correlation values in both elderly and healthy adults while walking along a figure-eight walkway (SL (ICC = 0.91), FC (ICC = 0.96), SV (ICC = 0.93)) (Mariani et al., 2010). Stride length and stride velocity measures derived from inertial sensors were not sensitive enough to distinguish between young and elderly adults, however that variability associated with consistent direction changes and acceleration phases may confound those differences. Elderly adults exhibited lower foot clearance values measured with inertial sensors compared to young healthy adults during straight walking and turning. Minimum clearance distinguished between populations but magnitude of angular velocity at minimum foot clearance was not significantly different between ages showing the utility for deriving spatial measures (Greene et al., 2011; McGrath et al., 2011). Detecting vertical displacement of the foot can evaluate the ability to avoid obstacles in everyday life. Increases in height of the foot during obstacle crossing is detectable with IMU devices and not significantly different than gold-standard measures (Trojaniello et al., 2015). Due to surgical outcomes, the amputee population can have difficulty increasing their foot during swing phase, which increases their risk of tripping. There has been little work applying IMUs to describe vertical displacements in foot elevation to distinguish between normal and compensatory movements. The ability to detect changes in vertical displacement of the foot expands the utility of wearable sensors to examine different tasks and populations.

Inertial sensors applied to the amputee population explore asymmetries, step lengths, and walking speed. Integrating acceleration from a single tri-axial accelerometer on the lower back was able estimate

step lengths in healthy and amputee subjects (Major, Raghavan, & Gard, 2015). Estimates of step length in the healthy controls showed mean error of -0.1 (17.1) percent of the gold standard measure, while amputee mean errors increased to -1.0 (15.3) percent of gold standard. Differences between the devices were step dependent. Initial steps were significantly larger when estimated from accelerometry compared to motion capture, while subsequent steps appear to underestimate step length (Major et al., 2015). The large amount of variability associated with the step length error are attributed to common initial step outlier's however a bias would most likely exist if first steps were removed due to consistent underestimation. Placement of IMU is most likely to attribute to these differences. Event detection from trunk worn IMUs extrapolates acceleration for event detection causing error in temporal events of gait (Zijlstra & Hof, 2003), accelerometers attached closer to the event of interest may have better gait event detection due to the impulse of the ground reaction force. Error in event detection can cause exacerbated differences in spatial estimation after double integration. Ankle-worn IMUs have been shown to produce accurate event detection across variable gait patterns (Trojaniello et al., 2014), which is important for the accuracy of temporal measures. ZUPT technique calculates drift-free velocity under the assumption that zero-velocity occurs at certain time points in the gait cycle (Peruzzi et al., 2011) or foot orientation such as flat foot (Kitagawa & Ogihara, 2016; Mariani, Rouhani, Crevoisier, & Aminian, 2013; Rebula et al., 2013). During level ground walking, with negligible change in vertical height of the walkway, removing drift in the second iteration of integration can improve the ground clearance estimation (Kitagawa & Ogihara, 2016). Stride length measurements have similar error rates to other studies estimating stride length but improved the estimation of vertical trajectory from ~10-20 mm (Mariani et al., 2010, 2012) to 2 ± 7 mm (Kitagawa & Ogihara, 2016). Improvements to vertical trajectory tracking during obstacle avoidance are also shown with ankle worn IMUs in elderly (1 ± 10 mm) and PD patients (2 ± 20 mm) when compared to motion capture (Trojaniello et al., 2015). Little research has begun investigating the frontal plane kinematics with inertial sensors. Lateral swing parameters between genders is not different when calculated using inertial sensors attached to the foot (Dadashi et al., 2013). During level ground walking, mean lateral deviation is estimated at 0.04 (0.01) m. Determining differences between groups

during compensatory movements is unclear. Frontal plane kinematic outcome measures are topical for populations with lower limb mechanical dysfunction (e.g. amputees, knee replacement, etc.) and those who adopt frontal plane movements (Bowker et al., 1992; Byrne & Prentice, 2003; Hill et al., 1997; Vrieling et al., 2007). If IMU devices can characterize frontal plane compensatory movements, assessment and quality of care for these populations could utilize quantifiable measures to improve the care of these patients.

3.1.6 Rationale, Objective, and Hypothesis

The clinical use of wearable sensors could improve intervention and rehabilitation by providing quantitative measures to better guide clinical decision making. As revealed in study 1 of this thesis, inertial sensors can be used, unobtrusively, to quantify kinematic outcome measurements to characterize human movement. The ability to distinguish specific lower limb movement characteristics is unknown.

The main objective of this study is to determine if spatial and temporal features of movement kinematics can be determined from IMU-based outcome measures by comparing normal and compensatory movements when obstacle avoidance and mechanical restriction challenge healthy individuals. Compensatory movements during obstacle stepping tasks were evoked in healthy population who wore a range limiting knee brace. Task conditions replicate amputee movement restrictions and reveal the utility of orthotic devices as a tool to research the amputee community. Specifically, the study set out to determine if it was possible to measure lateral limb movement, hip hiking, and limb clearance during knee joint constraint conditions (mechanical bracing) during stepping over obstacles. As noted, these task challenges are initially tested in this study in young healthy adults in an attempt to evoke the types of gait adaptations expected among individuals with restriction occurring due to disease or prosthetic intervention.

(1) It is hypothesized that spatially derived kinematic measures from IMUs during braced knee conditions will be characterize by increased lateral end point deviation compared to unlocked and no brace conditions for obstacle crossing and level ground walking. Further, there will

only be a significant difference for the obstacle condition when the subject has restricted range of motion (locked brace).

(2) It is hypothesized that spatially derived kinematic measures from IMUs of maximum endpoint limb elevation will have a main effect of obstacle condition. Obstacle crossing limb elevation will be significantly different from level ground walking for all brace conditions.

(3) It is hypothesized that spatially derived kinematic measures from IMUs of hip hiking will have a main effect of brace and obstacle condition. Locked brace hip hiking will be significantly different from both no and unlocked brace conditions. Further, increase of hip hiking will occur during obstacle avoidance compared to level ground walking.

3.2 Methods

3.2.1 Participants

Twelve young healthy adults, absent of neurological or mechanical dysfunction, were recruited for this study and provided informed consent. This project was reviewed and approved by University of Waterloo Office of Research and Ethics. Exclusion criteria included: (1) if participants had previous knee injury and were accustom to a external frame knee brace, (2) had current lower limb injury that caused movement deviation from their normal pattern, (3) lower limb injury within the last 6 months that caused tissue damage, or (4) had any health complications that may interfere with exercise. Participant anthropometric data was collected at the beginning of each collection: mean (SD) age 23.17 (4.17) years, height 1.73 (0.13) m, weight 78.32 (21.04) kg, right leg length 0.92 (0.07), left leg length 0.92 (0.07) and leg dominance (Table 15).

Table 15. Participant anthropometric and descriptive information for Study #2.

Subject	Age (years)	Gender	Height (cm)	Weight (kg)	Right Leg Length (cm)	Left Leg Length (cm)	Leg Dominance	Brace Size
001	22	M	1.84	91.4	0.96	0.97	Right	L
002	26	F	1.66	57.4	0.84	0.84	Right	M
003	25	M	1.93	105.6	1.01	1.01	Right	XL
004	27	M	1.57	88.4	0.86	0.86	Right	L
005	19	F	1.63	54.9	0.84	0.83	Right	M
006	19	F	1.59	107	0.88	0.88	Left	M
007	20	M	1.81	48.6	0.99	0.98	Right	L
008	23	M	1.90	87	0.98	0.98	Right	L
009	24	M	1.89	88.6	0.99	0.99	Right	L
010	33	M	1.70	93.2	0.92	0.91	Right	XL
011	19	F	1.67	58.5	0.90	0.90	Right	M
012	21	F	1.62	59.2	0.83	0.84	Right	M

3.2.2 Collection Protocol

Participants completed 15 level ground and obstacle avoidance trials under three different brace conditions for the duration of this collection (Figure 19). An orthotic off-the-shelf knee brace was used to manipulate the attainable knee flexion, in specific locked brace trials, with the goal to replicate movement patterns in pathological gait (Figure 20). In total, participants were to complete 45 successful level ground walking and 45 obstacle avoidance walking trials during this collection (15 trails of each brace condition). Trials were excluded if participant cleared the obstacle with their right limb as the lead limb, tripped the obstacle, false starts, or any stumbling during starting. Participant starting position adjustments ensure lead limb consistency across all brace and obstacle conditions. No brace walking conditions were completed as the first and last block of conditions. Dividing this condition ensured that learning effects of compensatory movements did not linger into normal walking patterns.

Block 1 - NB PRE	**Block 2 - UB**	**Block 3 - LB**	**Block 4 - NB POST**
- 7 Level ground walking trials - 8 Obstacle avoidance - No knee brace	- 15 Level ground walking trials - 15 Obstacle avoidance - Unlocked knee brace	- 15 Level ground walking trials - 15 Obstacle avoidance - Locked knee brace	- 8 Level ground walking trials - 7 Obstacle avoidance - No knee brace

Figure 19. Block diagram outlining collection block details and sequence for Study #2.

Figure 20. (a) CTI® OTS Knee Brace (Ossur (UK) Ltd, Stockport, UK) used on the present study. (b) Flexion Stops (Ossur (UK) Ltd, Stockport, UK) used as the locking mechanism for the knee brace to reduce knee flexion.

Baseline level ground and obstacle avoidance movement patterns were collected with participants under normal walking conditions. The brace with full range of motion (unlocked brace) was affixed to the participant's right limb (sizing followed suggestions from brace website) (Table 16) and was fitted for comfort of the participant. Participants completed walking trials with unlocked knee brace to determine if there was an affect of unlocked knee brace (passive restriction) to level ground and obstacle avoidance strategies. Lastly, flexion stops added to the knee brace to limit the attainable knee flexion and examine the ability to detect compensatory kinematic outcome measures during level ground and obstacle avoidance walking trials.

Table 16. Brace sizing guideline.

Size	Caliper Measurement (Knee Width)
Small	90 – 100 mm
Medium	100 – 115 mm
Large	115 – 120 mm
X-Large	120 – 130 mm
XX-Large	130 – 145 mm

3.2.2.1 Walking Path

The walking path was 1.25 metre wide and six metres in length. Participants were able to walk both ways on the walking path. Therefore, at the end participants were given instruction to turn around to

prepare for the subsequent trial. Instructions were read at the beginning of each block when the brace condition changed:

"The goal of this task is to walk at a comfortable speed, down the walkway and just past the end line. It is not necessary to stop directly at the end line but you can stop when you are comfortable after the line. At the beginning of each trial please try to stand as still as possible and you can start walking on my cue. When you stop at the end, please remain still until I cue you to turn around and step up to the start line."

During the obstacle avoidance trails an obstacle was setup at the three metre mark, halfway down the walkway. The obstacle was square wooden bar (1.25 m length x 0.04 m wide x 0.04 m height). The obstacle was set up to be 0.14 m high measured to the top edge and was placed on top of two blocks that were 1.25 metre apart. The obstacle was setup so that if a participant was unable to clear the obstacle, the bar would fall to the ground (Figure 21).

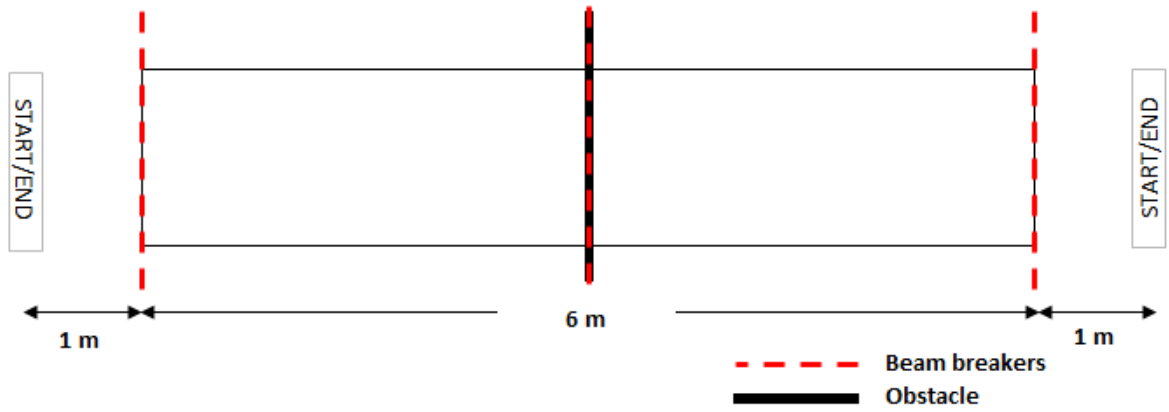

Figure 21. Gait task walkway. Obstacle was placed halfway between the start and end sections and was removed on level ground walking tasks. Beam breakers were start up at start, end and middle of walkway to synchronize step counts within a certain distance and obstacle crossing timing.

3.2.3 Instrumentation

3.2.3.1 Inertial Measurement Units

Shimmer3 Bridge Amplifier+ IMUs attached bilaterally to the ankles and Shimmer3 IMU attached to a belt above the right hip recorded human movement. A comfortable strap wrapped around the ankle and secured the IMU 0.04 m above the lateral malleolus. Hook and loop secured the hip worn IMU to a fabric belt around the subject's waist (ideally placed around the iliac crests of the pelvis). Shimmer

IMUs were calibrated following the same protocol in Study 1. Unit configurations were completed using proprietary software ConsensysPRO (Shimmer Sensing Inc., Dublin, Ireland). Shimmer3 IMUs were configured with both low-noise (±2g) and wide-range (±8g) accelerometers, gyroscope (±1000 degrees per second), magnetometer (1.3 kPa), quaternion orientation (9- and 6-degrees of freedom), the resistance amplifier, and a UNIX time stamp. Shimmer3 IMU units streamed via Bluetooth for visual purposes and logged data onto a 32 GB SD card for data analysis purposes to avoid missing data points lost in the streaming system. IMU collection frequency was set to a priori available frequencies, determined by Shimmer Sensing Inc., at 102.4 Hz.

3.2.3.2 Foot Switches

Participants were fitted with foot switches on the heel pad and forefoot of both right and left feet. Hypafix® tape managed wire placement and secured footswitches to bottoms of feet. An amplifier box is attached to the participant's waist belt that sends a 3.5 V signal to the Shimmer3 Bridge Amplifier+ resistance channel that will be used to confirm foot fall detection algorithms with IMU generated signals.

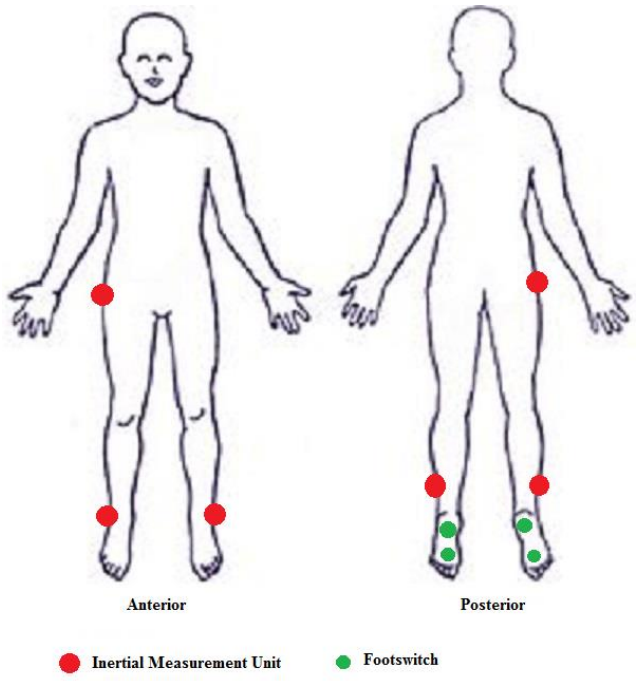

Figure 22. IMU placement on lower limb (4 cm above lateral malleolus). Footswitches were secured with Hypafix® tape to the bottom of the heel and forefoot for gait event confirmation.

3.2.3.3 Data Synchronization

Three beam breakers were setup at each end of the walking path and at the location of the obstacle, 2 metre across the walking path. When the beam is interrupted, a 3.5 V square wave is recorded onto a single Shimmer3 Bridge Amplifier+ unit sitting off the side of the walking path. The 3.5 V square wave indicates when participants are stepping over the obstacle and would be used to capture the crossing stride characteristics to describe compensatory movement while participants were stepping over the obstacle (Figure 21). The single IMU also receives signals when the start and end beams are broken, which indicate the beginning and ending of each walking trial.

UNIX timestamp recorded at the leading and last edge of the square wave recorded from the beam breakers along the walking path synchronized the Shimmer3 IMU units. Using the corresponding timestamps, data was sectioned into window of walking trial data.

3.2.4 Data Processing

Inertial measurement units were filtered using a dual pass 2nd order Butterworth band-pass filter. Low-pass frequency cut-off was determined with a residual analysis (Winter, 2009) and high-pass cut-offs were determined from previous conducted research studies (Trojaniello et al., 2014; Zok et al., 2004). Band-pass filter had a passband of 0.05-18 Hz. Data was filtered using the Matlab® filtfilt function for dual pass filtering.

After processing and windowing data into walking trials from SD log data, three distinct steps are used to output kinematic outcome measures: (1) stride segmentation, (2) rotation of IMU signals into motor task frame of reference, and (3) double integration and drift removal of acceleration signals.

3.2.4.1 Stride Segmentation

Walking trials are segmented into stride-by-stride analysis that allows definition of walking characteristics per stride and reduce integration drift effect. For drift removal, the final integration value is known. Instances of assumed zero velocity have been previously used to de-drift estimated velocity signals after acceleration. Periods of zero-velocity are not common during walking, however when the

foot comes in contact with the ground, it is assumed no movement occurs unless there is a slip or shuffling gait pattern. Under this assumption instances of zero-velocity have been assumed as the whole stance period (Rebula et al., 2013) or specific instances, such as 40% of stance phase, which was used for this study (Peruzzi et al., 2011; Trojaniello et al., 2014). To segment walking trials to stride data consecutive footfall data is determined. Trojaniello et al. (2014) developed a footfall detection algorithm to detect footfall events in healthy, elderly, choreic, hemiparetic, and parkinsonian gait patterns. The algorithm utilizes angular velocity and linear acceleration waveforms to detect initial and final contact instances and relies on outlining periods of known stance and swing phases according to these sensors. Swing phase was defined as a period of angular velocity that is greater 30% of local maximum angular velocities recorded in the sagittal plane (about the z-axis). During swing phase the contralateral limb is assumed to be in contact with the ground. Two minimum duration thresholds are applied to known swing and stance phases to accommodate signal drop-out or quick oscillations around a previously used threshold. Detected swing periods had to be at least 100 ms in duration and time between consecutive swing phases minimum time duration was 200 ms (Trojaniello et al., 2014). After determining swing and stance phases footfall search windows are defined. Toe-off search window is the period of time between stance phase and swing phase, while heel strike search window is between the swing and stance phases. Final contact is defined as the minimum mediolateral angular velocity in FC search window. Initial contact is defined as the minimum anterior posterior acceleration in the IC search window (Diana Trojaniello et al., 2014). These footfall detection methods were applied to all walking trials to segment the data, walking trials were segmented into strides with final contact events as stride definition boundaries.

Footswitch data confirmed gait event detection with IMU algorithm. Square wave foot switch data was used to detect initial and final contact using a threshold crossing. FSW threshold was calculated as the average of the signal recorded by the resistance amplifier received from the footswitch on ankle worn IMUs. Threshold crossing with a positive slope indicated initial contact and a negative slope

indicated final contact. After confirmation, 40% stance phase was calculated and used for de-drifting the velocity and position estimations.

3.2.4.2 Rotation to Task Frame of Reference

Local frame acceleration vectors are rotated into a global frame of reference using methods described in Study 1 (McGinnis & Perkins, 2012). Inertial frame of reference was created such that, the x-axis was anterior posterior with the direction of progression measuring positive, the y-axis was vertical and aligned with gravity, and the z-axis was the mediolateral axis with positive values pointing to the right of the participant. With this reference frame, all rightwards movements were recorded as positive and all leftwards movements were recorded and negative.

3.2.4.3 Double Integration and Drift Removal

Position data was estimated by double integrating accelerometer data in the global reference frame and removing drift with linear function subtraction, similar study 1. During walking trials, integration period occurred between assumed zero-velocity instances within each gait cycle (at 40% stance phase).

With the advantage of small time intervals, linear drift is assumed during stride integration time periods (between 40% stance). Linear drift removal was applied to vertical and mediolateral acceleration signals. Drift removal to vertical acceleration signals assumes the foot returns to the level ground after swing phase. Since walking path is assumed to be level ground (any change in walking surface is negligible) this linear drift removal technique is considered acceptable. Frontal plane swing characteristics are improved significantly when data is de-drifted in a similar fashion along the ML axis as conducted on the vertical axis (Mariani et al., 2010). Therefore, de-drifting techniques were applied to both vertical and mediolateral acceleration signals.

3.2.5 Outcome Measures

Kinematic outcome measures derived from double integrated, drift corrected accelerometer signals describe the movement pattern adopted to overcome obstacles. Maximum peak elevation of the foot during swing phase represents the change in height of foot to clear the ground or obstacle when walking. Maximum lateral deviation of foot during swing phase represents the frontal plane movement of the swinging foot during level ground and obstacle clearance. Hip hiking is the total vertical displacement of the hip during ipsilateral swing phase. Temporal measures of interest are defined by the gait events detected with the IMU footfall algorithm. Swing time is the time in seconds between the final contact (foot leaves the ground) to the initial contact of the ipsilateral limb (foot is in contact with ground). Double support time is the time between one limb's heel strike and the contralateral limb's toe-off. Left double support time is between the left heel strike and the right toe-off, while right double support time is between the right heels trike and left toe-off.

Table 17. Outcome measure description to characterize compensatory movements typically seen in the amputee population.

Outcome Measure	IMU Sensor	Definition
Maximum Elevation	Bilateral Shank-mounted	• Maximum vertical distance attained within the swing phase of gait
Peak Lateral Deviation	Bilateral Shank-mounted	• Maximum lateral deviation of the swinging foot
Hip Hiking	Hip	• Maximum change in height of hip during swing phase

Double Support Time	Bilateral Shank-mounted	• Time spent with two feet on the ground
		• Right DST:
		  ○ Time (s) from RHS to LTO
		• Left DST:
		  ○ Time (s) from LHS to RTO

Swing Time	Bilateral Shank-mounted	• Time between final and initial contact of ipsilateral limb

3.2.6 Statistical Analysis

All statistical tests performed in SPSS Statistics (IBM Corporation, Armonk, New York, United States) and significance was evaluated at $p = 0.05$. Pearson ® correlation determined the association of footfall

events between switches and algorithm. To compare PRE and POST brace condition outcome variables a one-way repeated measures analysis of variance was conducted on both level ground and obstacle avoidance. For the brace and obstacle avoidance conditions a two way repeated measures analysis of variance (ANOVA) to determine differences between outcome variables. Dependent variables are listed in Table 17. Violations to sphericity were corrected with the Greenhouse-Geisser correction factor. Post-hoc tests were completed with a Bonferroni correction to determine significant differences. When interaction effects were significant, t-test pairwise comparisons were completed with a Bonferroni correction applied to detect significance.

3.3 Results

3.3.1 Gait Event Detection Algorithm

To ensure the ability to identify foot falls using IMUs in order to segment the movement comparisons were initially made between IMUs and footswitch data. Descriptive footfall statistics were used to summarize the total number of events detected (e.g. right final/initial contact, left final/initial contact). Footfall algorithms were successful in reporting gait events during all conditions. Algorithm and footswitch techniques successfully detected 99.87% of all data, with an error rate of 0.13% for all gait events and conditions. Pearson (*r*) and mean average error are described in Table 18.

Table 18. Results from correlations of gait event detection using IMU algorithm compared to the timing from foot-switches on the bottom of feet.

Brace Condition		**Right IC**		**Right FC**		**Left IC**		**Left FC**	
		R^2	*P*	R^2	*p*	R^2	*p*	R^2	*p*
No Brace	No Obstacle	1.000	<.001	1.000	<.001	1.000	<.001	1.000	<.001
	Obstacle	0.999	<.001	1.000	<.001	1.000	<.001	1.000	<.001
Unlocked Brace	No Obstacle	0.998	<.001	1.000	<.001	0.999	<.001	1.000	<.001
	Obstacle	0.999	<.001	1.000	<.001	0.999	<.001	1.000	<.001

Locked Brace	No Obstacle	0.999	<.001	1.000	<.001	0.999	<.001	1.000	<.001
	Obstacle	0.999	<.001	1.000	<.001	0.999	<.001	1.000	<.001

3.3.2 Effect of Unlocked and Locked Brace Conditions on Normal Unrestricted Movement Patterns

To ensure that there was no carryover effects of wearing the brace (no long-term training effects) it was initially important to compare pre brace condition level ground and obstacle clearance to post brace condition movement patterns. This allowed evaluation of the effect of restricted knee range of motion on normal walking patterns to determine the potential of learning. Descriptive statistics for spatial and temporal level ground walking characteristics are present in Table 19. There was no significant main effect for pre or post brace condition for any level ground walking right and left temporal or spatial measures. One-way repeated measures ANOVA also compared obstacle clearance values for pre and post brace conditions. No significant differences were found for obstacle clearance measures (Table 19). No significant difference suggest no long lasting brace effects for kinematic outcome measures when comparing pre and post brace worn conditions. Results suggest trials prior to and after can be collapsed to a single factor (no brace) for further analysis.

Table 19. Summary of results of PRE and POST brace condition outcome measures**.**

		MEAN (SD)		**ANOVA RESULTS PRE vs. POST BRACE**	
Level Ground Walking		*PRE BRACE*	*POST BRACE*	*F*	*p*
Right Swing Time	(s)	0.40 (0.032)	0.40 (0.031)	0.001	0.980
Right Stance Time	(s)	0.69 (0.054)	0.67 (0.044)	0.357	0.556
Right Max Elevation	(m)	0.15 (0.015)	0.14 (0.014)	1.472	0.238
Right Max Lateral Deviation	(m)	0.01 (0.019)	0.009 (0.020)	0.056	0.815
Hip Hiking	(m)	0.03 (0.013)	0.03 (0.012)	0.038	0.847
Left Swing Time	(s)	0.38 (0.045)	0.37 (0.033)	0.014	0.906
Left Stance Time	(s)	0.71 (0.051)	0.69 (0.033)	1.144	0.296
Left Max Elevation	(m)	0.14 (0.013)	0.14 (0.018)	0.318	0.579
Left Max Lateral Deviation	(m)	-0.03 (0.021)	-0.03 (0.021)	0.010	0.919

Obstacle Crossing		*PRE*	*POST*	*F*	*p*
Right Swing Time	(s)	0.49 (0.036)	0.50 (0.033)	0.296	0.592
Right Stance Time	(s)	0.67 (0.060)	0.67 (0.037)	0.004	0.951
Right Max Elevation	(m)	0.37 (0.041)	0.37 (0.037)	0.021	0.887
Right Max Lateral Deviation	(m)	0.003 (0.022)	0.006 (0.026)	0.109	0.745
Hip Hiking	(m)	0.03 (0.020)	0.03 (0.018)	0.004	0.948
Left Swing Time	(s)	0.55 (0.040)	0.57 (0.042)	0.788	0.384
Left Stance Time	(s)	0.75 (0.081)	0.74 (0.055)	0.182	0.674
Left Max Elevation	(m)	0.31 (0.033)	0.32 (0.039)	0.406	0.531
Left Max Lateral Deviation	(m)	-0.09 (0.038)	-0.09 (0.036)	0.108	0.746

3.3.3 Main Effect of Brace and Obstacle Condition

3.3.3.1 Lateral Deviation of Right (braced/trailing) and Left Limb (unrestricted/lead)

For level ground walking mean (SD) of right lateral deviation during NB is 0.01 (0.019) m, UB is 0.009 (0.02) m, and LB is 0.01 (0.018) m. During obstacle crossing mean (SD) of NB is 0.005 (0.023) m, UB is -0.008 (0.032) m, and LB is -0.157 (0.068) m (Figure 23). Two-way repeated measures ANOVA evaluated the effect of brace and obstacle conditions on lateral deviation of the left foot obstacle crossing. Main effect of both brace, $F(2,22) = 71.115$, $p < .05$, and obstacle conditions, $F(1,11) = 57.918$, $p < .05$. Interaction effects between obstacle and brace conditions were also statistically significant, $F(2,22) = 67.026$, $p < .05$. Post-hoc pairwise comparisons with a Bonferroni correction were used to compare obstacle and brace conditions. Locked brace lateral foot deviation during obstacle avoidance was significantly larger than during level ground walking, $t(11) = 8.608$, $p < .05$. Locked brace lateral deviations was significantly different from no brace, $t(11) = 8.954$, $p < .001$, and unlocked brace, $t(11) = 7.974$, $p < .001$, condition during obstacle avoidance. No significant difference of right foot lateral deviation was found between no brace and unlocked brace conditions during either level ground walking or obstacle crossing.

During level ground walking left mean (SD) lateral deviation for NB is -0.029 (0.021) m, UB is -0.029 (0.023) m, and LB is -0.029 (0.020) m. For obstacle crossing mean (SD) for NB is -0.09 (0.034) m, UB is -0.096 (0.036) m, and LB is -0.083 (0.03) (Figure 24). No significant differences were found with left foot lateral deviation during swing for brace conditions, $F(2,22) = 2.266$, $p = .146$. Lateral deviation of the left foot was significantly lower (larger medial deviated foot movement during swing) during obstacle avoidance compared to level ground walking, $F(1,11) = 83.344$, $p < .05$. No significant interactions existed between obstacle and brace conditions ($F(2,22) = 2.075$, $p = .160$).

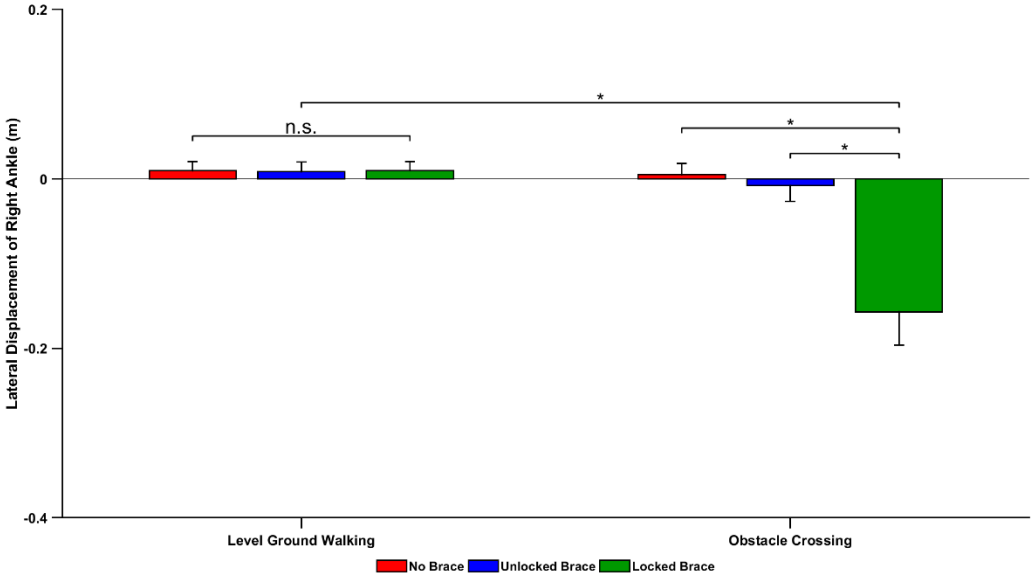

Figure 23. Lateral deviation of the right limb during clinical gait tasks comparing the lateral deviation that is present during obstacle avoidance and level ground walking with three different brace conditions (no brace, unlocked, locked brace). Negative values represent movement to the right (laterally) for the right limb. Significant differences (*) and not significant differences (*n.s.*) are denoted on figure.

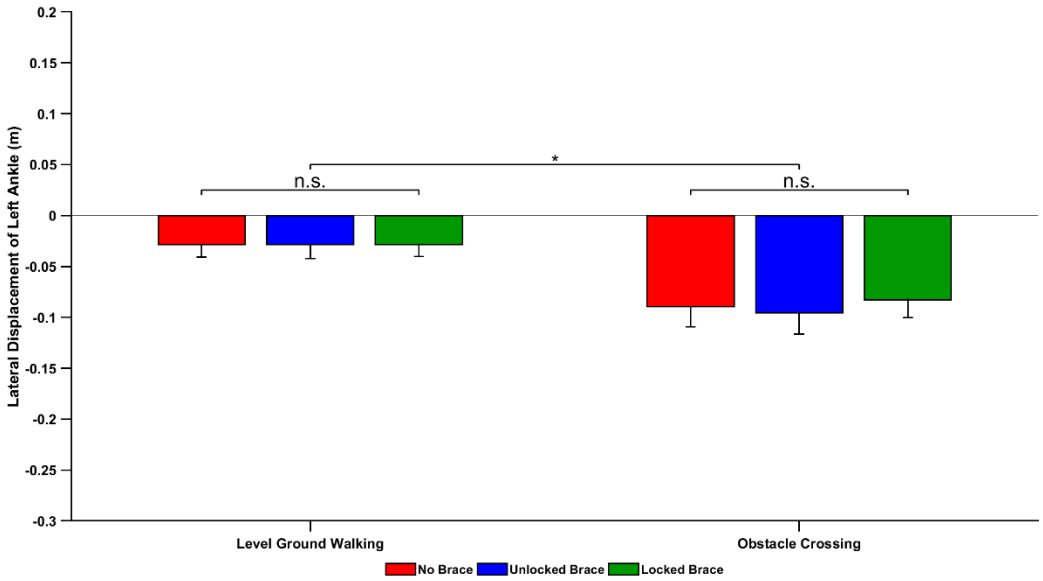

Figure 24. Lateral deviation of the left limb during clinical gait tasks comparing the lateral deviation that is present during obstacle avoidance and level ground walking with three different brace conditions (no brace, unlocked, locked brace). Negative values represent movement to the right (medially) for the left limb. Significant differences (*) and not significant differences (*n.s.*) are denoted on figure.

3.3.3.2 Max Elevation of Right (braced/trailing) and Left Limb (unrestricted/lead)

Table 20 provides a summary of spatial estimates for right and left foot maximum elevation and lateral deviation during level ground walking and obstacle crossing for all brace conditions. For level ground walking conditions, the mean (SD) of NB are 0.148 (0.013) m, UB are 0.138 (0.014) m, and LB are 0.114 (0.017) m (Figure 25). Obstacle crossing conditions means (SD) for NB are 0.373 (0.034), UB are 0.335 (0.034), and LB are 0.269 (0.039). Two-way repeated measures ANOVA results indicated a main effect of brace condition, $F(2,22) = 50.741$, $p < .05$, and obstacle condition, $F(1,11) = 704.230$, $p < .05$, for right foot max elevation measures. ANOVA results also indicate an interaction effect of brace and obstacle conditions, $F(2,22) = 36.291$, $p < .05$. Post-hoc pairwise comparisons with a Bonferroni correction factor on both brace and obstacle variables indicated significant differences between level ground walking and obstacle clearance right foot elevation between all conditions. Right foot max elevation for obstacle crossing was significantly larger than level ground walking for all brace conditions (no brace, $t(11) = -28.123$, $p < .001$, unlocked brace, $t(11) = -24.464$, $p = < .001$, locked brace, $t(11) = -$

15.600, $p < .001$). When subjects had full range of motion their max elevation value was significantly larger during NB level ground walking compared to UB, $t(11) = 4.915$, $p < .001$, and LB conditions, $t(11) = 5.881$, $p < .001$ and during obstacle crossing compared to unlocked, $t(11) = 4.761$, $p < .001$, and locked brace conditions, $t(11) = 8.000$, $p < .001$. Further, there were significant differences between unlocked brace compared to locked for both level ground walking, $t(11) = 4.034$, $p < .05$, and obstacle avoidance, $t(11) = 6.934$, $p < .05$.

For level ground walking, the mean (SD) of NB is 0.138 (0.016) m, UB is 0.136 (0.013) m, and LB is 0.130 (0.02) m for left foot maximum elevation values. During obstacle crossing the mean (SD) for NB is 0.312 (0.33) m, UB is 0.311 (0.03) m, and LB is 0.340 (0.027) m (Figure 26. ANOVA results indicate a main effect of obstacle, $F(2,22) = 501.878$, $p < .05$, but not brace conditions, $F(1, 11) = 3.130$, $p = .086$, for the left foot max elevation measures. A significant interaction effect between brace and obstacle conditions for left foot max elevation, $F(2,22) = 704.230$, $p < .05$, was calculated. Post-hoc pairwise comparisons with Bonferroni correction factor conducted on left foot max elevations measures to reveal differences within obstacle and brace factor levels. Left foot max elevation for obstacle crossing was significantly larger than level ground walking for no brace, $t(11) = -17.727$, $p < .001$, unlocked brace, $t(11) = -18.170$, $p < .001$, and locked brace conditions, $t(11) = -20.436$, $p < .001$. No differences were found in elevation values between brace conditions during level ground walking or obstacle avoidance.

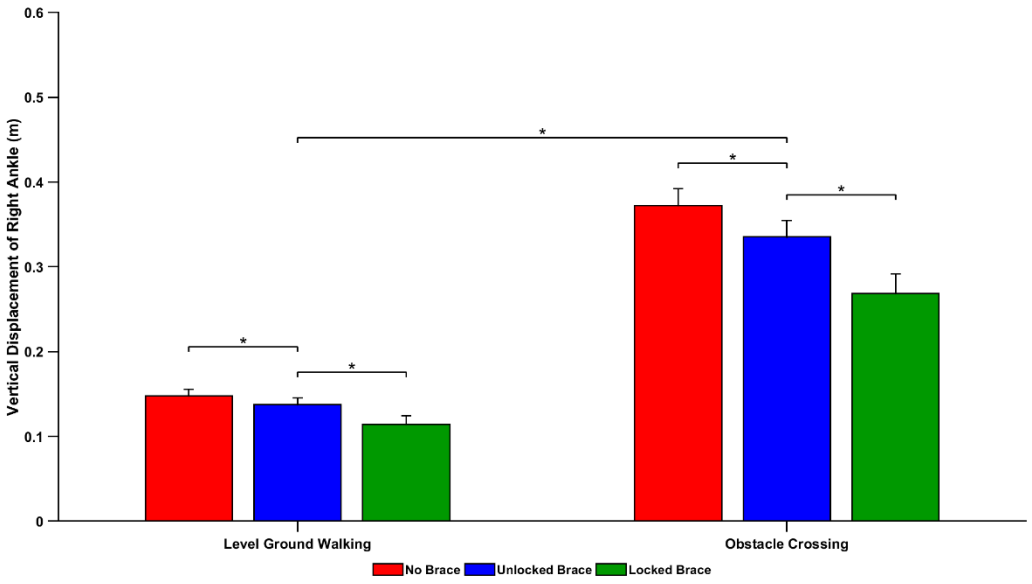

Figure 25. Maximum elevation of the right ankle during clinical gait tasks comparing the maximum vertical deviation that is present during obstacle avoidance and level ground walking with three different brace conditions (no brace, unlocked, locked brace). Significant differences (*) and not significant differences (*n.s.*) are denoted on figure.

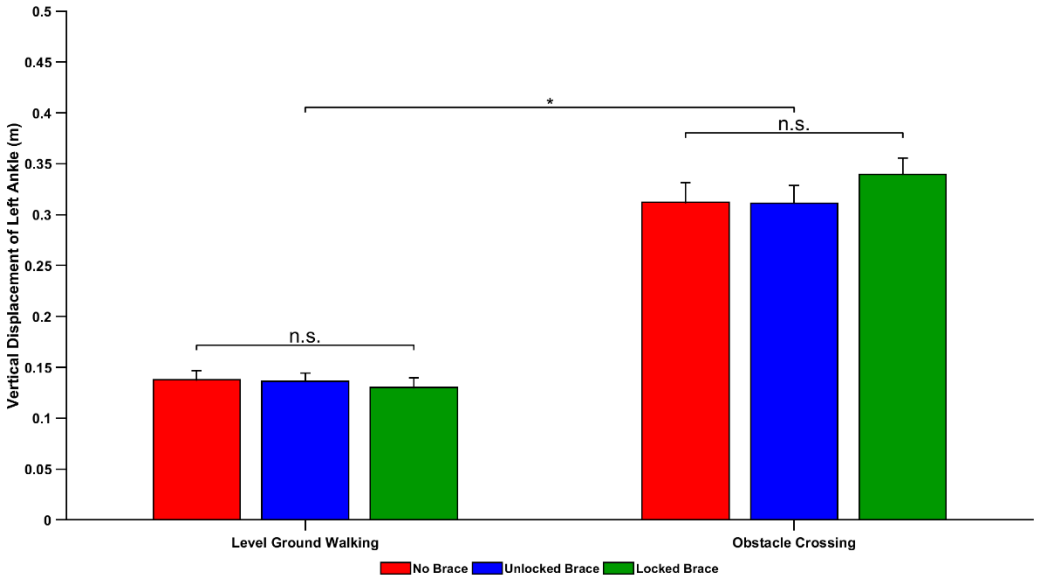

Figure 26. Maximum elevation of the left ankle during clinical gait tasks comparing the maximum vertical deviation that is present during obstacle avoidance and level ground walking with three different brace conditions (no brace, unlocked, locked brace). Significant differences (*) and not significant differences (*n.s.*) are denoted on figure.

Right Limb (braced and trailing limb) Hip Hiking

During level ground walking braced limb hip hiking mean (SD) for NB is 0.031 (0.013) m, UB is 0.031 (0.013), and LB is 0.037 (0.019) m and during obstacle crossing mean (SD) for NB is 0.034 (0.018) m, UB is 0.040 (0.025) m, and LB is 0.076 (0.046) m (Figure 27). ANOVA results indicate there are main effects of brace, $F(2,22) = 17.986$, $p < .05$, and obstacle condition, $F(1,11) = 7.516$, $p < .05$, on braced side hip hiking measures. A significant interaction effect also exists between brace and obstacle condition, $F(2,22) = 20.898$, $p < .05$. Post-hoc pairwise comparisons with a Bonferroni correction compared obstacle and brace conditions. Locked brace hip hiking was significantly different than both no brace, $t(11) = -4.530$, $p < .001$, and unlocked brace conditions, $t(11) = -4.462$, $p < .001$, during obstacle crossing. There was also a significant difference in hip hiking measures between level ground walking and obstacle crossing with a locked knee brace, $t(11) = -3.826$, $p < .05$.

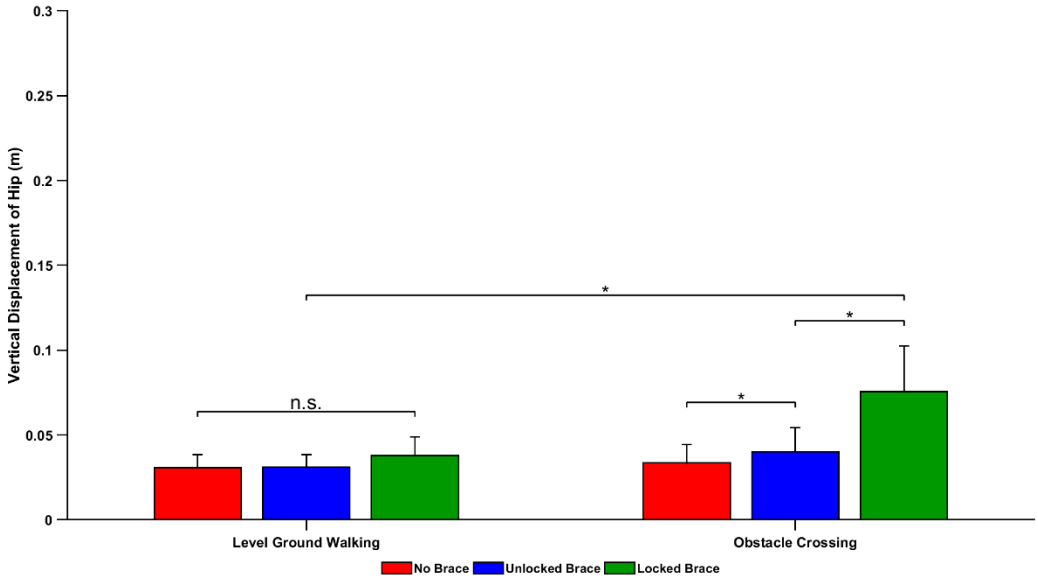

Figure 25. Hip hiking measures of the right hip during clinical gait task comparing hip vertical deviation during obstacle avoidance and level ground walking with three different brace conditions (no brace, unlocked, locked brace). Significant differences (*) and not significant differences (*n.s.*) are denoted on figure.

	IMU	No Brace		Unlocked Brace		Locked Brace		
		Level Ground	Obstacle Crossing	Level Ground	Obstacle Crossing	Level Ground	Obstacle Crossing	
Right	Max Elevation (m)	0.148 (0.013)	0.373 (0.034)	0.138 (0.014)	0.335 (0.034)	0.114 (0.017)	0.269 (0.039)	Obs ($p < .001$) Brace ($p < .001$) Int ($p < .001$)
	Lateral Deviation (m)	0.010 (0.019)	0.005 (0.023)	0.009 (0.02)	-0.008 (0.032)	0.010 (0.018)	-0.157 (0.068)	Obs ($p < .001$) Brace ($p < .001$) Int ($p < .001$)
Left	Max Elevation (m)	0.138 (0.016)	0.312 (0.033)	0.136 (0.013)	0.311 (0.03)	0.130 (0.02)	0.340 (0.027)	Obs ($p < .001$) Brace ($p = .064$) Int ($p < .01$)
	Lateral Deviation (m)	-0.029 (0.021)	-0.090 (0.034)	-0.029 (0.023)	-0.096 (0.036)	-0.029 (0.02)	-0.083 (0.03)	Obs ($p < .001$) Brace ($p = .127$) Int ($p = .015$)

Table 20. Mean, SD and ANOVA results summarizing spatial measures during clinical gait task

3.3.3.3 Right Limb (braced limb and trailing limb) Swing time

During level ground walking there mean (SD) braced limb swing times for NB are 0.40 (0.031) s, UB are 0.40 (0.033) s, and LB are 0.45 (0.054) s and during obstacle crossing NB are 0.49 (0.032), UB are 0.53 (0.060) s, and LB are 0.67 (0.100) s (Figure 28). Two way repeated measures ANOVA evaluated the effect of obstacle and brace on the right trailing limb during obstacle crossing. Main effects for brace, $F(1,11) = 56.753$, $p < .05$, and obstacle, $F(1,11) = 143.453$, $p < .05$, conditions were calculated. Interaction effect between brace and obstacle were also determined from ANOVA results, $F(2,22) = 170.854$, $p < .05$. Post-hoc pairwise comparison with a Bonferroni correction factor calculated differences between obstacle and brace conditions. Right swing time was significantly larger when obstacle crossing compared to level ground walking within all brace conditions (no brace, $t(11) = -13.790$, $p < .05$, unlocked brace, $t(11) = -10.733$, $p < .05$, locked brace, $t(11) = -10.154$, $p < .05$). There were no significant differences between no brace and unlocked brace conditions for each of obstacle crossing,

$t(11) = -3.662$, $p > .05$, and level ground walking, $t(11) = -0.551$, $p > .05$. Locked brace conditions are significantly longer when compared to no brace condition obstacle crossing, $t(11) = -7.887$, $p < .05$, as well as level ground walking, $t(11) = -5.057$, $p > .05$.

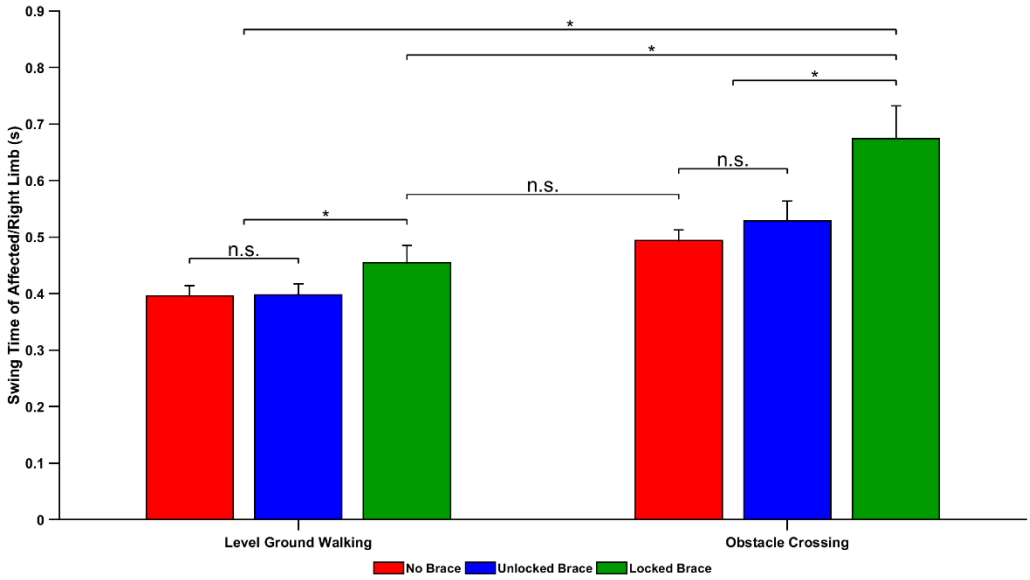

Figure 26. Right limb swing time during clinical gait task comparing swing time during obstacle avoidance and level ground walking with three different brace conditions (no brace, unlocked, locked brace). Significant differences (*) and not significant differences (*n.s.*) are denoted on figure.

3.3.3.4 Left Limb (unbraced and lead limb) Swing time

During level ground walking unbraced mean (SD) limb swing time for NB are 0.38 (0.038) s, UB are 0.38 (0.035) s, and LB are 0.37 (0.039) s and obstacle crossing NB are 0.56 (0.039), UB are 0.57 (0.054) s, and LB are 0.57 (0.046) s (Figure 29). Two-way repeated measures ANOVA evaluated the effect of obstacle and brace on the left leading limb during obstacle crossing. Main effect of obstacle condition exists, $F(1,11) = 170.854$, $p < .05$, but no main effect of brace or interaction effects exist. Significant differences in obstacle condition indicates obstacle crossing was longer compared to level ground walking.

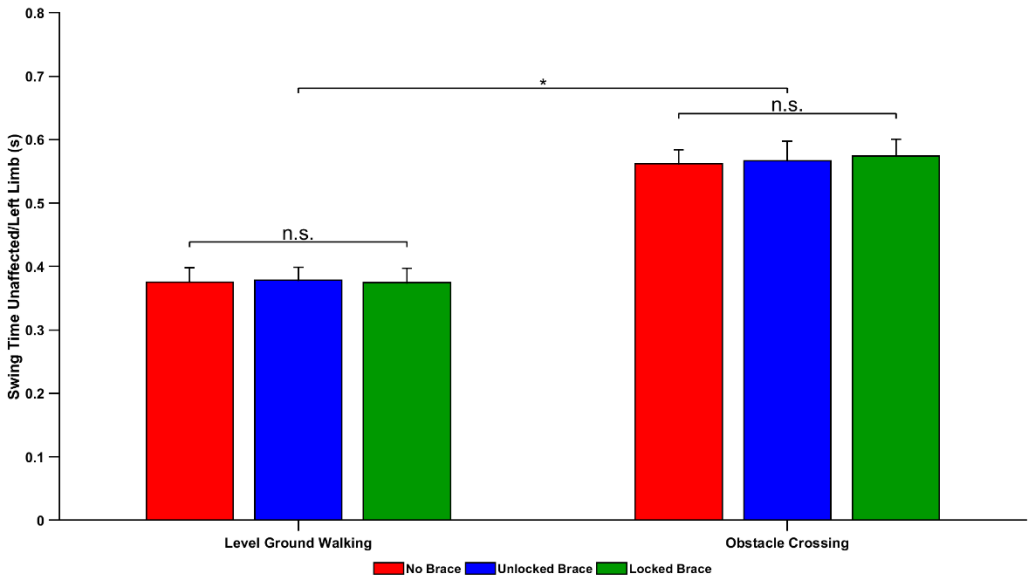

Figure 27. Left limb swing time during clinical gait task comparing swing time during obstacle avoidance and level ground walking with three different brace conditions (no brace, unlocked, locked brace). Significant differences (*) and not significant differences (*n.s.*) are denoted on figure.

3.3.3.5 Left Double Support Time (LDS_{+1})

During level ground walking transferring weight to the braced limb described as left double support means (SD) after obstacle clearance/location of obstacle for NB are 0.15 (0.052) s, UB are 0.15 (0.052) s, and LB are 0.16 (0.055) s, and during obstacle clearance NB are 0.14 (0.046) s, UB are 0.14 (0.045) s, and LB are 0.14 (0.039) s. Two-way repeated measures ANOVA compared the first instance of left double support time after the location of the obstacle between obstacle and brace conditions. ANOVA results indicated there was a main effect of obstacle condition, $F(1,11) = 8.466$, $p < .05$, but no main or interaction effect with the brace conditions. Post-hoc comparison indicated the left double support time after obstacle clearance was shorter compared to the same iteration of left double support time during level ground walking.

3.3.3.6 Right Double Support Time (RDS_{0})

During level ground walking right double support time means (SD) while over the obstacle or where the obstacle would be for NB are 0.15 (0.036) s, UB are 0.15 (0.035) s, and LB are 0.14 (0.029), and during obstacle crossing mean (SD) for NB are 0.12 (0.048) s, UB are 0.13 (0.042) s, and LB 0.14

(0.042) s. Two-way repeated measures ANOVA compared the instance of right double support time when the participant is clearing the obstacle or where the obstacle would be during level ground walking. Main effect of obstacle, $F(1,11) = 5.362$, $p < .05$, and interaction effects, $F(1,11) = 6.527$, $p < .05$, were significant. Post-hoc tests with a Bonferroni correction found no significant differences for all pairwise comparisons.

3.4 Discussion

The objective was to determine if wearable IMU sensors could distinguish differences in spatial and temporal kinematic outcome variables between normal and compensatory movement patterns. Specifically the purpose was to determine if frontal plane compensatory movements (e.g. hip circumduction characterized by lateral deviation and hip hiking) could be described with kinematic measures calculated with IMU sensors.

Overall, the study revealed the ability to detect lateral and vertical deviation of the braced limb as well as differences in hip hiking between the different task conditions. Differences were also observed in temporal characteristics, including longer swing times. These findings indicated that participants employed some amount of lateral deviation of the swinging foot and trunk motion when challenged with restricted range of motion to overcome obstacles. Overall findings from this study show the utility of IMU wearable sensors to distinguish lateral deviation, temporal measures, and other multi-planar compensatory movements from normal walking patterns.

Part of the main objective was to determine if kinematic outcome measures were significantly different between obstacle and brace conditions when subjects were crossing the obstacle. Calculations from IMUs were able to detect gait compensations related to peak lateral deviation of the affected limb, maximum elevation, and hip hiking during clearance. Frontal plane movement of the swinging foot is a typical compensatory movement to aid in obstacle avoidance and is a product of hip circumduction when limb range of motion is modified for achieve safe swing limb trajectory (Lewek et al., 2012). Spatially derived frontal plane kinematic outcome measures were significantly larger for restricted sagittal plane

knee motion and obstacle avoidance tasks when compared to normal knee movement during over ground walking and obstacle avoidance. Further, there was no difference in frontal plane outcome measures when comparing unlocked knee brace and no brace conditions for all obstacle conditions. A similar method has been applied to a large healthy older adult population during level ground walking conditions using bilaterally worn ankle IMUs to characterize normal walking patterns with IMU devices (Dadashi et al., 2013). No differences of gender or gait speed were revealed when walking over level ground in this older adult population. The magnitude of frontal plane swing kinematics in the previous study, 0.04 ± 0.01 m (Dadashi et al., 2013), reflect similar measures found in no brace and unlocked brace conditions of the present study, NB = 0.01 ± 0.02 m, UB = 0.009 ± 0.02 m. During obstacle avoidance, spatial kinematic lateral deviation of the foot during swing is not commonly reported. One study examining total knee arthroplasty patients reported lateral deviation measures in surgically affected, healthy, and healthy control limbs. When total knee arthroplasty (TKA) patients stepped over the obstacle with their surgically repaired limb, they experience reduced knee flexion (patients = 108.2 ± 2.48^{o}; control = 137.5 ± 7.58^{o}) (Byrne & Prentice, 2003). Byrne & Prentice (2003), calculated the lateral deviation of the foot in global space during obstacle avoidance and reported similar values (TKA patients lateral toe deviation mean = .187 m) as reported in this thesis project (affected limb lateral deviation mean = .157 m). Lateral deviation of the surgical foot was significantly larger than healthy and control limb deviations during clearance for TKA patients. The minimal differences between these reported values suggests clinical value for wearable sensors to describe compensatory movements. There are several main differences in these measures. For the current study, the affected limb was the trailing limb to reflect initial amputee obstacle clearance but the lead limb was target limb for TKA patients. Limb clearance strategies have different biomechanical mechanisms driving obstacle clearance. Hip flexion is a main contributor for lead limb clearance while knee flexion drives trial limb clearance (H. L. Chen & Lu, 2006; Patla et al., 1996). Byrne & Prentice (2003) also calculate lateral deviation from the swinging limb toe, whereas the current study calculated from the shank (location of IMU). This study used bilaterally ankle mounted IMUs to replicate placement for a lower limb amputation (absence of ankle articulation) and reduce the effects of

foot rotation, inversion/eversion, on kinematic outcome measure. Due to ankle articulations, Byrne & Prentice (2003) measured deviations may include ankle movement compared to our measurement of ankle movement that is not influenced by ankle articulations. Ankle articulations may also manifest in many of the foot-worn IMU studies looked at previously (Dadashi et al., 2013; Mariani et al., 2010; Rebula et al., 2013). Lewek et al. (2012) used mechanical and physiological constraints to reduce range of motion of the knee joint. Lateral deviation was significantly larger in physiological constrained conditions and larger but not significant in mechanical constraints during treadmill walking. Although mechanical constraints were not significantly larger and may be due to the properties of the orthotic device. During functional movements, reported and attainable knee flexion values are different than knee flexion restrictions outlined on mechanical device (Butler, Queen, Wilson, Stephenson, & Barnes, 2014), which may allow more flexion compared to other methods used for restriction. Although limb differences in these studies is important to acknowledge, these findings confirmed the main hypothesis because wearable sensors were able to distinguish between limbs and tasks.

Lower limb joint angle control is important for safe swing limb trajectory (Winter, 1992). Interaction of joint angles to produces sufficient limb clearance during level ground walking and obstacle avoidance. Estimated maximum elevation of the lower limb during clearance from wearable sensors has enough precision to distinguish between obstacle and brace conditions. Crossing obstacles requires a higher maximum elevation compared to level ground walking, however when sagittal plane knee mobility is constrained maximum elevation is lower than unconstrained level ground walking and obstacle crossing. Joint constraint influences the maximum elevation attained during obstacle crossing because limb elevation is largely driven by knee flexion in the trailing limb (H.-L. Chen et al., 2008). Wearable sensors have estimated foot elevation in two previous studies. Healthy older adults during level ground walking have a similar maximum elevation values, male = 0.16 ± 0.003 m, female = 0.11 ± 0.002 m (Dadashi et al., 2013), to no brace and unlocked brace level ground walking values found in this study, NB = 0.148 ± 0.013 m, UB = 0.138 ± 0.014 m. These two studies defined elevation in a different

manner. A foot worn accelerometer and rigid foot segment reported heel and toe clearance values (Mariani et al., 2012), whereas the current study simply examine change in elevation during swing phase. This thesis project cannot accurately describe clearance strategies because characteristics of the foot segment orientation are unknown when describing elevation values, however utilizing a rigid foot segment to estimate foot orientation may also introduce unwanted error in estimated clearance measures due to gait speed and foot size estimation. The ankle worn IMU has been used in obstacle clearance studies prior to the current thesis. Obstacle crossing characteristics in older adults reported max vertical displacements for level ground walking, 0.124 ± 0.26 m, and obstacle crossing, 0.297 ± 0.25 m (Trojaniello et al., 2015). These vertical deviations are very similar to the reported values in the current thesis project for level ground walking, 0.148 ± 0.013 m, obstacle crossing elevations, 0.373 ± 0.034 m. Differences could be attributed to obstacle characteristics that may influence the clearance strategy (Patla & Rietdyk, 1993; Patla et al., 1996) or the populations being evaluated (Lu et al., 2006). Obstacles that appear to be less stable or have wider dimensions and populations that may be more prone to instability have higher clearance patterns, thus increased maximum elevation, during obstacle crossing. Higher toe clearance increases the margin of safety and this is exemplified in patient populations (e.g. older adults and amputees) where stability may be a concern for the control system (Hill et al., 1997; Lu et al., 2006). Knee restriction affects the maximum elevation during obstacle crossing such that elevation is scaled lower as knee restriction increases (NB = 0.373 (0.034) m, UB = 0.335 (0.034), LB = 0.269 (0.039)). Knee flexion is contributing factor in clearance patterns these end range of motion knee angles may work in parallel with ankle dorsiflexors for fine-tuning the desired clearance parameters. When imposed constraints are present, slight but significant differences emerge to indicate a significant contribution of knee flexion to toe clearance. Evangelopoulou et al. (2016), found similar differences when applying ankle range limiting orthotic devices to a young healthy population during obstacle avoidance (e.g. 11.5 cm obstacle: Unrestricted ankle = 0.095 (0.029) m; Restricted ankle = 0.084 (0.019) m). Healthy subjects with reduced ankle mobility have lower clearance values compared to obstacle crossing with full range of motion. The accuracy of IMU vertical displacement estimate replicates sensitivity of elevation differences

when knee restriction is involved. Another potential source for lower maximum elevation may be reveal in the hip hiking measure. IMUs were able to distinguish significant hip hiking during locked brace obstacle avoidance trails, which coincides with the most knee restriction applied to the lower limb. If the clearance strategy changes from limb flexion to hip hiking as the main contributor to clearance this may also manifest as lower clearance values. In previous research, hip hiking was also seen as a response to mechanical knee ROM restriction but not physiological restriction (Delafontaine, Fourcade, Honeine, Ditcharles, & Yiou, 2018; Lewek et al., 2012). This research study is was able to show the potential changes from lower limb flexion to hip hiking as restriction increased during obstacle avoidance.

There were also important differences measured in step timing specifically when subject crossed obstacle with normal and limited knee flexion. Essential to this was the accuracy of footfall detection with IMU data worn at the ankle. The present study confirmed the high reliability of using such sensors to capture these footfall events. It is important to assess both spatial and temporal measures as they both reflect elements of compensation to comprised or restricted limb or body control during walking. Specifically, when subjects were challenged with reduced range of motion their braced limb swing phase was longer compared to unrestricted movement. When no restrictions are present (no brace, unlocked brace, or unbraced limb) swing time did not change during level ground walking. Amputees exhibit shorter swing times for their intact limbs and longer swing time with affected limbs (Hak et al., 2014). This is in response to stability of the single leg support, however it is unlikely that healthy subjects exhibit this pattern for the same reason and increase in swing time may be a response to new limb dynamics and safe trajectory. As expected, swing time is larger when crossing an obstacle compared to level ground walking because the limb trajectory is larger. Unlike amputee populations, healthy subjects did not exhibit any differences in double support time. Amputee populations increase their intact stance time and decrease their affected limb stance time as a control strategy for stability. This asymmetric pattern allows amputees to spend more time in single support with their intact limb providing more control to dynamic stability during walking (Grumillier, Martinet, Paysant, André, & Beyaert, 2008; Highsmith, Schulz,

Hart-Hughes, Latlief, & Phillips, 2010; Schaarschmidt et al., 2012). Changes to swing time in the amputee population tend to reflect stability concerns and safe swing limb trajectory (Hak et al., 2014); however, it is likely in the healthy population these differences are present to reflect safe trajectory rather than stability control. When prosthetic limb and socket interface are misaligned, (e.g. internally/externally rotated 5-10^{o}) patient stability concerns increase and subsequently increase their single leg intact limb stance time. Further, amputees modify their double support transition times and increase their double support for a more stable stance period (longer transitions to affected limb single leg support) (Grumillier et al., 2008). This allows for a slow progression to the less stable single leg support and allows the control system to achieve these differences. These differences in double support time were absent in the healthy population. Healthy subjects have full mechanical and neurological control over their joint unlike the amputee population. During single leg support healthy subjects are able to provide sufficient extensor moments to maintain upright stance and postural control (Winter, 1991). Differences in these control mechanisms and abilities performed by the healthy and impaired population decrease the application of orthotic devices to investigate amputee movement patterns in a comprehensive manner.

The application of wearable devices to clinical settings should be able to describe a variety of compensatory mechanisms exhibited by the population of interest. One limitation of IMU devices is the dissociation of specific movement strategies and their contribution to kinematic outcome measure, such as vertical displacement of the swinging hip. Reduced knee range of motion can dissociate between the different brace and obstacle conditions however the vertical displacement is a product of a variety of movement patterns: limb flexion, hip hiking, and vaulting (plantarflexion of stance limb) (Hill et al., 1999; Winter, 1992). These are all spatial compensatory movements adopted by the amputee population. Hip hiking estimated by the inertial measurement unit is significantly larger in the locked brace obstacle crossing condition compared to other brace and level ground walking conditions. Hip hiking is a compensatory movement that is adopted by the amputee population (Bowker et al., 1992), during limited knee range of motion (Lewek et al., 2012), and walking with bilateral ankle immobilization

(Nepomuceno, Major, Stine, & Gard, 2017). Pelvic tilt increases ipsilateral hip height during swing phase but trunk lateral bending can also cause hip hiking and contralateral limb to deviate laterally, in a similar fashion that has been detected with the IMUs. Trunk bending and increased mediolateral COM movement are postural adjustments used by healthy subjects during unilateral knee hypomobility (Delafontaine et al., 2018). Placement of accelerometers (on the belt and ankles) may be influenced by trunk rotation or lateral bending which are two trunk movements that are also adopted by the amputee population (Bowker et al., 1992). These IMU locations are useful due to ease of access, however it decreases the ability to distinguish the mechanism employed by patients to achieve successful gait. Clinically the Amputee Mobility Predictor defines the lateral deviation, or marked deviation, as "extreme substitute movements made to permit the foot to clear the floor" (Gailey et al., 2002). Based on these instructions to detect lateral deviation, clinical assessments could benefit from supplementary information supplied by the IMUs. Another area the IMU location limits the ability to describe biological mechanism is outlined by the differences in max elevation of the foot as affected by brace conditions. Significant differences exist across obstacle and brace conditions, which could indicate how the knee joint angles contribute to successful toe clearance (Evangelopoulou et al., 2016; Winter, 1992); however, implications of brace conditions are limited to speculation because of the IMU placement and limited descriptive ability. Another marked limitation of these tools revolves around processing assumptions. The ZUPT decreases the robustness of these tools to describe compensatory movements during a limb in stance phase because it assumes a zero-velocity timepoint. The zero velocity update reduces the ability to detect stance limb ankle plantarflexion and thus in ability to detect vaulting (Bowker et al., 1992) because of correcting the velocity during stance. In this current study, step width assumed negligible and during drift removal width was corrected to quantify the swinging foot characteristics. Processing techniques remove step width variability to extract improved swing foot characteristics. Limiting the ability reduces the potential for fall risk characterization using measures such as step width variability (Vanicek, Strike, & Polman, 2015), but improves swinging foot characterization (Mariani et al., 2010). Compensatory movements work

cohesively to overcome barriers in movement patterns, and these two limitations decrease the effectiveness of IMUs to fully describe compensatory movements using kinematic outcome measures.

Chapter 4: Conclusion

Quantitative measures could improve the quality of clinical gait analysis, particularly when movement patterns have subtle changes in response to interventions. Amputation, as a surgical intervention, is increasing with the rise of diabetic complications the risk of increasing population of amputees grows. Lower limb amputees are unique individuals since people innately have both mechanical and neurologically differences with their movement pattern. Cost-effective IMUs are a viable option to help intervene with improving clinical gait analysis because they are portable and inexpensive tools. This thesis sought to determine if spatially derived kinematic outcomes measures could distinguish common amputee compensatory movements from normal unaffected movement patterns, such as lateral deviation of the swinging foot. As a first step, it was pertinent to outline the numerical accuracy of IMU spatially derived outcome measures compared to a gold standard system before applying these tools to clinical settings. It was hypothesized that IMU spatially derived measures would not be significantly different from optical motion capture. Findings indicated the numeric agreeance between the two devices is mainly dependent on the task and axes calculated. Those movements with increased transverse rotation had less agreeance compared to linear measures that focused on single axes of movement. Overall mean error bias were not different from the line of equality but coefficients of repeatability did not satisfy the requirements for repeatability. Statistically spatially derived measures are not precise enough to replace optical motion capture measures. Precision requirements utilized in this current study may misinterpret the potential for applying these tools to a clinical setting (±18 mm). Other measures have clearly defined clinical differences, ±5^{o} mean error differences (Bolink et al., 2016), while these kinematic outcome measures are less definite. Further, subject mean errors for the majority of tasks ranged ~0.05 m between the two devices. If mean error is the only requirement for detectable clinical differences, these tools satisfy the requirements for clinical application. Next steps, the utility of IMUs to distinguish between compensatory and normal movement patterns is uninvestigated. The second objective shifts focus to determine the ability of IMUs to detect lateral deviation during a clinical obstacle avoidance task. Young

healthy subjects were challenged with reduce knee range of motion and obstacle avoidance to determine if compensatory movements were present. IMU spatially derived kinematic outcome measures were able to distinguish between locked brace obstacle avoidance tasks and unrestricted level ground walking conditions. Lateral deviation of the braced limb has larger deviations compared to all other braced (i.e. NB, UB) and obstacle conditions (i.e. level ground walking). Measures were comparable to previously defined lateral deviation in a TKA post-surgery cohort during an obstacle avoidance task (Byrne & Prentice, 2003). Other compensatory movements were also detectable with the spatially derived IMU data. Maximum elevation of the limb had high precision and distinguished between all obstacle and brace conditions. Elevation was lower as brace condition reduce range of motion and was significantly higher when crossing the obstacle. This reflected clearance patterns seen in optical motion capture results when young healthy adults had reduce ankle range of motion (Evangelopoulou et al., 2016). Footfall event detection was highly accurate for all brace and obstacle conditions, which allows accurate description of all temporal characteristics of gait. As predicted, swing times were longer during obstacle avoidance because of higher limb trajectory compared to level ground walking. Double support changes seen in the amputee population (Hak, Van Dieën, et al., 2013) were not present in the healthy population. Changes to DST occur in response to stability concerns, however in a young healthy population stability concerns less likely because of full neurological and mechanical control. Overall, IMU devices can detect spatial and temporal compensatory movements and have the potential to support clinical gait analysis with quantitative measures. Future research should focus on the ability of IMUs devices to detect these changes in a patient population to discern the differences in temporal measure related to stability and probe the control system as a whole with wearable devices. Application of wearable devices to populations with stability concerns could help advance detection of temporal differences in gait. Further, a more concise outline of the minimal number of devices to describe features of interest should be outlined for these particular populations. These two themes will promote the discussion of wearable sensors in clinical setting to support current rehabilitation.

References

Aminian, K., Najafi, B., Büla, C., Leyvraz, P. F., & Robert, P. (2002). Spatio-temporal parameters of gait measured by an ambulatory system using miniature gyroscopes. *Journal of Biomechanics*, *35*(5), 689–699. http://doi.org/10.1016/S0021-9290(02)00008-8

Aminian, K., Trevisan, C., Najafi, B., Dejnabadi, H., Frigo, C., Pavan, E., … Leyvraz, P. F. (2004). Evaluation of an ambulatory system for gait analysis in hip osteoarthritis and after total hip replacement. *Gait and Posture*, *20*(1), 102–107. http://doi.org/10.1016/S0966-6362(03)00093-6

Austin, G. P., Garrett, G. E., & Bohannon, R. W. (1999). Kinematic analysis of obstacle clearance during locomotion. *Gait and Posture*, *10*(2), 109–120. http://doi.org/10.1016/S0966-6362(99)00022-3

Barak, Y., Wagenaar, R. C. C., & Holt, K. G. G. (2006). Gait characteristics of elderly people with a history of falls: a dynamic approach. *Physical Therapy*, *86*(11), 1501–1510. http://doi.org/10.2522/ptj.20050387

Bland, J. M., & Altman, D. G. (1986). Statistical methods for assessing agreement between two methods of clinical measurement. *Lancet (London, England)*, *1*(8476), 307–10. Retrieved from http://www.ncbi.nlm.nih.gov/pubmed/2868172

Bolink, S. A. A. N., Naisas, H., Senden, R., Essers, H., Heyligers, I. C., Meijer, K., & Grimm, B. (2016). Validity of an inertial measurement unit to assess pelvic orientation angles during gait, sit-stand transfers and step-up transfers: Comparison with an optoelectronic motion capture system. *Medical Engineering & Physics*, *38*(3), 225–31. http://doi.org/10.1016/j.medengphy.2015.11.009

Bolink, S. A. A. N., Van Laarhoven, S. N., Lipperts, M., Heyligers, I. C., & Grimm, B. (2012). Inertial sensor motion analysis of gait, sit-stand transfers and step-up transfers: Differentiating knee patients from healthy controls. *Physiological Measurement*, *33*(11), 1947–1958. http://doi.org/10.1088/0967-3334/33/11/1947

Bonato, P. (2005). Advances in wearable technology and applications in physical medicine and rehabilitation. *Journal of Neuroengineering and Rehabilitation*, *2*(1), 2. http://doi.org/10.1186/1743-0003-2-2

Boonstra, M. C., Van Der Slikke, R. M. A., Keijsers, N. L. W., Van Lummel, R. C., De Waal Malefijt, M. C., & Verdonschot, N. (2006). The accuracy of measuring the kinematics of rising from a chair with accelerometers and gyroscopes. *Journal of Biomechanics*, *39*(2), 354–358. http://doi.org/10.1016/j.jbiomech.2004.11.021

Bowker, J. H., Michael, J. W., & American Academy of Orthopaedic Surgeons. (1992). Atlas of limb prosthetics: surgical, prosthetic, and rehabilitation principles, 930. Retrieved from http://www.oandplibrary.org/alp/chap14-01.asp

Brodie, M. A., Walmsley, A., & Page, W. (2008a). Dynamic accuracy of inertial measurement units during simple pendulum motion. *Computer Methods in Biomechanics and Biomedical Engineering*, *11*(3), 235–242. http://doi.org/10.1080/10255840802125526

Brodie, M. A., Walmsley, A., & Page, W. (2008b). The static accuracy and calibration of inertial measurement units for 3D orientation. *Computer Methods in Biomechanics and Biomedical Engineering*, *11*(6), 641–648. http://doi.org/10.1080/10255840802326736

Buckley, J. G., De Asha, A. R., Johnson, L., & Beggs, C. B. (2013). Understanding adaptive gait in lower-limb amputees: insights from multivariate analyses. *Journal of NeuroEngineering and*

Rehabilitation, *10*(1). http://doi.org/10.1186/1743-0003-10-98

Bugané, F., Benedetti, M. G., Casadio, G., Attala, S., Biagi, F., Manca, M., & Leardini, A. (2012). Estimation of spatial-temporal gait parameters in level walking based on a single accelerometer: Validation on normal subjects by standard gait analysis. *Computer Methods and Programs in Biomedicine*, *108*(1), 129–137. http://doi.org/10.1016/j.cmpb.2012.02.003

Butler, R. J., Queen, R. M., Wilson, B., Stephenson, J., & Barnes, C. L. (2014). The effect of extension constraint knee bracing on dynamic balance, gait mechanics, and joint alignment. *PM and R*, *6*(4), 309–315. http://doi.org/10.1016/j.pmrj.2013.09.011

Byrne, J. M., & Prentice, S. D. (2003). Swing phase kinetics and kinematics of knee replacement patients during obstacle a v oidance, *18*.

Cain, S. M., McGinnis, R. S., Davidson, S. P., Vitali, R. V., Perkins, N. C., & McLean, S. G. (2016). Quantifying performance and effects of load carriage during a challenging balancing task using an array of wireless inertial sensors. *Gait and Posture*, *43*, 65–69. http://doi.org/10.1016/j.gaitpost.2015.10.022

Cappozzo, A., Della Croce, U., Leardini, A., & Chiari, L. (2005). Human movement analysis using stereophotogrammetry. Part 1: Theoretical background. *Gait and Posture*, *21*(2), 186–196. http://doi.org/10.1016/j.gaitpost.2004.01.010

Cereatti, A., Trojaniello, D., & Croce, U. Della. (2015). Accurately measuring human movement using magneto-inertial sensors: Techniques and challenges. In *2nd IEEE International Symposium on Inertial Sensors and Systems, IEEE ISISS 2015 - Proceedings*. http://doi.org/10.1109/ISISS.2015.7102390

Chen, H.-C., Ashton-Miller, J. A., Alexander, N. B., & Schultz, A. B. (1991). Stepping Over Obstacles: Gait Patterns of Healthy Young and Old Adults. *Journal of Gerontology*, *46*(6), M196–M203. http://doi.org/10.1093/geronj/46.6.M196

Chen, H.-L., Lu, T.-W., Wang, T.-M., & Huang, S.-C. (2008). Biomechanical strategies for successful obstacle crossing with the trailing limb in older adults with medial compartment knee osteoarthritis. *Journal of Biomechanics*, *41*(4), 753–761. http://doi.org/10.1016/j.jbiomech.2007.11.017

Chen, H. L., & Lu, T. W. (2006). Comparisons of the joint moments between leading and trailing limb in young adults when stepping over obstacles. *Gait and Posture*, *23*(1), 69–77. http://doi.org/10.1016/j.gaitpost.2004.12.001

Chiari, L., Dozza, M., Cappello, A., Horak, F. B., Macellari, V., & Giansanti, D. (2005). Audio-biofeedback for balance improvement: An accelerometry-based system. *IEEE Transactions on Biomedical Engineering*, *52*(12), 2108–2111. http://doi.org/10.1109/TBME.2005.857673

Cole, M. J., Durham, S., & Ewins, D. (2008). An evaluation of patient perceptions to the value of the gait laboratory as part of the rehabilitation of primary lower limb amputees. *Prosthetics and Orthotics International*, *32*(770885181), 12–22. http://doi.org/10.1080/03093640701554045

Condie, E., Scott, H., & Treweek, S. (2006). Lower limb prosthetic outcome measures: A review of the literature 1995 to 2005. *Journal of Prosthetics and Orthotics*, *18*(1), 13–45. http://doi.org/10.1097/00008526-200601001-00004

Cutti, A. G., Ferrari, A., Garofalo, P., Raggi, M., Cappello, A., & Ferrari, A. (2010). "Outwalk": A protocol for clinical gait analysis based on inertial and magnetic sensors. *Medical and Biological Engineering and Computing*, *48*(1), 17–25. http://doi.org/10.1007/s11517-009-0545-x

Dadashi, F., Mariani, B., Rochat, S., Büla, C. J., Santos-Eggimann, B., & Aminian, K. (2013). Gait and foot clearance parameters obtained using shoe-worn inertial sensors in a large-population sample of older adults. *Sensors (Switzerland)*, *14*(1), 443–457. http://doi.org/10.3390/s140100443

De Asha, a. R., & Buckley, J. G. (2014). The effects of walking speed on minimum toe clearance and on the temporal relationship between minimum clearance and peak swing-foot velocity in unilateral trans-tibial amputees. *Prosthetics and Orthotics International*, *39*(2), 120–125. http://doi.org/10.1177/0309364613515493

de Pasquale, G., & Somà, A. (2010). Reliability testing procedure for MEMS IMUs applied to vibrating environments. *Sensors*, *10*(1), 456–474. http://doi.org/10.3390/s100100456

de Vries, W. H. K., Veeger, H. E. J., Baten, C. T. M., & van der Helm, F. C. T. (2009). Magnetic distortion in motion labs, implications for validating inertial magnetic sensors. *Gait and Posture*, *29*(4), 535–541. http://doi.org/10.1016/j.gaitpost.2008.12.004

Del Pilar, M., Orozco, D., Abousamra, O., Church, C., Lennon, N., Henley, J., … Miller, F. (2016). Reliability and validity of Edinburgh visual gait score as an evaluation tool for children with cerebral palsy. *Gait & Posture*, *49*, 14–18. http://doi.org/10.1016/j.gaitpost.2016.06.017

Delafontaine, A., Fourcade, P., Honeine, J. L., Ditcharles, S., & Yiou, E. (2018). Postural adaptations to unilateral knee joint hypomobility induced by orthosis wear during gait initiation. *Scientific Reports*, *8*(1), 1–15. http://doi.org/10.1038/s41598-018-19151-1

Devan, H., Hendrick, P., Ribeiro, D. C., A Hale, L., & Carman, A. (2014). Asymmetrical movements of the lumbopelvic region: Is this a potential mechanism for low back pain in people with lower limb amputation? *Medical Hypotheses*, *82*(1), 77–85. http://doi.org/10.1016/j.mehy.2013.11.012

Dillingham, T. R., Pezzin, L. E., & MacKenzie, E. J. (2002). Limb amputation and limb deficiency: epidemiology and recent trends in the United States. *Southern Medical Journal*, *95*(8), 875–83. Retrieved from http://www.thefreelibrary.com/Limb+amputation+and+limb+deficiency:+epidemiology+and+recent+trends...-a090569925

Ephraim, P. L., Wegener, S. T., MacKenzie, E. J., Dillingham, T. R., & Pezzin, L. E. (2005). Phantom pain, residual limb pain, and back pain in amputees: Results of a national survey. *Archives of Physical Medicine and Rehabilitation*, *86*(10), 1910–1919. http://doi.org/10.1016/j.apmr.2005.03.031

Esser, P., Dawes, H., Collett, J., & Howells, K. (2009). IMU: Inertial sensing of vertical CoM movement. *Journal of Biomechanics*, *42*(10), 1578–1581. http://doi.org/10.1016/j.jbiomech.2009.03.049

Evangelopoulou, E., Twiste, M., & Buckley, J. G. (2016). Restricting ankle motion via orthotic bracing reduces toe clearance when walking over obstacles. *Gait & Posture*, *43*, 251–256. http://doi.org/10.1016/j.gaitpost.2015.10.006

Evans, M. D., Goldie, P. A., & Hill, K. D. (1997). Systematic and random error in repeated measurements of temporal and distance parameters of gait after stroke. *Archives of Physical Medicine and Rehabilitation*, *78*(7), 725–729. http://doi.org/10.1016/S0003-9993(97)90080-0

Gailey, R. S., Roach, K. E., Applegate, E. B., Cho, B., Cunniffe, B., Licht, S., … Nash, M. S. (2002). The Amputee Mobility Predictor: An instrument to assess determinants of the lower-limb amputee's ability to ambulate. *Archives of Physical Medicine and Rehabilitation*, *83*(5), 613–627. http://doi.org/10.1053/ampr.2002.32309

Geil, M. D. (2009). Assessing the state of clinically applicable research for evidence-based practice in

prosthetics and orthotics. *The Journal of Rehabilitation Research and Development*, *46*(3), 305. http://doi.org/10.1682/JRRD.2008.02.0019

Giavarina, D. (2015). Understanding Bland Altman analysis. *Biochemia Medica*, *25*(2), 141–151. http://doi.org/10.11613/BM.2015.015

Greene, B. R., McGrath, D., Foran, T. G., Doheny, E. P., & Caulfield, B. (2011). Body-worn sensor based surrogates of minimum ground clearance in elderly fallers and controls. *Proceedings of the Annual International Conference of the IEEE Engineering in Medicine and Biology Society, EMBS*, (May), 6499–6502. http://doi.org/10.1109/IEMBS.2011.6091732

Grumillier, C., Martinet, N., Paysant, J., André, J. M., & Beyaert, C. (2008). Compensatory mechanism involving the hip joint of the intact limb during gait in unilateral trans-tibial amputees. *Journal of Biomechanics*, *41*(14), 2926–2931. http://doi.org/10.1016/j.jbiomech.2008.07.018

Hahn, M. E., & Chou, L.-S. (2004). Age-related reduction in sagittal plane center of mass motion during obstacle crossing. *Journal of Biomechanics*, *37*(6), 837–844. http://doi.org/10.1016/j.jbiomech.2003.11.010

Hak, L., Houdijk, H., Beek, P. J., & Van Dieë, J. H. (2013). Steps to take to enhance gait stability: The effect of stride frequency, stride length, and walking speed on local dynamic stability and margins of stability. *PLoS ONE*, *8*(12). http://doi.org/10.1371/journal.pone.0082842

Hak, L., van Dieën, J. H., van der Wurff, P., & Houdijk, H. (2014). Stepping Asymmetry Among Individuals With Unilateral Transtibial Limb Loss Might Be Functional in Terms of Gait Stability. *Physical Therapy*. http://doi.org/10.2522/ptj.20130431

Hak, L., Van Dieën, J. H., Van Der Wurff, P., Prins, M. R., Mert, A., Beek, P. J., & Houdijk, H. (2013). Walking in an unstable environment: Strategies used by transtibial amputees to prevent falling during gait. *Archives of Physical Medicine and Rehabilitation*, *94*(11). http://doi.org/10.1016/j.apmr.2013.07.020

Hall, L. A., & McCloskey, D. I. (1983). Detections of movements imposed on finger, elbow and shoulder joints. *The Journal of Physiology*, *335*(1), 519–533. http://doi.org/10.1113/jphysiol.1983.sp014548

Hanlon, M., & Anderson, R. (2009). Real-time gait event detection using wearable sensors. *Gait & Posture*, *30*(4), 523–7. http://doi.org/10.1016/j.gaitpost.2009.07.128

Heijnen, M. J. H., Muir, B. C., & Rietdyk, S. (2012). Interpolation techniques to reduce error in measurement of toe clearance during obstacle avoidance. *Journal of Biomechanics*, *45*(1), 196–198. http://doi.org/10.1016/j.jbiomech.2011.09.019

Highsmith, M. J., Schulz, B., Hart-Hughes, S., Latlief, G., & Phillips, S. (2010). Differences in the Spatiotemporal Parameters of Transtibial and Transfemoral Amputee Gait. *Journal of Prosthetics and Orthotics*, *22*(1), 26–30.

Hill, S. W., Patla, A. E., Ishac, M. G., Adkin, A. L., Supan, T. J., & Barth, D. G. (1997). Kinematic patterns of participants with a below-knee prosthesis stepping over obstacles of various heights during locomotion. *Gait and Posture*, *6*(3), 186–192. http://doi.org/10.1016/S0966-6362(97)01120-X

Hill, S. W., Patla, A. E., Ishac, M. G., Adkin, A. L., Supan, T. J., & Barth, D. G. (1999). Altered kinetic strategy for the control of swing limb elevation over obstacles in unilateral below-knee amputee gait. *Journal of Biomechanics*, *32*(5), 545–549. http://doi.org/10.1016/S0021-9290(98)00168-7

Hof, A. L., van Bockel, R. M., Schoppen, T., & Postema, K. (2007). Control of lateral balance in walking.

Experimental findings in normal subjects and above-knee amputees. *Gait and Posture*, *25*(2), 250–258. http://doi.org/10.1016/j.gaitpost.2006.04.013

Howarth, S. J., & Callaghan, J. P. (2010). Quantitative assessment of the accuracy for three interpolation techniques in kinematic analysis of human movement. *Computer Methods in Biomechanics and Biomedical Engineering*, *13*(6), 847–855. http://doi.org/10.1080/10255841003664701

Huang, S. C., Lu, T. W., Chen, H. L., Wang, T. M., & Chou, L. S. (2008). Age and height effects on the center of mass and center of pressure inclination angles during obstacle-crossing. *Medical Engineering and Physics*, *30*(8), 968–975. http://doi.org/10.1016/j.medengphy.2007.12.005

J.Woodman, O. (2007). An introduction to inertial navigation. *University of Cambridge - Computer Laboratory*, *UCAM-CL-TR*(3B), 961–2. http://doi.org/10.1017/S0373463300036341

Johnson, L., Buckley, J. G., Scally, A. J., & Elliott, D. B. (2007). Multifocal spectacles increase variability in toe clearance and risk of tripping in the elderly. *Investigative Ophthalmology and Visual Science*, *48*(4), 1466–1471. http://doi.org/10.1167/iovs.06-0586

Kayssi, A., de Mestral, C., Forbes, T. L., & Roche-Nagle, G. (2016). A Canadian population-based description of the indications for lower-extremity amputations and outcomes. *Canadian Journal of Surgery*, *59*(2), 99–106. http://doi.org/10.1503/cjs.013115

Kendell, C., Lemaire, E. D., Kofman, J., & Dudek, N. (2015). Gait adaptations of transfemoral prosthesis users across multiple walking tasks. *Prosthetics and Orthotics International*. http://doi.org/10.1177/0309364614568410

Kingma, H. (2005). Thresholds for perception of direction of linear acceleration as a possible evaluation of the otolith function. *BMC Ear, Nose and Throat Disorders*, *5*(1), 5. http://doi.org/10.1186/1472-6815-5-5

Kiss, R. M. (2010). Comparison between kinematic and ground reaction force techniques for determining gait events during treadmill walking at different walking speeds. *Medical Engineering and Physics*, *32*(6), 662–667. http://doi.org/10.1016/j.medengphy.2010.02.012

Kitagawa, N., & Ogihara, N. (2016). Estimation of foot trajectory during human walking by a wearable inertial measurement unit mounted to the foot. *Gait and Posture*, *45*, 110–114. http://doi.org/10.1016/j.gaitpost.2016.01.014

Kose, A., Cereatti, A., & Della Croce, U. (2012). Bilateral step length estimation using a single inertial measurement unit attached to the pelvis. *Journal of NeuroEngineering and Rehabilitation*, *9*(1), 9. http://doi.org/10.1186/1743-0003-9-9

Kulkarni, J., Gaine, W. J., Buckley, J. G., Rankine, J. J., & Adams, J. (2005). Chronic low back pain in traumatic lower limb amputees. *Clinical Rehabilitation*, *19*(1), 81–86. http://doi.org/10.1191/02692b15505cr8l9oa

Lajoie, K., Bloomfield, L. W., Nelson, F. J., Suh, J. J., & Marigold, D. S. (2012). The contribution of vision, proprioception, and efference copy in storing a neural representation for guiding trail leg trajectory over an obstacle. *Journal of Neurophysiology*, *107*(8), 2283–2293. http://doi.org/10.1152/jn.00756.2011

Landy, E. (2010). *Strategies Utilizaed while Minimizing Ankle Motion Bilaterally and Unilaterally during Level Ground Walking and Obstacle Clearace Tasks*. University of Waterloo.

Leardini, A., Lullini, G., Giannini, S., Berti, L., Ortolani, M., & Caravaggi, P. (2014). Validation of the angular measurements of a new inertial-measurement-unit based rehabilitation system: Comparison

with state-of-the-art gait analysis. *Journal of NeuroEngineering and Rehabilitation*, *11*(1), 1–7. http://doi.org/10.1186/1743-0003-11-136

Levinger, P., Lai, D. T. H., Menz, H. B., Morrow, A. D., Feller, J. a., Bartlett, J. R., … Begg, R. (2012). Swing limb mechanics and minimum toe clearance in people with knee osteoarthritis. *Gait & Posture*, *35*(2), 277–281. http://doi.org/10.1016/j.gaitpost.2011.09.020

Lewek, M. D., Osborn, A. J., & Wutzke, C. J. (2012). The influence of mechanically and physiologically imposed stiff-knee gait patterns on the energy cost of walking. *Archives of Physical Medicine and Rehabilitation*, *93*(1), 123–128. http://doi.org/10.1016/j.apmr.2011.08.019

Litman, K. (2015). *Accuracy and Precision of Microelectronic Measuring Systems (MEMS)*. McMaster University.

Lu, T. W., Chen, H. L., & Chen, S. C. (2006). Comparisons of the lower limb kinematics between young and older adults when crossing obstacles of different heights. *Gait and Posture*, *23*(4), 471–479. http://doi.org/10.1016/j.gaitpost.2005.06.005

Lugade, V., Lin, V., & Chou, L. S. (2011). Center of mass and base of support interaction during gait. *Gait and Posture*, *33*(3), 406–411. http://doi.org/10.1016/j.gaitpost.2010.12.013

Maathuis, K. G. B., van der Schans, C. P., van Iperen, A., Rietman, H. S., & Geertzen, J. H. B. (2005). Gait in children with cerebral palsy: observer reliability of Physician Rating Scale and Edinburgh Visual Gait Analysis Interval Testing scale. *Journal of Pediatric Orthopedics*, *25*(3), 268–272. http://doi.org/10.1097/01.bpo.0000151061.92850.74

Madgwick, S. O. H., Harrison, A. J. L., & Vaidyanathan, R. (2011). Estimation of IMU and MARG orientation using a gradient descent algorithm. *IEEE International Conference on Rehabilitation Robotics*. http://doi.org/10.1109/ICORR.2011.5975346

Major, M. J., Raghavan, P., & Gard, S. (2015). Assessing a low-cost accelerometer-based technique to estimate spatial gait parameters of lower-limb prosthesis users. *Prosthetics and Orthotics International*, 1–6. http://doi.org/10.1177/0309364614568411

Mariani, B., Hoskovec, C., Rochat, S., Büla, C., Penders, J., & Aminian, K. (2010). 3D gait assessment in young and elderly subjects using foot-worn inertial sensors. *Journal of Biomechanics*, *43*(15), 2999–3006. http://doi.org/10.1016/j.jbiomech.2010.07.003

Mariani, B., Rochat, S., Büla, C. J., & Aminian, K. (2012). Heel and toe clearance estimation for gait analysis using wireless inertial sensors. *IEEE Transactions on Biomedical Engineering*, *59*(12 PART2), 3162–3168. http://doi.org/10.1109/TBME.2012.2216263

Mariani, B., Rouhani, H., Crevoisier, X., & Aminian, K. (2013). Quantitative estimation of foot-flat and stance phase of gait using foot-worn inertial sensors. *Gait and Posture*, *37*(2), 229–234. http://doi.org/10.1016/j.gaitpost.2012.07.012

Mazza, C., Donati, M., Mccamley, J., Picerno, P., Cappozzo, A., Mazzà, C., … Cappozzo, A. (2012). An optimized Kalman filter for the estimate of trunk orientation from inertial sensors data during treadmill walking. *Gait & Posture*, *35*(1), 138–142. http://doi.org/10.1016/j.gaitpost.2011.08.024

McGinnis, R. S., & Perkins, N. C. (2012). A highly miniaturized, wireless inertial measurement unit for characterizing the dynamics of pitched baseballs and softballs. *Sensors (Switzerland)*, *12*(9), 11933–11945. http://doi.org/10.3390/s120911933

McGrath, D., Greene, B. R., Walsh, C., & Caulfield, B. (2011). Estimation of minimum ground clearance (MGC) using body-worn inertial sensors. *Journal of Biomechanics*, *44*(6), 1083–1088.

http://doi.org/10.1016/j.jbiomech.2011.01.034

Millor, N., Lecumberri, P., Gómez, M., Martínez-Ramírez, A., & Izquierdo, M. (2014). Drift-free position estimation for periodic movements using inertial units. *IEEE Journal of Biomedical and Health Informatics*, *18*(4), 1131–1137. http://doi.org/10.1109/JBHI.2013.2286697

Moore, K. L., DalleyII, A. F., & Agur, A. M. R. (2006). *Clinically Oriented Anatomy, 5th Edition*. *Clinical Anatomy*.

Morgenroth, D. C., Orendurff, M. S., Shakir, A., Segal, A., Shofer, J., & Czerniecki, J. M. (2010). The relationship between lumbar spine kinematics during gait and low-back pain in transfemoral amputees. *American Journal of Physical Medicine & Rehabilitation / Association of Academic Physiatrists*, *89*(8), 635–643. http://doi.org/10.1097/PHM.0b013e3181e71d90

Muro-de-la-Herran, A., García-Zapirain, B., & Méndez-Zorrilla, A. (2014). Gait analysis methods: An overview of wearable and non-wearable systems, highlighting clinical applications. *Sensors (Switzerland)*, *14*(2), 3362–3394. http://doi.org/10.3390/s140203362

Nepomuceno, A., Major, M. J., Stine, R., & Gard, S. (2017). Effect of foot and ankle immobilization on able-bodied gait as a model to increase understanding about bilateral transtibial amputee gait. *Prosthetics and Orthotics International*. http://doi.org/10.1177/0309364617698521

Noble, J. W., & Prentice, S. D. (2006). Adaptation to unilateral change in lower limb mechanical properties during human walking. *Experimental Brain Research*, *169*(4), 482–495. http://doi.org/10.1007/s00221-005-0162-3

Ojeda, L., & Borenstein, J. (2007). Non-GPS navigation for security personnel and first responders. *Journal of Navigation*, *60*(3), 391–407. http://doi.org/10.1017/S0373463307004286

Ong, A. M. L., Hillman, S. J., & Robb, J. E. (2008). Reliability and validity of the Edinburgh Visual Gait Score for cerebral palsy when used by inexperienced observers. *Gait and Posture*, *28*(2), 323–326. http://doi.org/10.1016/j.gaitpost.2008.01.008

Owings, T. M., & Grabiner, M. D. (2004). Step width variability, but not step length variability or step time variability, discriminates gait of healthy young and older adults during treadmill locomotion. *Journal of Biomechanics*, *37*(6), 935–938. http://doi.org/10.1016/j.jbiomech.2003.11.012

Patla, A. E., & Greig, M. (2006). Any way you look at it, successful obstacle negotiation needs visually guided on-line foot placement regulation during the approach phase. *Neuroscience Letters*, *397*(1–2), 110–114. http://doi.org/10.1016/j.neulet.2005.12.016

Patla, A. E., & Rietdyk, S. (1993). Visual control of limb trajectory over obstacles during locomotion: effect of obstacle height and width. *Gait & Posture*, *1*(1), 45–60. http://doi.org/10.1016/0966-6362(93)90042-Y

Patla, A. E., Rietdyk, S., Martin, C., & Prentice, S. (1996). Locomotor Patterns of the Leading and the Trailing Limbs as Solid and Fragile Obstacles are Stepped over: Some Insights into the Role of Vision During Locomotion. *Journal of Motor Behavior*, *28*(1), 35–47. http://doi.org/10.1080/00222895.1996.9941731

Peruzzi, A., Della Croce, U., & Cereatti, A. (2011). Estimation of stride length in level walking using an inertial measurement unit attached to the foot: A validation of the zero velocity assumption during stance. *Journal of Biomechanics*, *44*(10), 1991–1994. http://doi.org/10.1016/j.jbiomech.2011.04.035

Pezzack, J. C., Norman, R. W., & Winter, D. a. (1977). An assessment of derivative determining techniques used for motion analysis. *Journal of Biomechanics*, *10*(5–6), 377–382.

http://doi.org/10.1016/0021-9290(77)90010-0

Picerno, P., Cereatti, A., & Cappozzo, A. (2011). A spot check for assessing static orientation consistency of inertial and magnetic sensing units. *Gait and Posture*, *33*(3), 373–378. http://doi.org/10.1016/j.gaitpost.2010.12.006

Pitkin, M. R. (2010). Biomechanics of lower limb prosthetics. In *Biomechanics of Lower Limb Prosthetics* (pp. 1–141). http://doi.org/10.1007/978-3-642-03016-1

Powers, C. M., Rao, S., & Perry, J. (1998). Knee kinetics in trans-tibial amputee gait. *Gait and Posture*, *8*(1), 1–7. http://doi.org/10.1016/S0966-6362(98)00016-2

Read, H. S., Hazlewood, M. E., Hillman, S. J., Prescott, R. J., & Robb, J. E. (2002). Edinburgh visual gait score for use in cerebral palsy. *Journal of Pediatric Orthopedics*, *23*(3), 296–301. Retrieved from http://www.ncbi.nlm.nih.gov/pubmed/12724590

Rebula, J. R., Ojeda, L. V., Adamczyk, P. G., & Kuo, A. D. (2013). Measurement of foot placement and its variability with inertial sensors. *Gait & Posture*, *38*(4), 974–980. http://doi.org/10.1016/j.gaitpost.2013.05.012

Ricci, L., Taffoni, F., & Formica, D. (2016). On the orientation error of IMU: Investigating static and dynamic accuracy targeting human motion. *PLoS ONE*, *11*(9), 1–15. http://doi.org/10.1371/journal.pone.0161940

Roetenberg, D., Luinge, H., & Slycke, P. (2009). Xsens MVN: full 6DOF human motion tracking using miniature inertial sensors. *Xsens Motion Technologies …*, (July 2016). Retrieved from https://www.researchgate.net/profile/Per_Slycke/publication/239920367_Xsens_MVN_Full_6DOF_Human_Motion_Tracking_Using_Miniature_Inertial_Sensors/links/0f31752f1f60c20b18000000.pdf

Rouhani, H., Favre, J., Crevoisier, X., & Aminian, K. (2012). Measurement of Multi-segment Foot Joint Angles During Gait Using a Wearable System. *Journal of Biomechanical Engineering*, *134*(June 2012), 061006. http://doi.org/10.1115/1.4006674

Sabatini, A. M., Martelloni, C., Scapellato, S., & Cavallo, F. (2005). Assessment of walking features from foot inertial sensing. - Sabatini et al. - 2005.pdf, *52*(3), 486–494.

Salarian, A., Burkhard, P. R., Vingerhoets, F. J. G., Jolles, B. M., & Aminian, K. (2013). A novel approach to reducing number of sensing units for wearable gait analysis systems. *IEEE Transactions on Biomedical Engineering*, *60*(1), 72–77. http://doi.org/10.1109/TBME.2012.2223465

Schaarschmidt, M., Lipfert, S. W., Meier-Gratz, C., Scholle, H. C., & Seyfarth, A. (2012). Functional gait asymmetry of unilateral transfemoral amputees. *Human Movement Science*, *31*(4), 907–917. http://doi.org/10.1016/j.humov.2011.09.004

Schmalz, T., Blumentritt, S., & Reimers, C. D. (2001). Selective thigh muscle atrophy in trans-tibial amputees: An ultrasonographic study. *Archives of Orthopaedic and Trauma Surgery*, *121*(6), 307–312. http://doi.org/10.1007/s004020000227

Schmid, M., Beltrami, G., Zambarbieri, D., & Verni, G. (2005). Centre of pressure displacements in trans-femoral amputees during gait. *Gait and Posture*, *21*(3), 255–262. http://doi.org/10.1016/j.gaitpost.2004.01.016

Sejdić, E., Lowry, K. A., Bellanca, J., Perera, S., Redfern, M. S., & Brach, J. S. (2016). Extraction of Stride Events from Gait Accelerometry during Treadmill Walking. *IEEE Journal of Translational Engineering in Health and Medicine*, *4*(February 2015).

http://doi.org/10.1109/JTEHM.2015.2504961

Seymour, R. (2002). *Prosthetics and Orthotics: Lower Limb and Spinal*. (T. Julet, U. Lushnycky, N. Peterson, D. Hartman, & J. Ajello, Eds.). Baltimore, Maryland, United States, Maryland, United States: Lippincott Williams & Wilkins.

Shrout, P. E., & Fleiss, J. L. (1979). Intraclass correlations: Uses in assessing rater reliability. *Psychological Bulletin*, *86*(2), 420–428. http://doi.org/10.1037/0033-2909.86.2.420

Shull, P. B., Jirattigalachote, W., Hunt, M. A., Cutkosky, M. R., & Delp, S. L. (2014). Quantified self and human movement: A review on the clinical impact of wearable sensing and feedback for gait analysis and intervention. *Gait and Posture*, *40*(1), 11–19. http://doi.org/10.1016/j.gaitpost.2014.03.189

Singer, J. C., McIlroy, W. E., & Prentice, S. D. (2014). Kinetic measures of restabilisation during volitional stepping reveal age-related alterations in the control of mediolateral dynamic stability. *Journal of Biomechanics*, *47*, 1–7. http://doi.org/10.1016/j.jbiomech.2014.08.022

Singer, J. C., Prentice, S. D., & McIlroy, W. E. (2013). Age-related changes in mediolateral dynamic stability control during volitional stepping. *Gait and Posture*, *38*(4), 679–683. http://doi.org/10.1016/j.gaitpost.2013.03.003

Sparrow, W. a., Shinkfield, A. J., Chow, S., & Begg, R. K. (1996). Characteristics of gait in stepping over obstacles. *Human Movement Science*, *15*(4), 605–622. http://doi.org/10.1016/0167-9457(96)00022-X

Stevens-lapsley, J. E., Schenkman, M. L., & Dayton, M. R. (2011). Comparison of Self-Reported Knee Injury and Osteoarthritis Outcome Score to Performance Measures in Patients After Total Knee Arthroplasty. *PMRJ*, *3*(6), 541–549. http://doi.org/10.1016/j.pmrj.2011.03.002

Takeda, R., Lisco, G., Fujisawa, T., Gastaldi, L., Tohyama, H., & Tadano, S. (2014). Drift Removal for Improving the Accuracy of Gait Parameters Using Wearable Sensor Systems. *Sensors*, *14*(12), 23230–23247. http://doi.org/10.3390/s141223230

Takeda, R., Tadano, S., Natorigawa, A., Todoh, M., & Yoshinari, S. (2009a). Gait posture estimation by wearable acceleration and gyro sensor. *IFMBE Proceedings*, *25*(9), 111–114. http://doi.org/10.1007/978-3-642-03889-1-30

Takeda, R., Tadano, S., Natorigawa, A., Todoh, M., & Yoshinari, S. (2009b). Gait posture estimation by wearable acceleration and gyro sensor. *IFMBE Proceedings*, *25*(9), 111–114. http://doi.org/10.1007/978-3-642-03889-1-30

Taylor, L., Miller, E., & Kaufman, K. R. (2017). Static and dynamic validation of inertial measurement units. *Gait and Posture*, *57*(April), 80–84. http://doi.org/10.1016/j.gaitpost.2017.05.026

Temel, M., Rudolph, K. S., & Agrawal, S. K. (2010). Gait recovery in healthy subjects: Perturbations to the knee motion with a Smart Knee Brace. *IEEE/ASME International Conference on Advanced Intelligent Mechatronics, AIM*, *1864*(November 2014), 527–532. http://doi.org/10.1109/AIM.2010.5695918

Thong, Y. K., Woolfson, M. S., Crowe, J. A., Hayes-Gill, B. R., & Jones, D. A. (2004). Numerical double integration of acceleration measurements in noise. *Measurement: Journal of the International Measurement Confederation*, *36*(1), 73–92. http://doi.org/10.1016/j.measurement.2004.04.005

Thong, Y. K., Woolfson, M. S., Crowe, J. a, Hayes-Gill, B. R., & Challis, R. E. (2002). Dependence of inertial measurements of distance on accelerometer noise. *Measurement Science and Technology*,

13(8), 1163–1172. http://doi.org/10.1088/0957-0233/13/8/301

Tong, K., & Granat, M. H. (1999). A practical gait analysis system using gyroscopes, *21*, 87–94.

Trojaniello, D., Cereatti, A., & Croce, U. Della. (2014). Gait direction of progression estimate using shank worn MIMUs. *Gnb2014*, (1), 25–27. http://doi.org/10.13140/2.1.1682.9443

Trojaniello, D., Cereatti, A., & Della Croce, U. (2015). Foot clearance estimation during overground walking and vertical obstacle passing using shank-mounted MIMUs in healthy and pathological subjects. *Conference Proceedings : ... Annual International Conference of the IEEE Engineering in Medicine and Biology Society. IEEE Engineering in Medicine and Biology Society. Annual Conference*, *2015*(July 2016), 5505–8. http://doi.org/10.1109/EMBC.2015.7319638

Trojaniello, D., Cereatti, A., Pelosin, E., Avanzino, L., Mirelman, A., Hausdorff, J. M., & Della Croce, U. (2014). Estimation of step-by-step spatio-temporal parameters of normal and impaired gait using shank-mounted magneto-inertial sensors: application to elderly, hemiparetic, parkinsonian and choreic gait. *Journal of Neuroengineering and Rehabilitation*, *11*(1), 152. http://doi.org/10.1186/1743-0003-11-152

Vanicek, N., Strike, S. C., & Polman, R. (2015). Kinematic differences exist between transtibial amputee fallers and non-fallers during downwards step transitioning. *Prosthetics and Orthotics International*, *39*(4), 322–332. http://doi.org/10.1177/0309364614532867

Vaz, S., Falkmer, T., Passmore, A. E., Parsons, R., & Andreou, P. (2013). The Case for Using the Repeatability Coefficient When Calculating Test-Retest Reliability. *PLoS ONE*, *8*(9), 1–7. http://doi.org/10.1371/journal.pone.0073990

Vrieling, a. H., van Keeken, H. G., Schoppen, T., Otten, E., Halbertsma, J. P. K., Hof, A. L., & Postema, K. (2007). Obstacle crossing in lower limb amputees. *Gait & Posture*, *26*(4), 587–594. http://doi.org/10.1016/j.gaitpost.2006.12.007

Vrieling, A. H., van Keeken, H. G., Schoppen, T., Hof, A. L., Otten, B., Halbertsma, J. P. K., & Postema, K. (2009). Gait adjustments in obstacle crossing, gait initiation and gait termination after a recent lower limb amputation. *Clinical Rehabilitation*, *23*(7), 659–671. http://doi.org/10.1177/0269215509102947

Winter, D. (1992). Foot trajectory in human gait: a precise and multifactorial motor control task. *Physical Therapy*, *72*(1), 45-53; discussion 54–6.

Winter, D. A. (2009). *Biomechanics and motor control of human movement* (4th ed.). Hoboken, New Jersey: John Wiley & Sons, Inc. Retrieved from https://books.google.ca/books?hl=en&lr=&id=_bFHL08IWfwC&oi=fnd&pg=PA14&dq=the+biomechanics+and+motor+control+of+human+gait:+normal,+elderly+and+pathological&ots=Jlku9uegN4&sig=03Qu3rmO3Elh0bCw1zM8Or_4KFk

Winter, D. A. D. A. (1991). *Biomechanics and motor control of human gait: normal, elderly and pathological* (2nd ed.). Waterloo. Retrieved from http://trid.trb.org/view.aspx?id=770965

Winter, D. A., & Sienko, S. E. (1988). Biomechanics of below-knee amputee gait. *Journal of Biomechanics*, *21*(5), 361–367. http://doi.org/10.1016/0021-9290(88)90142-X

Wu, G., Siegler, S., Allard, P., Kirtley, C., Leardini, A., Rosenbaum, D., … Stokes, I. (2002). ISB recommendation on definitions of joint coordinate system of various joints for the reporting of human joint motion--part I: ankle, hip, and spine. International Society of Biomechanics. *Journal of Biomechanics*, *35*(4), 543–548. http://doi.org/10.1016/S0021-9290(01)00222-6

Yang, M., Zheng, H., Wang, H., McClean, S., & Newell, D. (2012). IGAIT: An interactive accelerometer based gait analysis system. *Computer Methods and Programs in Biomedicine*, *108*(2), 715–723. http://doi.org/10.1016/j.cmpb.2012.04.004

Zeni, J. A., Richards, J. G., & Higginson, J. S. (2008). Two simple methods for determining gait events during treadmill and overground walking using kinematic data. *Gait & Posture*, *27*(4), 710–714. http://doi.org/10.1016/j.gaitpost.2007.07.007

Ziegler-Graham, K., MacKenzie, E. J., Ephraim, P. L., Travison, T. G., & Brookmeyer, R. (2008). Estimating the Prevalence of Limb Loss in the United States: 2005 to 2050. *Archives of Physical Medicine and Rehabilitation*, *89*(3), 422–429. http://doi.org/10.1016/j.apmr.2007.11.005

Zijlstra, W., & Hof, A. L. (2003). Assessment of spatio-temporal gait parameters from trunk accelerations during human walking. *Gait and Posture*, *18*(2), 1–10. http://doi.org/10.1016/S0966-6362(02)00190-X

Zok, M., Mazzà, C., & Della Croce, U. (2004). Total body centre of mass displacement estimated using ground reactions during transitory motor tasks: application to step ascent. *Medical Engineering & Physics*, *26*(9), 791–798. http://doi.org/10.1016/j.medengphy.2004.07.005